TECHNICAL REPORT STANDARD TITLE PAGE

1. Report No.	2. Government Accession No.	3. Recipient's Catalog No.
FHWA/TX-88+459-2F		

4. Title and Subtitle	5. Report Date
METHODS OF ANALYZING AND FACTORS INFLUENCING FRICTIONAL EFFECTS OF SUBBASES	November 1987
	6. Performing Organization Code
7. Author(s)	8. Performing Organization Report No.
Andrew J. Wimsatt, B. Frank McCullough, and Ned H. Burns	Research Report 459-2F
9. Performing Organization Name and Address	10. Work Unit No.
Center for Transportation Research The University of Texas at Austin Austin, Texas 78712-1075	11. Contract or Grant No. Research Study 3-8-86-459
	13. Type of Report and Period Covered
12. Sponsoring Agency Name and Address Texas State Department of Highways and Public Transportation; Transportation Planning Division P. O. Box 5051 Austin, Texas 78763-5051	Final
	14. Sponsoring Agency Code

15. Supplementary Notes
Study conducted in cooperation with the U. S. Department of Transportation, Federal Highway Administration. Research Study Title: "Development of Subbase Friction Information for Use in Design of Concrete Pavement"

16. Abstract

This final report for Research Project 459 reviews available information relating to the subbase frictional effect, especially an unpublished Portland Cement Association report for the Federal Highway Administration on cement stabilized subbases. Experimental results of push off tests on an unbound shell subbase layer underlying an in-service jointed reinforced concrete pavement are given and discussed. The report also lists and discusses the results of push off tests to find the effects of subbase depth and surface texture on the frictional resistance of an asphalt concrete pavement. Actual crack spacing values for continuously reinforced concrete pavements were then correlated to values predicted by the CRCP computer program in this report, using the subbase friction information found from this project study. Results of estimating subbase friction using the indirect tensile strength testing of subbase cores are shown and discussed, and implications of the subbase frictional effect on concrete pavements are presented. The report ends with a summary of conclusions and recommendations for future testing.

17. Key Words	18. Distribution Statement
subbase, friction, concrete pavements, subbase depth, surface texture, crack spacing, indirect tensile test	No restrictions. This document is available to the public through the National Technical Information Service, Springfield, Virginia 22161.

19. Security Classif. (of this report)	20. Security Classif. (of this page)	21. No. of Pages	22. Price
Unclassified	Unclassified	84	

Form DOT F 1700.7 (8-69)

METHODS OF ANALYZING AND FACTORS INFLUENCING FRICTIONAL EFFECTS OF SUBBASES

by
Andrew J. Wimsatt
B. Frank McCullough
Ned H. Burns

Research Report 459-2F

Research Project 3-8-86-459
Development of Subbase Friction Information for Use in Design of Concrete Pavement

conducted for

Texas State Department of Highways
and Public Transportation

in cooperation with the

U. S. Department of Transportation
Federal Highway Administration

by the

Center for Transportation Research

Bureau of Engineering Research
The University of Texas at Austin

November 1987

The contents of this report reflect the views of the authors, who are responsible for the facts and the accuracy of the data presented herein. The contents do not necessarily reflect the official views or policies of the Federal Highway Administration. This report does not constitute a standard, specification, or regulation.

There was no invention or discovery conceived or first actually reduced to practice in the course of or under this contract, including any art, method, process, machine, manufacture, design or composition of matter, or any new and useful improvement thereof, or any variety of plant which is or may be patentable under the patent laws of the United States of America or any foreign country.

PREFACE

This is the final report for Research Project 3-8-86-459, "Development of Subbase Friction Information for Use in Design of Concrete Pavement." The study was conducted by the Center for Transportation Research, Bureau of Engineering Research, The University of Texas at Austin. This study was sponsored jointly by the Texas State Department of Highways and Public Transportation and the Federal Highway Administration under an agreement with the University of Texas and the Texas State Department of Highways and Public Transportation.

Special appreciation is expressed to Carl Bertrand, Chris Hartmann, Alan Durston, Lyn Gabbert, Michele Sewell, Dr. Nam, Moon Won, Chia Pei Chou, Don Dombroski, and all other Center for Transportation Research staff members for their assistance in the experimentation, data collection, and organization of this report.

Andrew J. Wimsatt
B. Frank McCullough
Ned H. Burns

LIST OF REPORTS

Report No. 459-1, "Stabilized Subbase Friction Study for Concrete Pavements," by James W. Wesevich, B. Frank McCullough, and Ned H. Burns, presents the following: (a) a review of all available literature of subbase friction studies; (b) a theoretical explanation of subbase friction and its effect on concrete pavements; (c) experimental results of concrete pavement behavior over several stabilized subbases; (d) experimental results of push-off tests run on several stabilized subbases; and (e) results of a state-wide survey in determining the prominent subbases used under concrete pavements.

Report No. 459-2F, "Methods of Analyzing and Factors Influencing Frictional Effects of Subbases," by Andrew J. Wimsatt, B. Frank McCullough, and Ned H. Burns, reports the following: (a) a review of more available information relating to the subbase frictional effect; (b) experimental results of push off tests on an unbound shell subbase layer underlying an in-service jointed reinforced concrete pavement in Houston, Texas; (c) results of push off tests to find the effects of subbase depth and surface texture on the frictional resistance of an asphalt concrete pavement; (d) results of correlating actual crack spacing values for continuously reinforced concrete pavements to values predicted by the CRCP computer program using the subbase friction information found from this study; (e) results of estimating subbase friction using the indirect tensile strength testing of subbase cores; and (f) implications of the subbase frictional effect on concrete pavements.

ABSTRACT

This final report for Research Project 459 reviews available information relating to the subbase frictional effect, especially an unpublished Portland Cement Association report for the Federal Highway Administration on cement stabilized subbases. Experimental results of push off tests on an unbound shell subbase layer underlying an in-service jointed reinforced concrete pavement are given and discussed. The report also lists and discusses the results of push off tests to find the effects of subbase depth and surface texture on the frictional resistance of an asphalt concrete pavement. Actual crack spacing values for continuously reinforced concrete pavements were then correlated to values predicted by the CRCP computer program in this report, using the subbase friction information found from this project study. Results of estimating subbase friction using the indirect tensile strength testing of subbase cores are shown and discussed, and implications of the subbase frictional effect on concrete pavements are presented. The report ends with a summary of conclusions and recommendations for future testing.

KEYWORDS: Subbase, friction, concrete pavements, subbase depth, surface texture, crack spacing, indirect tensile test.

SUMMARY

This is the final report for Research Project 459, "Development of Subbase Friction Information for Use in Design of Concrete Pavements." The final phase researched the effect of material depth and surface texture on Texas Specification Type "D" Asphalt Concrete Pavement.

This report discusses the construction of the test area, the experimentation, and the friction information obtained from the testing. It also discusses the results of using the CRCP computer program developed by the Center for Transportation Research (CTR) to predict pavement crack spacing for the stabilized subbases tested in this project, reviews literature and information about subbase friction, discusses the possibility of using the indirect split tensile test on subbase cores to estimate the subbase's frictional resistance, describes results of testing an unbound shell subbase under in-service pavement on IH-45 in Houston, and the implications of the findings in this project, using the PCP1 computer program, also developed by CTR, to formulate conclusions about the effect of the frictional resistance information obtained from the subbases researched in the study. From the results, it was determined that surface texture did not play a significant part in the frictional resistance of the asphalt concrete pavement. However, subbase depth was significant, since the failure planes resulting from the push off tests were at the interface between the asphalt concrete pavement and the underlying flexible subbase material for the thin subbase layer, and within the layer itself only for the thicker subbase layer. Temperature also affected the frictional resistance, with lower temperatures causing greater frictional restraints. Test slab thickness, or overburden pressure, was not a factor for the asphalt concrete pavement, agreeing with the conclusion made in Research Report 459-1 that, for stabilized subbases, overburden pressure was not significant. Also, the unbound shell subbase tested in Houston, exhibited a very low maximum frictional restraint, around 1 psi, which explains why the overlying jointed reinforced concrete pavement was in such good condition after four decades of traffic. Overburden pressure was not a factor for this subbase, either. The CRCP program predicted actual average crack spacing values very well, using the subbase frictional information derived from this research. Further experimentation is recommended, especially to see if the indirect tensile strength of subbase cores could be used to estimate a subbase's frictional resistance; the results from this study on this proposed procedure are preliminary but very promising.

IMPLEMENTATION STATEMENT

Findings from this study on the maximum frictional restraint for the unbound shell subbase and the two layers of asphalt concrete pavement can be used in concrete pavement design methods (such as the procedure in the AASHTO Pavement Design Guide) to produce more reliable traffic facilities.

TABLE OF CONTENTS

PREFACE iii

LIST OF REPORTS iii

ABSTRACT iii

SUMMARY iv

IMPLEMENTATION STATEMENT iv

CHAPTER 1. INTRODUCTION

BACKGROUND 1

OBJECTIVES 1

Project Objective 1

Report Objective 1

SCOPE OF THE REPORT 1

CHAPTER 2. AVAILABLE INFORMATION

LITERATURE REVIEW 2

Portland Cement Association Report for the FHWA (Ref 4) 2

Center For Highway Research Project 98 Reports 3

CTR REPORT 459-1 3

SUMMARY 7

CHAPTER 3. EVALUATION OF AN IN-SERVICE PAVEMENT SUBBASE LAYER

BACKGROUND 8

DESCRIPTION OF SITE 8

CONSTRUCTION OF THE TEST SLABS AND TEST APPARATUS 8

EXPERIMENTATION 10

RESULTS 10

SUMMARY 12

CHAPTER 4. A STUDY ON THE EFFECT OF SUBBASE TEXTURE AND THICKNESS ON AN ASPHALT STABILIZED SUBBASE

DISCUSSION OF THE EXPERIMENTATION 14

CONSTRUCTION OF THE TEST SITE 14

EXPERIMENTATION 15

SUMMARY 18

CHAPTER 5. CORRELATION OF THE ACTUAL WITH THE PREDICTED CRACK SPACING OF CONTINUOUSLY REINFORCED CONCRETE PAVEMENTS IN TEXAS USING THE CRCP COMPUTER MODEL

DISCUSSION OF THE PROCEDURE 21

DATA INPUT 21

Concrete Pavement Properties 21

Frictional Restraint - Movement Curves 21

COLLECTION OF ACTUAL CRACK SPACING DATA 22

RESULTS OF THE CORRELATION BETWEEN ACTUAL AND PREDICTED CRACK SPACING 22

CHAPTER 6. A PROPOSED PROCEDURE FOR ESTIMATING SUBBASE FRICTION
REASONS FOR AN ALTERNATE PROCEDURE 24
EXPERIMENTATION 24
RESULTS 25

CHAPTER 7. DISCUSSION OF RESULTS
UNBOUND SHELL SUBBASE TESTS AT THE HOUSTON TEST SITE 27
ASPHALT CONCRETE PAVEMENT TESTS AT THE CTR TEST SITE 27
Effect of Texture on Frictional Resistance 27
Effect of Subbase Depth on Frictional Resistance 27
Effect of Overburden Pressure on Frictional Resistance 27
Other Considerations 27
INDIRECT TENSILE TEST CORRELATION RESULTS 28
CRCP COMPUTER MODEL CORRELATION RESULTS 30

CHAPTER 8. IMPLICATIONS OF THE FINDINGS FROM THIS STUDY
BACKGROUND 31
PCP1 PROGRAM INPUT 31
RESULTS 31

CHAPTER 9. CONCLUSIONS AND RECOMMENDATIONS
CONCLUSIONS FROM THIS REPORT 33
RECOMMENDATIONS 33
MAJOR CONCLUSIONS FROM CENTER FOR TRANSPORTATION RESEARCH REPORT 459-1 (REF 6) 33

REFERENCES 35

APPENDICES
APPENDIX A INDIRECT TENSILE STRENGTH RESULTS FROM THE CENTER FOR HIGHWAY RESEARCH PROJECT 98 37
APPENDIX B RESULTS OF THE PUSH-OFF TESTS ON ASPHALT CONCRETE PAVEMENT AT THE BALCONES RESEARCH 40
APPENDIX C DATA INPUT FOR THE CRCP PROGRAM TO PREDICT CRACK SPACING 66
APPENDIX D CRCP CRACK SPACKING DATA FOR SELECTED TEXAS HIGHWAYS IN DISTRICTS 1, 3, 4, 10, 13, 17, 19, 20, AND 24 74

CHAPTER 1. INTRODUCTION

This chapter introduces the background to this study on the frictional characteristics of subbases, lists the project and report objectives, and states the scope of this final report.

BACKGROUND

Designing, constructing, and adequately maintaining concrete pavements under rigorous and unpredictable traffic and environmental loads is one of the most complex problems any pavement engineer faces. The effects of several of these environmental loads, including moisture and temperature, have been researched, but the effect of one very important environmental load, the frictional characteristics between concrete pavements and today's stabilized subbase materials, has not been adequately studied. Goldbeck (Ref 1), Timms (Ref 2), and others, whose reports were summarized in the previous report on this project (Ref 6), have studied the frictional characteristics of several unbound materials. Several specific tests have been conducted on cement-stabilized materials, including tests in Saudi Arabia (Ref 3), also covered in the previous project report (Ref 6), and tests conducted for the Federal Highway Administration by the Portland Cement Association (Ref 4). However, none of these studies tested a wide range of stabilized subbase materials, and only the Portland Cement Association study, which is discussed in this report, tested the effect of surface texture on frictional resistance.

OBJECTIVES

The project and study objectives are discussed in this section.

Project Objective

Research Project 459 was initiated to obtain stabilized subbase friction information. This was to be accomplished by reviewing literature on the subject; conducting push-off tests to obtain frictional resistance values for several stabilized subbases; and, using the test data as input, executing computer programs to see if they could predict actual concrete pavement behavior and distresses.

Report Objective

The first part of the study involved a review of literature on subbase friction and concrete slab push-off tests made in order to obtain friction information for five subbases: a flexible subbase, a cement-stabilized subbase, an asphalt-stabilized subbase, a lime-treated clay, and an untreated clay (Ref 6). This final phase of the study concentrated on determining whether or not texture and depth played a part in the subbases' frictional resistances. Computer programs, using friction data from this project as input, were executed to see how the programs were affected by this friction information. More literature was reviewed, and the idea of correlating frictional resistance to some aspect of the subbase's material properties was pursued.

SCOPE OF THE REPORT

This final phase of the project study researched the effect of material depth and surface texture on Texas Specification Type "D" Asphalt Concrete Pavement. This report discusses the construction of the test area, the experimentation, and the friction information obtained from the testing. It also discusses the results of using the CRCP computer program developed by CTR to predict pavement crack spacing for the stabilized subbases tested in this project, reviews more literature and information about subbase friction, discusses the possibility of using the indirect split tensile test on subbase cores to estimate the subbase's frictional resistance, describes results of testing an unbound shell subbase under in-service pavement on IH-45 in Houston, and discusses the implications of the findings in this project, using a computer program to formulate conclusions about the effect of the frictional resistance information obtained from the subbases researched in the study. The report ends with a summary of conclusions and recommendations.

CHAPTER 2. AVAILABLE INFORMATION

This chapter presents information gathered from a review of literature on a Portland Cement Association Report for the Federal Highway Administration concerning friction reducers on a cement-stabilized subbase. The chapter also reports indirect tensile strength information for asphalt-stabilized, cement-stabilized, and lime-treated clay subbases from Center for Highway Research Project 98. A summary of information and results obtained from the first part of this project study is also included.

LITERATURE REVIEW

Since the first report for this project, four additional references have been reviewed: a report by the Portland Cement Association concerning the effectiveness of certain friction reducers on cement-stabilized subbases and three reports for Center for Highway Research Project 98 concerning the indirect tensile strengths of asphalt-stabilized, lime-stabilized, and cement-stabilized subbase cores.

Portland Cement Association Report for the FHWA (Ref 4)

Researchers investigated the effect of friction reducing methods and texture on cement-stabilized subbases. Using the conventional push-off test procedure, concrete test slabs, most of them 4 feet wide, 4 feet long, and 6 inches thick, were cast over a limestone aggregate, cement-stabilized subbase coated with 0.2 gallon per square yard of Shell SS-1 asphalt emulsion curing compound. Each slab rested upon a particular texture and a friction reducing medium. In addition, one slab was cast over an uncoated, medium texture, cement-stabilized subbase with no friction reducer. The texture of the subbase was varied by "using different gradations of crushed limestone for each texture ...." The researchers measured the resulting textures using the sand-patch method (ASTM designation E965-83). Then, the slabs were pushed across the subbase, and the peak frictional forces required for the slabs were recorded.

The results, together with the friction reducers used and the subbase textures, are presented in Tables 2.1 through 2.4. Table 2.4, which lists values in psi, was obtained by dividing the applied loads in Table 2.3 by the surface areas of the respective slabs. The results show that, for the effective friction reducers, texture was not significant. However, for the 1/16-inch sand skin treatment, which was basically ineffective as a friction reducer, texture played a significant role in the frictional resistance.

The researchers also pushed and pulled the slabs across the cement-stabilized subbase material after the initial bond between the slabs and the subbase had been broken by the first push-off test. This is similar to what Stott did in his experimentation, in which he conducted his testing until a steady state of frictional resistance was reached, resulting in

TABLE 2.1. COEFFICIENTS OF FRICTION FROM THE CEMENT-STABILIZED SUBBASE TESTING (REF 4)

Friction Reducer	Subbase Texture	Max. Coeff. of Friction					Sliding Coeff. of Friction				
		Push	Pull	Push	Pull	Ave.	Push	Pull	Push	Pull	Ave.
1/4" Sand + Poly.	Medium	0.56	0.58	0.55	0.56	0.56	0.56	0.58	0.55	0.56	0.56
1/4" Sand	Smooth	0.55	0.55	0.54	0.56	0.55	0.55	0.55	0.54	0.55	0.55
	Medium	0.59	0.59	0.58	0.58	0.59	0.59	0.59	0.58	0.58	0.59
	Rough	0.52	0.50	0.56	0.52	0.53	0.51	0.50	0.56	0.52	0.52
1/16" Sand skin	Smooth	0.93	0.75	0.86	0.70	0.81	0.51	0.56	0.74	0.61	0.61
+ Poly.	Medium	0.76	0.77	0.65	0.70	0.72	0.65	0.67	0.65	0.65	0.65
	Rough	0.94	-	0.76	0.70	0.80	0.78	-	0.71	0.65	0.71
Double Poly.	Smooth	0.63	0.58	0.63	0.74	0.65	0.59	0.58	0.63	0.70	0.62
	Medium	0.68	0.81	0.66	0.75	0.72	0.67	0.65	0.65	0.68	0.66
	Rough	0.98	0.76	0.71	0.69	0.79	0.89	0.68	0.65	0.63	0.71
1/16" Sand Skin	Smooth	13.83 *	0.81	1.06	1.05	0.97	0.85	0.81	1.06	1.05	0.94
	Medium	44.47 *	1.24	1.13	1.40	1.26	1.04	0.93	1.00	1.07	1.10
	Rough	51.15 *	1.45	1.44	1.72	1.54	1.14	1.23	1.29	1.24	1.23
No friction reducer (CTB coated with curing compound)	Smooth		> 13.5 **								
	Medium		> 44.0 **								
	Rough		> 51.0 **								
No friction reducer (CTB uncoated)	Medium		> 8.0 **								

* Not included in average

** Values are based on the maximum load that could be applied to the slab with our testing equipment.

TABLE 2.2. EFFECT OF SLAB SIZE AND WEIGHT ON COEFFICIENT OF FRICTION* (REF 4)

Slab Size	Slab Weight	Max. Coeff. of Friction					Sliding Coeff. of Friction				
		Push	Pull	Push	Pull	Avg.	Push	Pull	Push	Pull	Avg.
2 ft x 4 ft x 6 in.	649	0.74	0.69	0.71	0.75	0.72	0.68	0.63	0.68	0.75	0.69
4 ft x 4 ft x 6 in.	1249	0.76	0.77	0.65	0.70	0.72	0.65	0.66	0.65	0.65	0.65
4 ft x 8 ft x 6 in.	2552	0.89	0.62	0.55	0.73	0.70	0.79	0.51	0.53	0.68	0.63
4 ft x 4 ft x 12 in.	2524	0.63	0.78	0.61	0.71	0.68	0.63	0.78	0.61	0.71	0.68
4 ft x 8 ft x 12 in.	5076	0.78	0.71	0.72	0.69	0.72	0.78	0.71	0.72	0.69	0.72
Average		0.71		0.67							
Standard Deviation		± 0.016		± 0.032							
Coefficient of Variation		2.3 percent		4.8 percent							

* All tests were conducted on the medium texture CTB with the 1/16-in. sand skin covered with a polyethylene friction reducer.

a hysteresis curve (Ref 5). The researchers also tried to reach such a steady state. Stott's study is also summarized in CTR Research Report 459-1 (Ref 6).

One important finding from the PCA study is that the three test slabs on the bituminous coated cement-stabilized subbase with no friction reducer had bonded so well to the subbase that they could not be pushed with the researchers' testing system. This was also the case for the test slab on the medium textured, uncoated, cement-stabilized subbase with no friction reducer. This fact accounts for the inability of the study by Wesevich et al to reach a peak frictional resistance for a cement-stabilized subbase material tested in Houston (Ref 6). The PCA researchers also found that, for the bituminous coated cement-stabilized subbase with the medium texture and the 1/16-inch sand skin layer, "sliding occurred primarily in the bituminous curing compound layer," not in the subbase.

Another finding of the study was that the coefficient of friction did not change significantly for a "medium texture CTB with the 1/16 inch sand skin covered with a polyethylene friction reducer" when push-off tests were conducted with slabs of varying thicknesses, as shown in Table 2.2. The finding suggests that the frictional restraint, in psi, does increase with overburden pressure (i.e., slab thickness) when the slab is placed on polyethylene, thus agreeing with the classical friction model (i.e., the frictional coefficient is directly affected by the weight of the object). This fact is shown by the frictional resistance values in psi for the 1/16-inch sand skin and polyethylene with different slab thicknesses at the bottom of Table 2.4. The researchers concluded that "polyethylene on a sand layer and double polyethylene were the most reliable and best all purpose friction reducers evaluated."

Center For Highway Research Project 98 Reports

Research Reports 98-2 (Ref 7), 98-3 (Ref 8), and 98-4 (Ref 9) include indirect split tensile strength data for cores on asphalt-stabilized, cement-stabilized, and lime-stabilized materials, respectively. The experimental results are presented in Appendix A, and a summary of these results is shown in Table 2.5. These reports were obtained for this study to see if indirect tensile strengths of subbase cores could be used to estimate frictional resistance. As expected, cores of cement-stabilized material had the highest indirect tensile strength average, followed by cores of asphalt-stabilized and lime-stabilized materials. However, standard deviations were high among the samples tested for each material, as shown in Table 2.5. Results of this correlation between the indirect tensile strength and frictional resistance are presented in Chapter 4 of this report.

CTR REPORT 459-1

In the report of the first phase of this project, Wesevich et al (Ref 6) stated that subbase friction does not follow the classical model of friction, since it is composed of three components: an adhesion, or gluing, component between the slab and subbase material; a bearing component that is influenced by the surface texture of the subbase; and a shear component which is induced by the movement of the slab across the subbase. Figure 2.1, reprinted from Research Report 459-1, graphically shows these components. The researchers found that subbase friction is an environmental restraint that affects concrete stresses, steel stresses, and slab movements. They also found from the literature review that very few studies researched stabilized subbases.

The researchers stated in Research Report 459-1 that subbase friction acts to counter concrete pavement movements. When the pavement's temperature increases, the pavement wants to expand, but subbase friction resists the movement, causing compressive stresses to develop in the concrete. Since concrete is strong in compression, this usually is not a problem. However, in situations in which the pavement's temperature decreases, or, as in the case of prestressed pavements, when post-tensioning forces are applied to the pavement, the pavement wants to contract.

TABLE 2.3. APPLIED LOADS AND SLAB WEIGHTS (REF 4)

Reducer	Subbase Texture	Size, ft	Move-ment	Maximum Coeff of Friction					Sliding Coeff of Friction					Slab Weight
				Push	Pull	Push	Pull	Avg.	Push	Pull	Push	Pull	Avg.	
1/4" Sand + Poly.	Medium	4x4x0.5	270	700	720	690	700	703	700	720	690	700	703	1240
1/4" Sand	Smooth	4x4x0.5	360	705	695	690	715	701	700	695	685	700	695	1273
	Medium	4x4x0.5	80	760	760	745	745	753	760	760	745	745	753	1279
	Rough	4x4x0.5	160	665	635	705	665	668	645	635	705	665	663	1269
1/16" Sand	Smooth	4x4x0.5	550	1190	960	1100	890	1035	650	715	940	780	771	1275
Skin + Poly.	Medium	4x4x0.5	580	950	960	815	875	900	810	830	805	810	814	1249
	Rough	4x4x0.5	250	1190	1460**	970	890	1017	995	1160**	900	820	905	1271
Double	Smooth	4x4x0.5	400	805	740	800	945	823	750	740	800	890	795	1273
Poly.	Medium	4x4x0.5	630	875	1030	840	960	926	850	835	830	870	846	1279
	Rough	4x4x0.5	480	1240	970	905	880	999	1125	865	820	795	901	1269
1/16" Sand	Smooth	4x4x0.5	17384	17384**	1020	1340	1315	1224	1070	1020	1340	1315	1186	1257
Skin	Medium	4x4x0.5	56252	56252**	1570	1430	1775	1592	1320	1180	1260	1350	1278	1265
	Rough	4x4x0.5	65272	65272**	1850	1840	2200	1963	1460	1570	1640	1580	1563	1276
NoFriction	Smooth	4x4x0.5						>17000					>17000	1266*
Reducer on	Medium	4x4x0.5						>56000					>56000	1266*
Bit. Curing Compound	Rough	4x4x0.5						>65000					>65000	1266*
No Friction Reducer	Medium	4x4x0.5						>10000					>10000	1266*
1/16" Sand	Medium	2x4x0.5	260	480	450	460	490	440	470	410	440	490	445	649
Skin + Poly	Medium	4x8x0.5	1520	2260	1580	1410	1860	1778	2010	1300	1350	1730	1598	2552
	Medium	4x4x1	500	1580	1970	1540	1790	1720	1580	1970	1540	1790	1720	2524
	Medium	4x8x1	1900	3960	1590	3640	3500	3673	3960	3590	3640	3500	3673	5076

Applied load values are in pounds. * Average weight for 4x4x0.5 slabs **Not used in average

TABLE 2.4. FRICTIONAL RESTRAINT VALUES (POUNDS/SQUARE INCH) OBTAINED FROM TABLE 2.3

Reducer	Subbase Texture	Size, ft	Move-ment	Maximum Coeff of Friction					Sliding Coeff of Friction					Slab Weight
				Push	Pull	Push	Pull	Avg.	Push	Pull	Push	Pull	Avg.	
1/4" Sand + Poly.	Medium	4x4x0.5	0.11	0.30	0.31	0.30	0.30	0.31	0.30	0.31	0.30	0.30	0.31	1240
1/4" Sand	Smooth	4x4x0.5	0.16	0.31	0.30	0.30	0.31	0.30	0.30	0.30	0.30	0.30	0.30	1273
	Medium	4x4x0.5	0.03	0.33	0.33	0.32	0.32	0.33	0.33	0.33	0.32	0.32	0.33	1279
	Rough	4x4x0.5	0.07	0.29	0.28	0.31	0.29	0.29	0.28	0.28	0.31	0.29	0.29	1269
1/16" Sand	Smooth	4x4x0.5	0.24	0.52	0.42	0.48	0.39	0.45	0.28	0.31	0.41	0.34	0.33	1275
Skin + Poly.	Medium	4x4x0.5	0.25	0.41	0.42	0.35	0.38	0.39	0.35	0.36	0.35	0.35	0.35	1249
	Rough	4x4x0.5	0.11	0.52	0.63**	0.42	0.39	0.44	0.43	0.50**	0.39	0.36	0.39	1271
Double	Smooth	4x4x0.5	0.17	0.35	0.32	0.35	0.41	0.36	0.33	0.32	0.35	0.39	0.35	1273
Poly.	Medium	4x4x0.5	0.27	0.38	0.45	0.36	0.42	0.40	0.37	0.36	0.36	0.38	0.37	1279
	Rough	4x4x0.5	0.21	0.54	0.42	0.39	0.38	0.43	0.49	0.38	0.36	0.35	0.39	1269
1/16" Sand	Smooth	4x4x0.5	7.55	7.55**	0.44	0.58	0.57	0.53	0.46	0.44	0.58	0.57	0.51	1257
Skin	Medium	4x4x0.5	24.4	24.4**	0.68	0.62	0.77	0.69	0.57	0.51	0.55	0.59	0.55	1265
	Rough	4x4x0.5	28.3	28.3**	0.80	0.80	0.95	0.85	0.63	0.68	0.71	0.69	0.68	1276
NoFriction	Smooth	4x4x0.5					>7.4						>7.4	1266*
Reducer on	Medium	4x4x0.5					>24.3						>24.3	1266*
Bit. Curing	Rough	4x4x0.5					>28.2						>28.2	1266*
Compound														
No Friction Reducer	Medium	4x4x0.5					>4.3						>4.3	1266*
1/16" Sand	Medium	2x4x0.5	0.22	0.41	0.39	0.40	0.43	0.41	0.38	0.36	0.38	0.43	0.39	649
Skin + Poly	Medium	4x8x0.5	0.33	0.50	0.34	0.30	0.40	0.39	0.44	0.28	0.29	0.38	0.35	2552
	Medium	4x4x1	0.22	0.69	0.86	0.67	0.78	0.75	0.69	0.86	0.67	0.78	0.75	2524
	Medium	4x8x1	0.41	0.86	0.35	0.79	0.76	0.80	0.86	0.78	0.79	0.76	0.80	5076

Frictional Restraint values are in lbs per square inch (psi) * Average weight for 4x4x0.5 slabs ** Not used in average

TABLE 2.5. RESULTS FROM CTR RESEARCH REPORTS 98-2, 98-3, AND 98-4

Type of Specimen	No. of Test Specimens	Mean (psi)	Standard Deviation (psi)	Max. Observed Tensile Strength (psi)	Min. Observed Tensile Strength (psi)
Asphalt Treated	68	94.8	54.2	231.3	7.6
Cement Treated	180	138.2	96.8	497.1	13.1
Lime Treated Clay	34	77.1	56.2	318.0	24.0

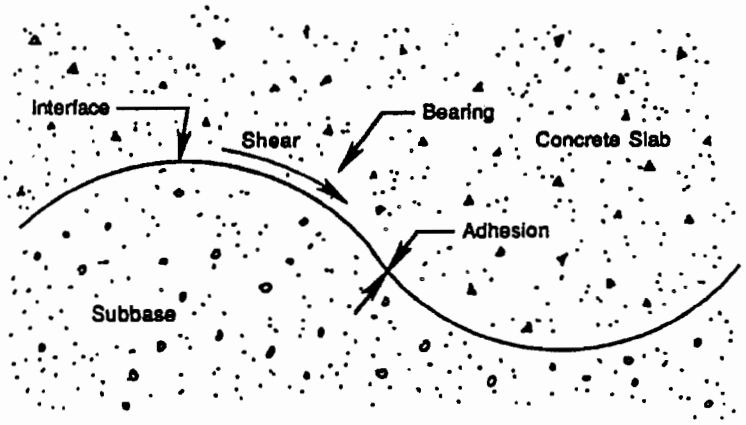

Fig 2.1. ***Adhesion, bearing, and shear components at the slab-subbase interface.***

Subbase friction, however, counters this movement, resulting in tensile stresses in the pavement. In prestressed pavements, this means that the desired amount of post-tensioning force is not achieved in the pavement, especially at the center of the pavement slab. For CRCP, JRCP, and other pavement types, the tensile stresses, in conjunction with traffic loads, cause cracking.

The researchers also conducted a survey of SDHPT Districts to see what subbases were used under their concrete pavements. From the survey, they selected and conducted push-off tests on these five subbase materials:

(1) 12–inch flexible subbase,

(2) 3/4-inch asphalt-stabilized subbase (bond breaker) over 6-inch cement-stabilized subbase, over 6-inch lime-stabilized subbase,

(3) 6-inch cement-stabilized subbase over 6-inch lime-stabilized subbase,

(4) 6-inch lime-stabilized subbase over untreated clay, and

(5) untreated clay.

Figure 2.2 is a graphical representation of the subbases tested in this phase of the study. Table 2.6 shows the results of the push-off tests in terms of the peak frictional resistances of each subbase and the corresponding test slab movement. They concluded that, for stabilized subbases and for flexible subbase, which acted as a stabilized subbase due to the cementing agents contained in it, overburden pressure was not a significant factor. They also found that the failure plane was within the subbase material for stabilized subbases and at the slab-subbase interface for unstabilized materials, such as untreated clay. The only exception to this fact was that the failure plane for the 3/4-inch asphalt-stabilized subbase was the interface between the asphalt-stabilized subbase and the cement-stabilized subbase.

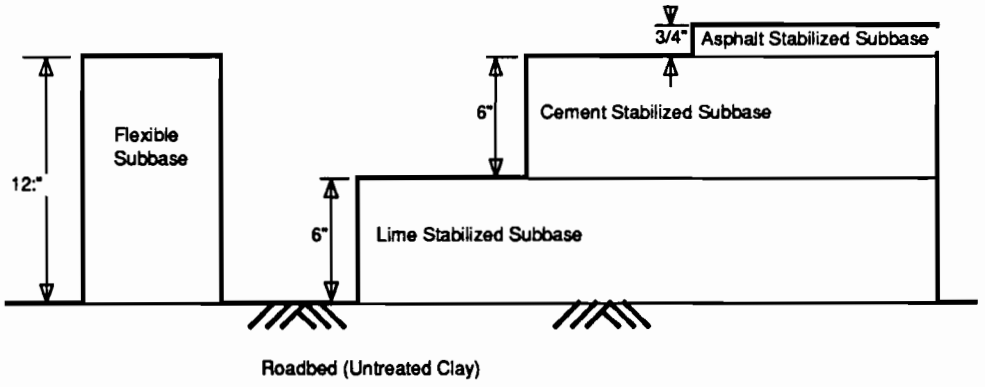

Fig 2.2. ***Subbases tested in CTR Research Report 459-1 (Ref 6).***

Research Report 459-1 includes several

TABLE 2.6. RESULTS OF TESTING - CTR RESEARCH REPORT 459-1

Subbase Type	Peak Frictional Resistance (psi)	Horizontal Movement at Sliding (inch)	Slab Depth (inches)
Flexible	3.0, 3.4	0.024, 0.020	4, 8
Asphalt Stabilized	1.6, 2.2	0.030, 0.038	3.5, 7
Cement Stabilized	15.4 +	0.001 +	3.5
Lime-treated Clay	1.6, 1.7	0.011, 0.012	3.5, 7
Untreated Clay	0.6, 1.1	0.030, 0.052	3.5, 7

important facts about stabilized subbases that the researchers were not able to find in the literature review. The report also raised several questions, the most important concerning the effect of texture and depth on subbase friction. This report tries to answer some of these questions for asphalt-stabilized subbase materials, since they are used as effective bond-breakers between concrete pavements and cement-stabilized subbases.

SUMMARY

The Portland Cement Association study for the FHWA resulted in several interesting discoveries. First, the resulting failure planes differed, depending on the type of treatment used on the cement-stabilized subbase. For the slabs on polyethylene, the failure planes were not within the subbase material, and the frictional characteristics followed the classical friction model mentioned in Research Report 459-1 (Ref 6). However, for the slabs on the 1/16–inch sand skin layer, the failure plane was within the curing compound layer applied on the cement-stabilized subbase. In addition, the peak frictional resistances varied widely, from 0.28 psi to 28.3 psi (a ratio of 1 to 100), depending on the treatment applied to the cement-stabilized subbase. Finally, the researchers were unable to push slabs across the cement-stabilized subbase with no friction reducer applied to the surface.

The average indirect tensile strength values from the three reports for Center for Highway Research Project 98 are revealing in that the cement-stabilized subbase cores had the highest values, although the standard deviations of all three core types are very high. A correlation between these average values and the peak frictional resistances, however, may be possible.

Finally, the first phase of the study for this project (Ref 6) discovered several important factors. The failure planes from the push-off tests on the stabilized subbases and on the flexible subbase were within the subbases, not at the interface between the test slabs and the subbases. In addition, overburden pressure, or test slab depth, was not significant in the frictional restraint for these subbases. Finally, the study found that, during the push-off tests, the cement–stabilized subbase would have had the highest peak frictional resistance. An actual value could not be found, however, since the subbase had adhered to the test slab so much that it was impossible to achieve a peak frictional resistance.

CHAPTER 3. EVALUATION OF AN IN-SERVICE PAVEMENT SUBBASE LAYER

This chapter covers the experimentation and results of the testing for the maximum frictional resistance of an unbound shell subbase material underlying jointed reinforced concrete pavement on Interstate 45 in Houston, Texas. The push-off test procedure used throughout this project in obtaining subbase friction information is described.

BACKGROUND

Interstate 45 south of downtown Houston was originally composed primarily of a JRC pavement consisting of slabs approximately 12 feet wide, 20 feet long, and 8 inches thick. This pavement was constructed in 1945 and was in service from 1947 to 1985, when the reconstruction and overlay of the highway commenced. During that time, the pavement itself stayed in excellent condition - in one observed area, out of approximately 155 jointed pavement sections, only two showed any cracking (Ref 8).

One hypothesis explaining why the pavement was in such good condition is that the underlying subbase had low friction properties, and thus the pavement was not subjected to large tensile stresses when it contracted, which would have lead to cracking. It was decided, then, to find the maximum frictional restraint of the subbase material under this pavement by using a push-off test procedure. The results of this experiment were also of interest to researchers on Projects 422 and 472 who were also investigating the condition of the IH-45 facility.

The subbase in this case consisted of an unbound seashell material dredged from the Texas Gulf Coast. This subbase was widely used under many concrete roadways constructed in the Gulf Coast area prior to the 1970's. To protect the subbase from construction operations, 0.3 gallon per square yard of base preservative OA-175 had been used to cover the surface of the subbase (Ref 11). A typical pavement section, plan, obtained from the Texas SDHPT, is shown in Fig 3.1 (Ref 12).

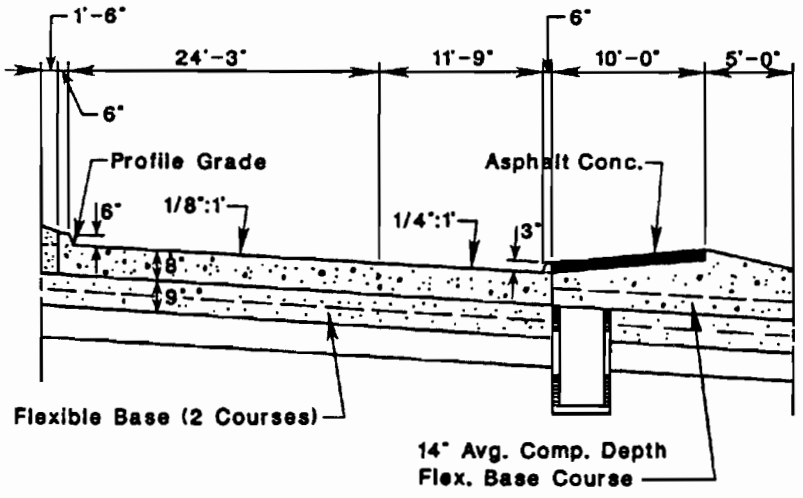

Fig 3.1. ***Houston IH-45 cross section (Ref 12).***

DESCRIPTION OF SITE

The site chosen for the testing was on the shoulder of the northbound lanes of IH-45, just at the end of the embankment north of Scott Street in downtown Houston. The asphalt pavement that made up the shoulder had been removed during construction operations, leaving the shell subbase exposed. The subbase was in excellent condition and had a relatively smooth surface texture. Figures 3.2 and 3.3 show the test area.

CONSTRUCTION OF THE TEST SLABS AND TEST APPARATUS

Two test slabs were constructed using 5 sack concrete containing 1–1/2–inch–size silicious river gravel aggregate. One test slab was 14 feet long, 2 feet wide, and 3–1/2 inches thick; the other slab was 14 feet long, 2 feet wide, and 8 inches thick. A hole 1–1/2 feet deep was excavated between the two slabs and a concrete anchor was placed in it. The anchor contained four rebars extending the depth of the anchor to provide shear strength. After the concrete was placed for the slabs, plastic inserts with thermocouples were inserted into the fresh concrete at midspan for both slabs. The thermocouples were placed on the inserts so that they would be embedded at mid-depth for both slabs. Figure 3.4 shows the plan view of this test site.

The plastic inserts provided a place to put a linear voltage distance transducer (LVDT) to measure the horizontal movement of each slab during the push–off testing. Another LVDT measured the vertical movement of the slab; it came in contact with a small plastic block that was epoxied to the slab surface after the concrete had set. Both LVDT's were mounted on a horizontal rebar that was suspended above each test slab by a pair of rebar stakes hammered into the subbase on both sides of each test slab.

The anchor provided a place for a hydraulic ram to push the test slab. A load cell was placed between the slab and the ram to measure the force that the ram exerted on the slab. A hydraulic pump pressurized the ram,

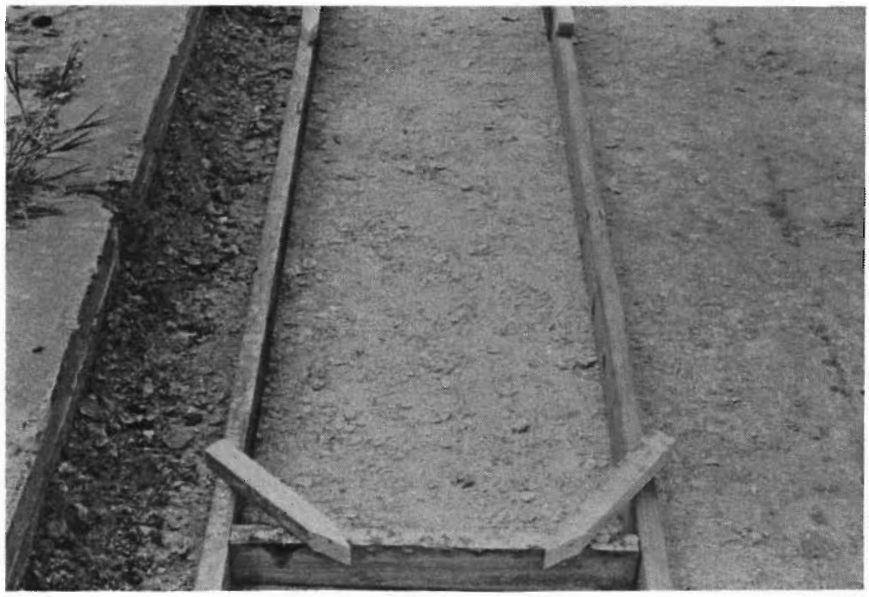

Fig 3.2. ***Houston IH-45 test site.***

Fig 3.3. *Test slabs and instrumentation.*

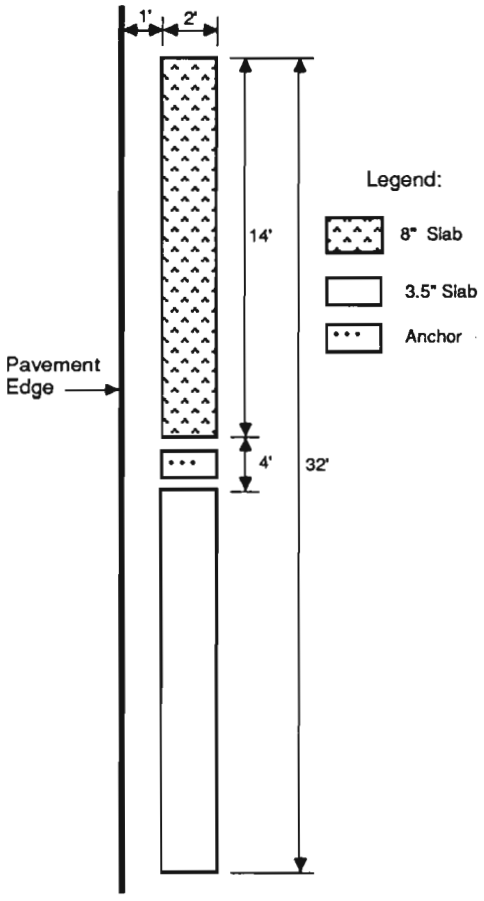

Fig 3.4. *Plan view of Houston IH-45 test site.*

and a pressure meter connected between the ram and pump measured the internal pressure of the ram.

When the concrete was placed for the slabs, the formwork for the 8-inch–thick slab bulged 3 inches at the bottom of one end. This was not a problem, however, since the actual surface area of the slab did not differ significantly from the desired value.

EXPERIMENTATION

The testing procedure and apparatus were the same as that used by Wesevich et al in the first phase of this study. Before testing began, the horizontal and vertical LVDT's were set to read approximately zero displacements and the slabs were preloaded by the load apparatus. Then, pressure was applied to the ram in 100 to 300–psi increments. A computerized data acquisition system recorded the force exerted on the slab as well as the horizontal and vertical movements of the slab after each pressure increment. The data generated from the tests on both slabs resulted in force-movement curves. The forces were converted to frictional resistances in psi by dividing the force values by the respective slab areas.

The conditions during the testing were not ideal, since the subbase was still moist from rain on the morning of the test, and the contractor had constructed a dirt road next to the test site. However, since there were time constraints, the experiment was conducted. The data seem valid.

RESULTS

The data generated from the tests are shown in Tables 3.1 through 3.3. The initial readings of –0.0001 inch in the

TABLE 3.1. RESULTS OF THE HOUSTON IH-45 UNBOUND SHELL PUSH-OFF TESTS

Test Slab Depth (in.)	Maximum Frictional Resistance (psi)	Corresponding Horizontal Movement (in.)
3.5	1.11	0.04
8.0	1.06	0.04

TABLE 3.2. PUSH-OFF TEST, 3-1/2-INCH SLAB ON UNBOUND SHELL SUBBASE

Push-off Test No.: 2 Houston I-45 Slab Area: 4032 in. ^{2}
Date: 13 May 1987 Slab Thickness: 3 1/2 in.
Subbase: Unbound Shell

Time (Hr:Min)	Load (kips)	Ram Pressure (ksi)	Horizontal Movement (in.)	Vertical Movement (in.)	Slab Temp. (°F)	Frictional Resistance (psi)	μ
17:31	0.569	0.100	0.0000	0.0000	84.380	0.141	0.48
17:32	0.586	0.100	–0.0001	0.0000	84.380	0.145	0.50
17:32	0.803	0.160	–0.0001	–0.0001	84.542	0.199	0.68
17:33	1.322	0.280	0.0001	0.0001	84.920	0.328	1.12
17:33	1.702	0.380	0.0005	–0.0001	84.038	0.422	1.45
17:33	1.987	0.440	0.0011	–0.0001	84.794	0.493	1.69
17:33	2.331	0.520	0.0019	0.0000	85.262	0.578	1.98
17:34	2.684	0.580	0.0030	0.0003	84.740	0.666	2.28
17:34	3.086	0.660	0.0047	0.0010	83.642	0.765	2.62
17:34	3.466	0.740	0.0064	0.0019	84.578	0.860	2.95
17:34	3.794	0.800	0.0097	0.0037	83.534	0.941	3.23
17:35	4.042	0.840	0.0147	0.0058	84.200	1.002	3.44
17:35	4.327	0.900	0.0225	0.0109	85.172	1.073	3.68
17:35	4.466	0.940	0.0356	0.0213	84.766	1.108	3.80
17:36	4.230	0.940	0.0433	0.0465	84.974	1.049	3.60
17:36	2.781	0.620	0.0433	0.1465	84.254	0.690	2.37

TABLE 3.3. PUSH-OFF TEST, 8-IN. SLAB ON UNBOUND SHELL SUBBASE

Push-off Test No.: 1 Houston I-45 Slab Area: 4032 in. ^{2}
Date: 13 May 1987 Slab Thickness: 8 in.
Subbase: Unbound Shell

Time (Hr:Min)	Load (kips)	Ram Pressure (ksi)	Horizontal Movement (in.)	Vertical Movement (in.)	Slab Temp. (°F)	Frictional Resistance (psi)	μ
17:01	0.480	80	0.0000	0.0000	84.506	0.119	0.18
17:02	1.440	300	0.0012	0.0003	84.416	0.357	0.54
17:02	2.325	520	0.0073	0.0022	85.866	0.577	0.87
17:03	3.401	640	0.0239	0.0097	85.298	0.844	1.27
17:04	3.989	760	0.0437	0.0251	85.226	0.989	1.48
17:04	4.250	880	0.0467	0.0472	84.974	1.054	1.58
17:04	4.282	880	0.0437	0.0730	85.190	1.062	1.59
17:05	4.242	860	0.0437	0.0967	85.226	1.052	1.58
17:06	4.079	760	0.0467	0.1517	84.938	1.012	1.52

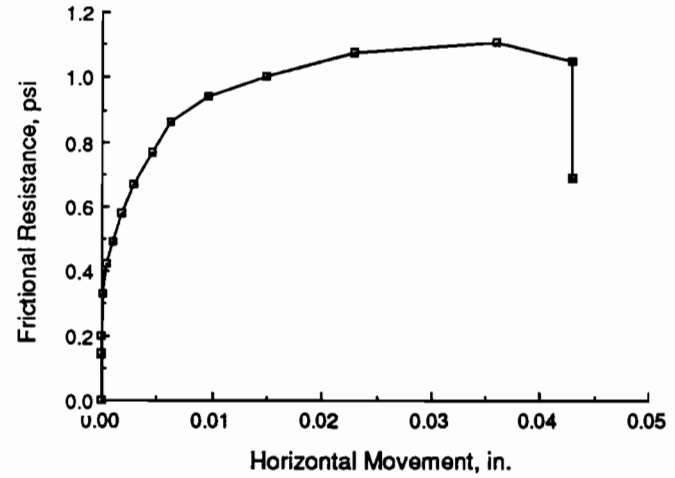

Fig 3.5. ***Horizontal movement for push-off test on 3-1/2-inch slab over unbound shell subbase.***

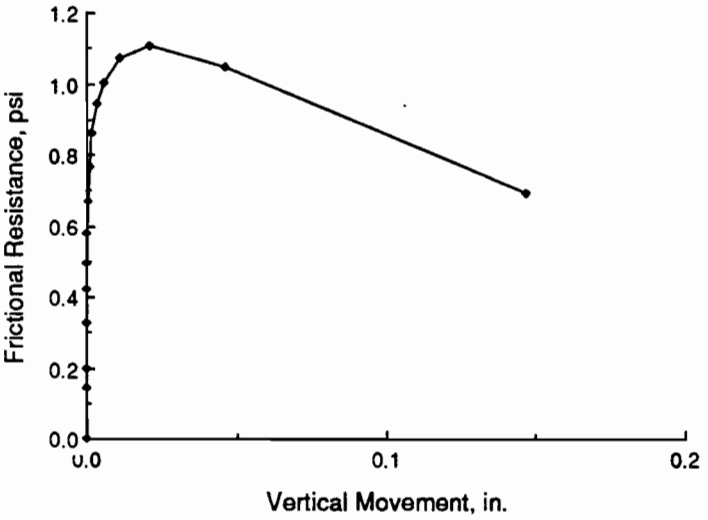

Fig 3.6. ***Vertical movement for push-off test on 3-1/2-inch slab over unbound shell subbase.***

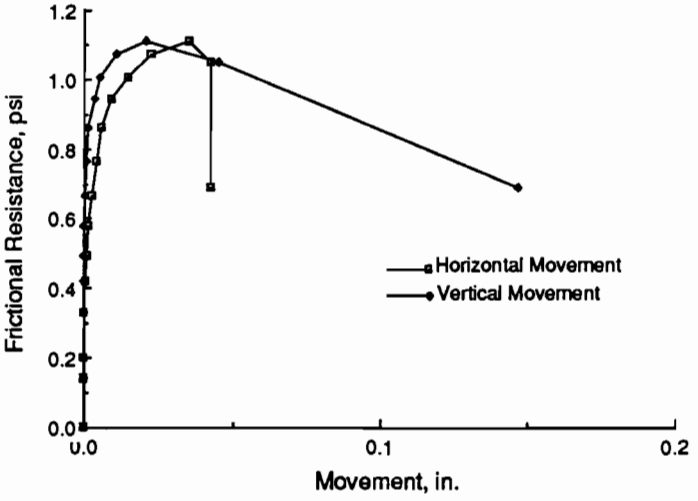

Fig 3.7. ***Horizontal and vertical movements for push-off test on 3-1/2-inch slab over unbound shell subbase.***

horizontal and vertical movements were due to small displacement errors and were considered zero for the data plots in Figs 3.5 through 3.10.

The maximum frictional resistance values for both slabs were very similar: 1.10 psi for the 3–1/2–inch slab and 1.06 psi for the 8–inch slab. This suggests that overburden pressure was not a factor for this subbase. Though the bottoms of the slabs could not be observed because of equipment constraints, the data suggest that the failure planes for the slabs were within the subbase; the vertical displacements of both slabs continued to rise when the horizontal displacements stopped at the peak frictional resistances of the slabs. This indicates that the shell material had adhered to the bottom of the slabs and that shear failure conditions occurred within the subbase itself, causing the slabs to move up over their respective failure planes. If the failure planes had been at the respective slab-subbase interfaces, the slabs would have moved horizontally with virtually no vertical movements, as was the case in the untreated clay push-off tests conducted by Wesevich et al. Thus, this material behaved as a stabilized subbase, most likely because of the cementing agents inherent in shell material.

SUMMARY

This subbase material's maximum frictional restraint of approximately one psi is very low compared to those of other subbases tested in this project. Since the unbound shell material does not adhere to the pavement as much as other subbases do, it does not induce large tensile stresses that could lead to excessive cracking and punchouts. This could explain why the overlying pavement exhibits very few distresses and has remained in excellent condition for nearly forty years.

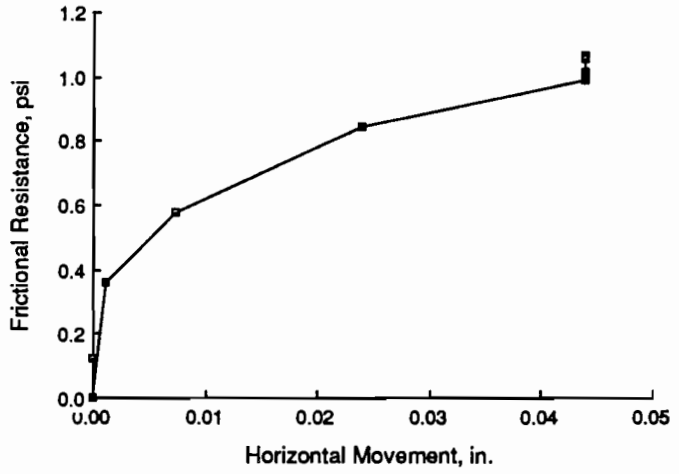

Fig 3.8. ***Horizontal movement for push-off test on 8-inch slab over unbound shell subbase.***

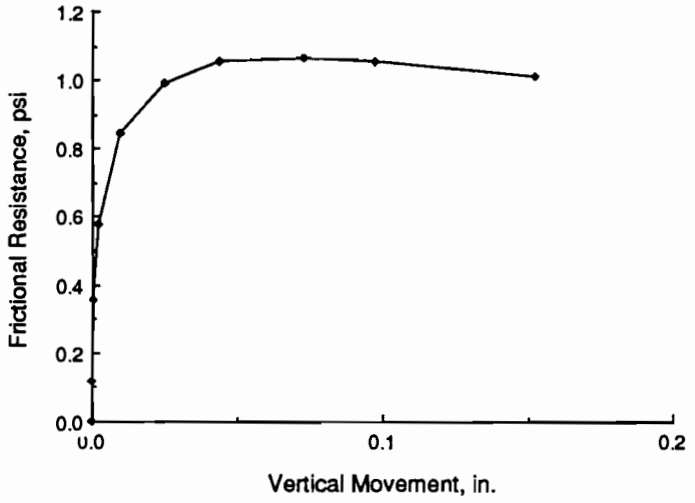

Fig 3.9. ***Vertical movement for push-off test on 8-inch slab over unbound shell subbase.***

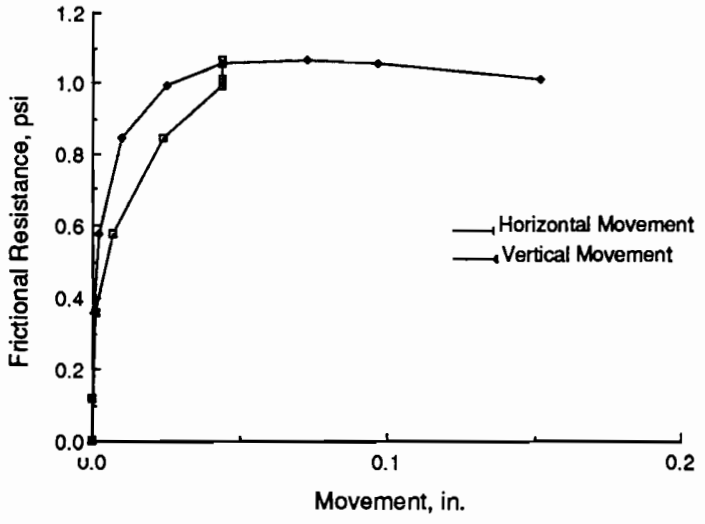

Fig 3.10. ***Horizontal and vertical movements for push-off test on 8-inch slab over unbound shell subbase.***

CHAPTER 4. A STUDY ON THE EFFECT OF SUBBASE TEXTURE AND THICKNESS ON AN ASPHALT STABILIZED SUBBASE

This chapter discusses the construction of a test area and experimentation, using the push-off test procedure, to find the frictional resistance of an asphalt concrete pavement material using three different surface textures and two different pavement thicknesses. The data generated from the testing results in frictional restraint-movement curves, which are shown in this chapter.

DISCUSSION OF THE EXPERIMENTATION

Several methods were discussed for varying the texture of the subbase material, including the variation of the aggregate gradation of the subbase. However, it was highly unlikely that a contractor would agree to such a request for a relatively small project such as this one, and the pavement was textured by hand with a wedge-shaped hammer. In addition, the subbase in this phase of the study consisted of Texas Specification Type D asphalt pavement, since it was more readily available than any other type asphalt concrete pavement or asphalt-stabilized subbase in the Austin area. It was expected to have approximately the same frictional restraint characteristics as any other asphalt pavement or asphalt-stabilized subbase material.

The testing involved the use of a combination of three surface textures (smooth, medium, and rough), two test slab thicknesses (3–1/2 inches and simulated 7 inches), and two asphalt pavement depths (2 inches and 5 inches). Twelve push-off tests were conducted, each test consisting of a specific asphalt pavement depth, surface texture, and test slab thickness. Six push-off tests were conducted per layer, with three slabs of 3–1/2–inch thickness and three slabs of simulated 7–inch thickness. The 7–inch slab thicknesses were simulated during the push-off testing by placing weighed precast concrete blocks on the respective slabs, a procedure also used by Wesevich et al in their experimentation.

CONSTRUCTION OF THE TEST SITE

At the Center for Transportation Research test site at the Balcones Research Center in Austin, two layers of Texas Specification Type D asphalt concrete pavement with limestone aggregate were placed and rolled on a 12–inch–thick flexible subbase. Both layers were 11 feet long and 36 feet wide. However, the layers differed in thickness - one was 5 inches deep, the other was 2 inches deep. A plan view of the asphalt layers, the locations of the test slabs and anchors, and the textures under each slab are shown in Fig 4.1. Figures 4.2 and 4.3 show the site before and after the asphalt pavement layers were placed.

After the pavement layers were constructed, the locations of the twelve test slabs and six anchors were marked on the respective surfaces. Six slabs were to be placed on the 5–inch layer, leaving the remaining six to be constructed on the 2-inch layer. Then, eight marked slab areas, four areas per asphalt layer, were textured by using a wedge hammer to place linear striations approximately 1/8 inch deep into the pavement. These striations were placed across the 2-foot widths of the marked areas. To simulate a medium texture, the striations were placed 4 inches apart on four marked slab areas, two areas per asphalt pavement layer. The other four slab areas that were textured, again two areas per layer, contained striations 2 inches apart to approximate a rough texture. The remaining four slab areas were left alone to approximate a smooth texture. An attempt was made to measure the texture using the ASTM approved sand patch method mentioned in the PCA report for the FHWA; however, the test is not valid for textures with localized indentations (or

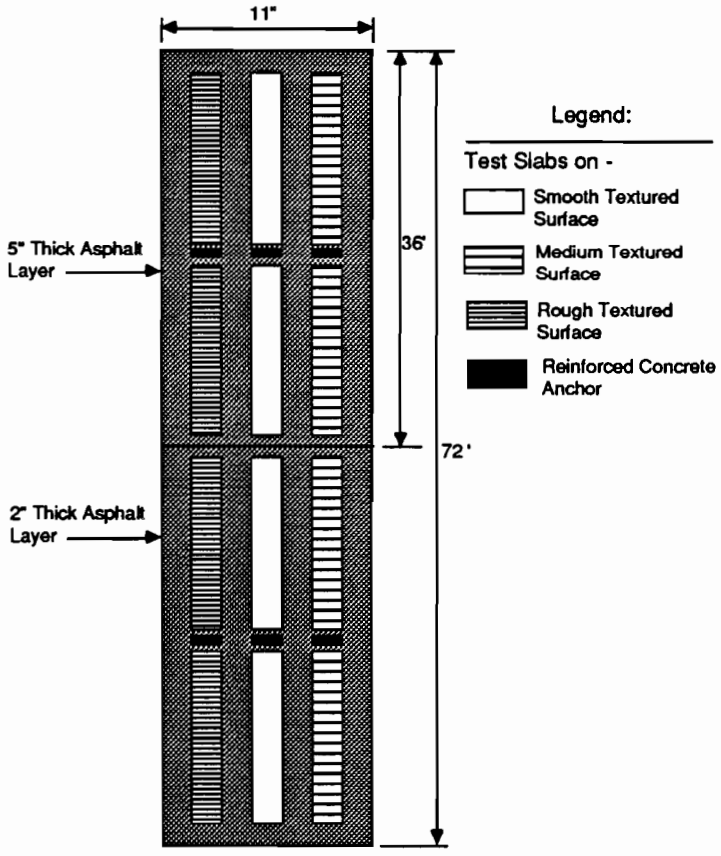

Fig 4.1. ***Plan view of test site.***

cracks) present in the pavement. The resulting asphalt pavement textures are shown in Figures 4.4 and 4.5.

Then, holes approximately 1 foot 4 inches deep were excavated for the placement of anchors. Each of the six anchors, as shown in Fig 4.1, was placed between two slabs to function as a place for the same hydraulic ram and load cell that were used in the Houston IH-45 testing to exert forces on the slabs. Four No. 6 rebars were then placed into the holes to reinforce the anchors.

The slabs and anchors were then cast using five sack concrete with crushed limestone aggregate. All slabs poured were 14 feet long, 2 feet wide, and 3–1/2 inches deep. Plastic inserts containing thermocouples (one per insert) were placed at the midspan of all twelve slabs before the concrete set, to serve the same function as the inserts used in the Houston IH-45 testing. The concrete was then coated with a curing compound. No cracking was observed in any of the slabs.

EXPERIMENTATION

The push-off test procedure used in the experimentation by Wesevich et al and the Houston IH-45 testing was used in this study. The first push-off test was conducted in the morning on a simulated 7–inch slab overlying the 5–inch–thick asphalt pavement with a medium texture,

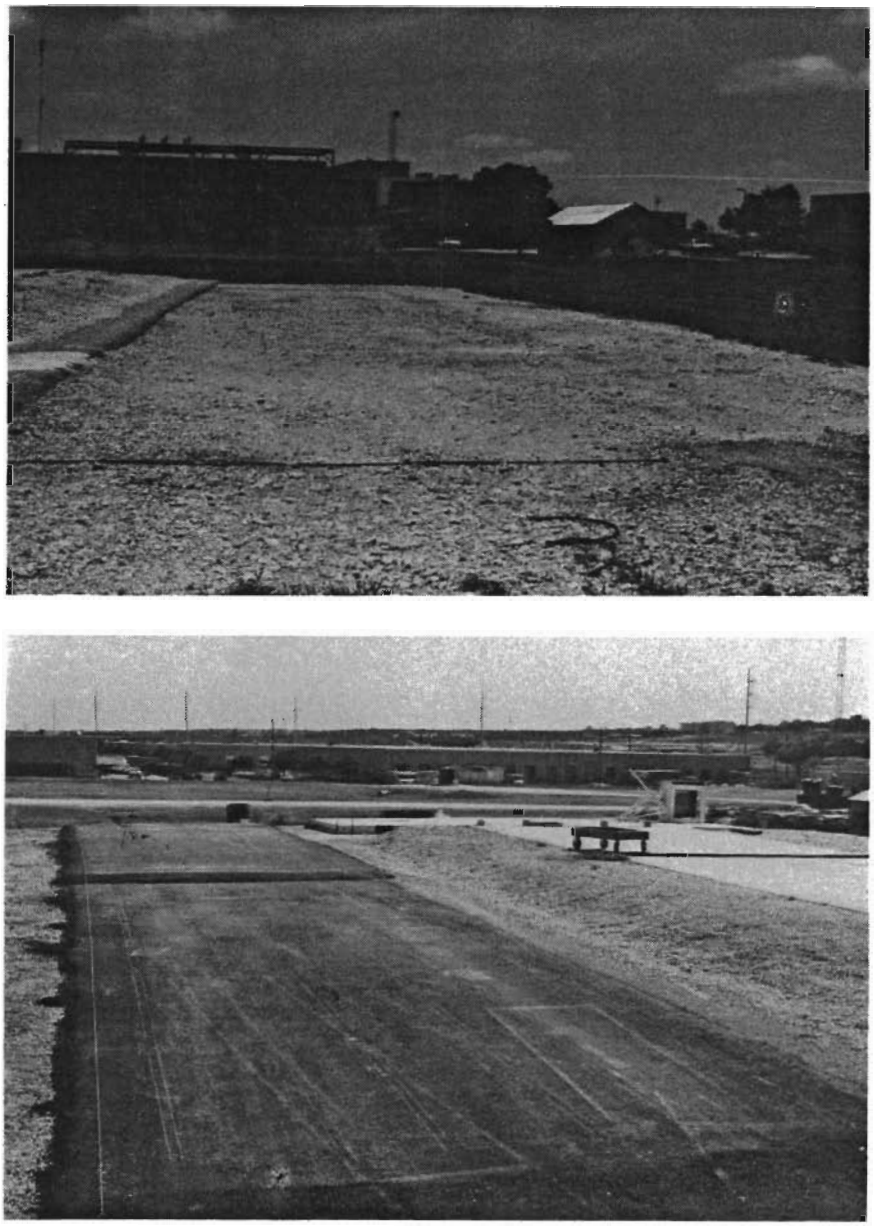

Fig 4.2. ***Site before and after the asphalt pavement layers were placed.***

when the mid-depth slab temperature was around 84 degrees. However, the maximum frictional restraint was never found, for several reasons. First, the 5–inch–thick asphalt layer could not take any bearing pressure, which resulted in the anchor's rotating under a load of 10,000 pounds. As a result, the ram and load cell were reoriented at an angle to the test slab, which caused a portion of the slab to uplift. The test slab then cracked 5 feet from the end of the load application when the force reached 16,000 pounds, near the 20,000 pound capacity of the load cell and hydraulic ram. These two factors stopped the experimentation and negated the further use of the slab. The 3–1/2–inch test slab on the medium-textured 5–inch asphalt layer was then tested, using the same anchor. This time, the anchor rotated even more than in the first push-off test, and a maximum frictional restraint could not be achieved. The testing, again, was stopped.

Because of the problems in the morning, the testing was conducted in the afternoon, when the temperature of the slabs at mid-depth reached 109 to 115 degrees. Though it was much more desirable to get frictional values for the asphalt pavement in the morning, when the frictional restraint was greater, the object of the study was to see specifically if subbase depth and surface texture affected the frictional resistance of the material. Thus, in essence, the temperature was kept constant by conducting the experiments in the afternoon.

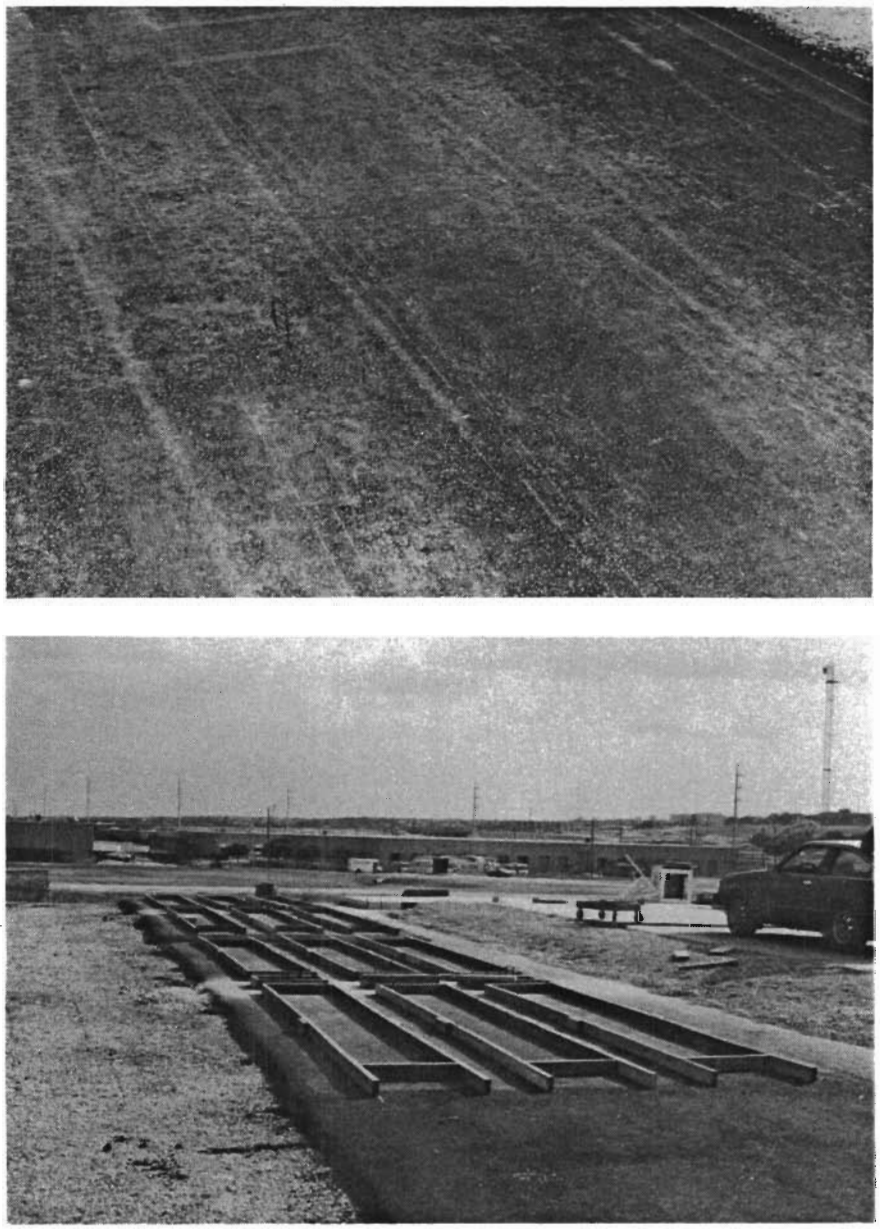

Fig 4.3. ***Asphalt surface before texturing and formwork for the test slabs.***

That afternoon, testing commenced on a 3–1/2–inch slab on the 5–inch asphalt pavement layer with a smooth texture. The testing was successful, though the anchor moved again. However, the maximum restraint was not achieved on the 7–inch slab with the same 5–inch depth and smooth texture and using the same anchor, since the anchor was rendered useless by the previous push-off test. To prevent further occurrences of this problem, a precast concrete block was placed in between the untested simulated 7–inch slab on the rough texture of the same layer and its anchor so that the anchor could stay in place for the push-off testing of the corresponding 3–inch slab with the same texture. The danger was that the resulting load applied on the 7–inch slab from anchor rotation could reach the maximum frictional resistance, but, fortunately, this did not occur. The testing on the 3–1/2–inch slab was successful. The block was then placed between the tested 3–1/2–inch slab and the anchor, and precast blocks were put on the 3–1/2–inch slab with the hope of providing some residual frictional resistance between the slab and the subbase. The ram, load cell, and LVDT's were placed on the 7–inch slab and testing commenced. The anchor, as a result of the preparation, did not rotate, and the maximum frictional resistance for the 7–inch slab on the 5–inch asphalt layer with rough texture was

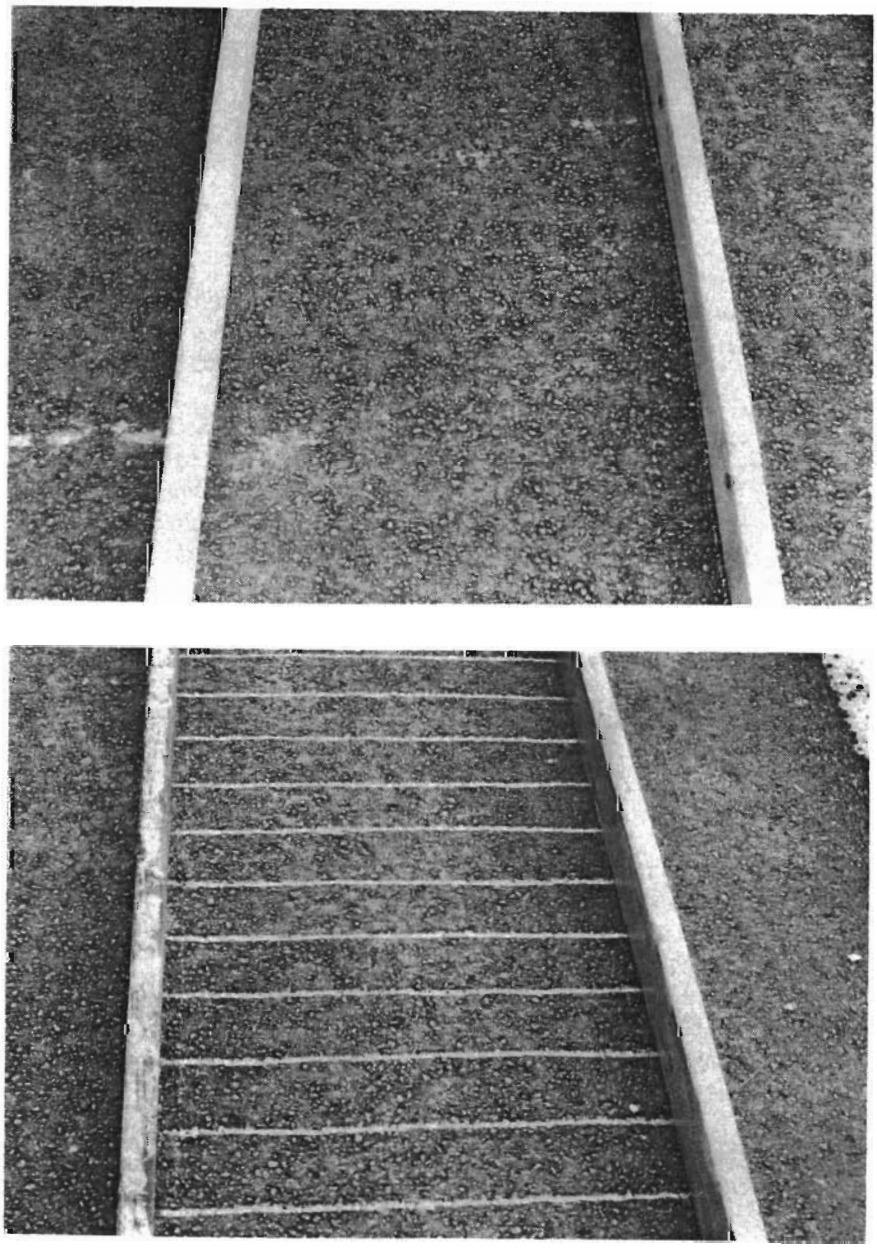

Fig 4.4. ***Smooth and medium textures.***

Fig 4.5. *Rough texture.*

TABLE 4.1. RESULTS OF PUSH-OFF TESTS ON TYPE D ASPHALT PAVEMENT

Subbase Depth (in.)	Texture	Concrete Thickness 3.5 inches	Concrete Thickness 7 inches
2	Smooth	1.65 psi* (0.03 in.)**	2.54 psi (0.04 in.)
	Medium	2.31 psi (0.06 in.)	2.56 psi (0.02 in.)
	Rough	2.30 psi (0.05 in.)	2.42 psi (0.03 in.)
5	Smooth	2.53 psi (0.07 in.)	--
	Medium	2.90 psi (0.03 in.)	--
	Rough	2.85 psi (0.06 in.)	3.23 psi (0.04 in.)

* Maximum frictional restraint.
** Movement at sliding.

found. The same preparation for retesting the two slabs was used on the slabs that couldn't be pushed off; for the 3–1/2–inch slab on the medium texture the test was completed, but it was not successful on the 7–inch slab on the smooth texture. As a result, four slabs on the 5–inch asphalt pavement layer generated frictional resistance data - one 7-inch-thick slab on the rough texture and three 3-1/2-inch-thick slabs on smooth, medium, and rough textures, respectively.

The next afternoon, testing commenced on the six slabs on the 2–inch-deep asphalt pavement layer. This time, the anchors held since they were more embedded in the flexible subbase layer. The same preparation was done for this situation as was done before on the 5–inch–thick asphalt pavement layer, but it was not needed; none of the anchors moved or rotated. All tests on this layer were successful. Figures 4.6 and 4.7 show the push-off tests on two simulated 7–inch slabs and the LVDT setup on a 3-1/2–inch slab.

Results of the ten successful push-off tests, using the same format as the tables and figures in Chapter 3, are shown in Table 4.1 and in Appendix B. As in the push-off tests on the unbound shell subbase in Houston, the initial readings of -0.0001 to -0.0002–inches in the horizontal and vertical movements for some of the push-off tests were due to small displacement errors and were considered essentially zero for the data plots, also in Appendix B. In addition, vertical movements beyond 1/10 inch were considered inaccurate, since, at this point, the vertical LVDT's could not move horizontally with the slab and, thus, could be registering horizontal movements of the slab. The results of the testing are discussed in Chapter 7.

SUMMARY

From the results of the testing, it seems that texture does not significantly affect the frictional resistance of the two layers. Overburden pressure, or test slab thickness, does not affect the results either, a fact which agrees with the results found in the first phase of the study (Ref 6). However, the pavement layer thicknesses seem to affect the frictional resistances, due to the resulting failure planes, which are discussed in Chapter 7. Finally, temperature has an effect on this material, with cooler temperatures increasing the frictional restraint.

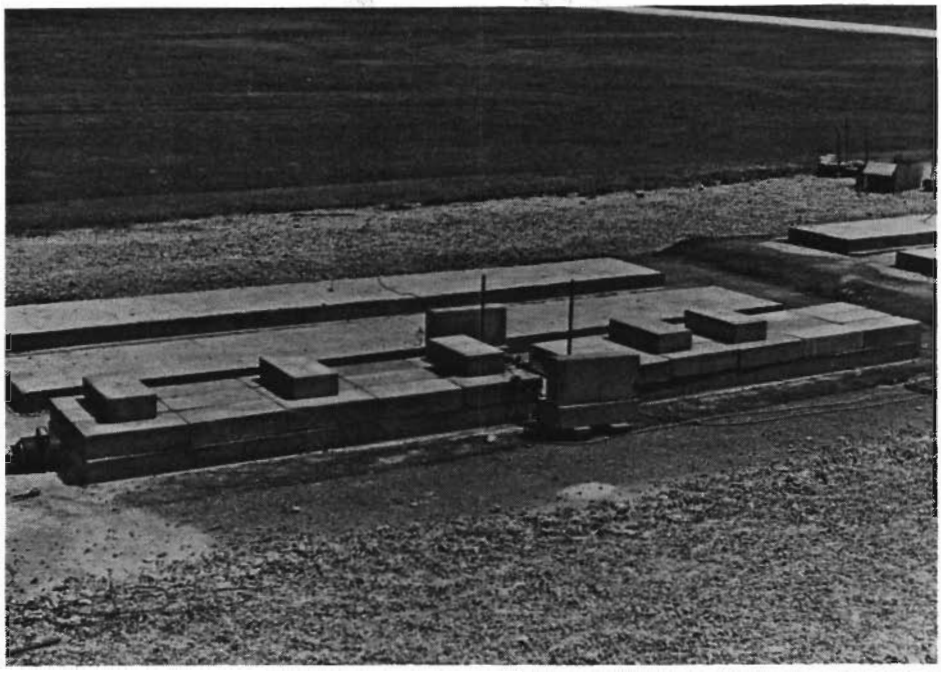

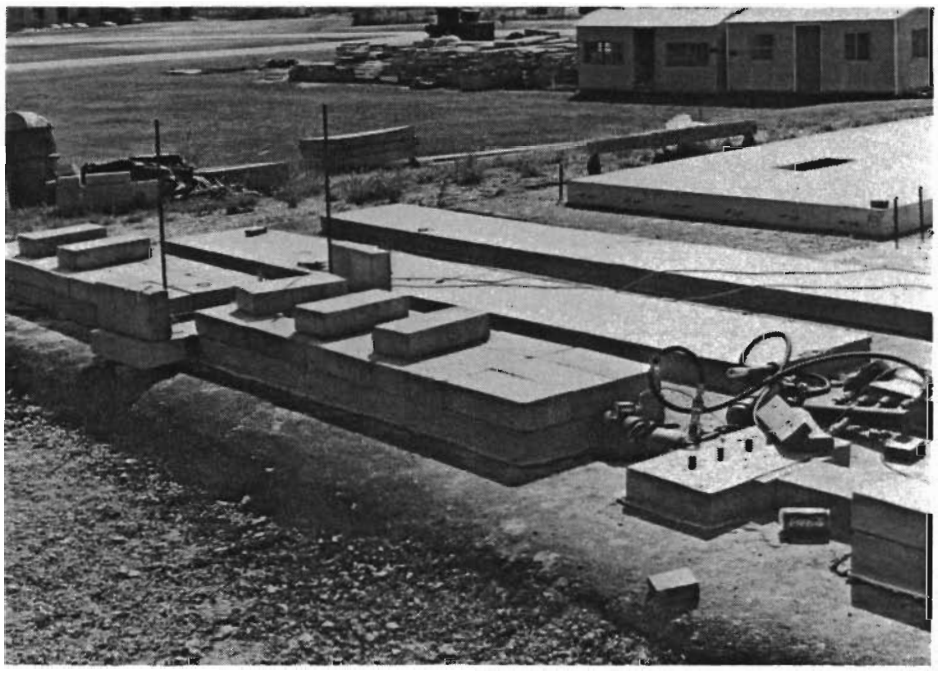

Fig 4.6. ***Push-off tests on simulated 7-inch-thick slabs.***

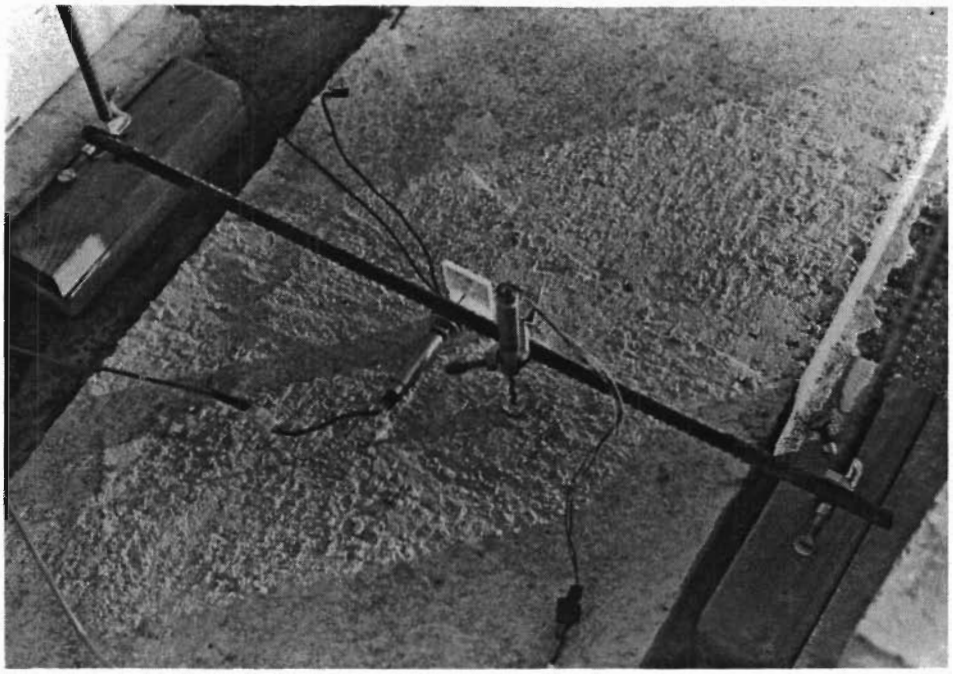

Fig 4.7. ***Horizontal and vertical LVDT's on a 3-1/2-inch test slab.***

CHAPTER 5. CORRELATION OF THE ACTUAL WITH THE PREDICTED CRACK SPACING OF CONTINUOUSLY REINFORCED CONCRETE PAVEMENTS IN TEXAS USING THE CRCP COMPUTER MODEL

This chapter presents the data input used in the CRCP computer model and the information obtained from actual crack spacing measurements conducted for the Texas SDHPT in the mid 1970's. The results of the correlation between measured crack spacing on CRCP roadways in Texas and the predicted crack spacing from the CRCP computer model are also presented.

DISCUSSION OF THE PROCEDURE

Since this study has collected frictional resistance values for several subbases, it was decided to find if the CRCP computer model developed at the Center for Transportation Research could predict actual crack spacings observed in CRCP pavements across the state. Chia-Pei Chou, involved in Project 472, had developed and compiled a database on several CRCP highways in the state. This database included values for pavement depth, coarse aggregate type used in the concrete, and subbase type. In addition, crack spacing was measured by the Texas SDHPT on several of the highways that the database listed. Thus, the CRCP program produced results with these data.

DATA INPUT

The data input into the CRCP program, listed in Appendix C, consisted of concrete pavement properties, the subbases' frictional restraint-movement curves, temperature data, external traffic loads, and iteration and tolerance control. The pavement and subbase friction properties are discussed in detail in this section.

Concrete Pavement Properties

Since the Texas SDHPT measured crack spacing mainly on 8–inch–thick concrete pavements, the program executions and resulting correlations were limited to this concrete thickness. In addition, only pavements containing either silicious river gravel or limestone were considered. The steel percentage was kept constant at 0.6 percent, which was determined from the Texas SDHPT Highway Design Manual as the standard reinforcement design for CRCP (Ref 10). The soil support factor was 640 pci, since no actual values for each subbase type could be determined.

The material properties of the concrete for each section could not be obtained, so the properties used in the program were estimated or standardized. The compressive strength of the concrete pavement entered into the program was 3500 psi. Thermal coefficient values used in the program were 4.00×10^{-6} and 6.00×10^{-6} for limestone aggregate concrete and silicious river gravel concrete, respectively. These values were used in another study on the effect of coarse aggregate type on concrete. A standardized tensile strength gain curve developed by the U.S. Bureau of Reclamation, which resulted in a tensile strength of 443 psi at 28 days, was used for pavements containing limestone aggregate. Since concrete containing silicious river gravel seems to have a lower tensile strength than limestone aggregate concrete, and since the program could not run with the standardized tensile strength curve and a concrete thermal coefficient of 6.00×10^{-6} for cement-stabilized subbases, another curve resulting in a lower tensile strength, 312 psi at 28 days, was used for pavements using silicious river gravel. This curve was obtained from another CRCP program data set with concrete having a thermal coefficient of 5.03×10^{-6} and a compressive strength of 3900 psi; this curve may be too conservative for silicious river gravel, but the program was able to execute with the data.

Frictional Restraint - Movement Curves

The frictional restraint-movement curves from each subbase for the CRCP computer program were developed from the information gathered in this study on push-off tests conducted on lime-treated clay, asphalt-stabilized, cement-stabilized, and flexible subbases. These values are also shown in Appendix C. The frictional data from the push-off tests for test slabs 14 feet long, 2 feet wide, and 7 inches thick were used as the program data input for lime–treated clay, asphalt-stabilized, and flexible subbases. The frictional data for the asphalt-stabilized subbase were from the test conducted for this report on the 5–inch–thick asphalt pavement layer with the rough texture; the data for the lime-treated clay subbase and the asphalt-stabilized subbase were from testing from the first phase of this study (Ref 6). For the cement-stabilized subbase, however, the 28–psi maximum frictional restraint value found from the PCA study for bituminous–coated, cement-stabilized subbase on the 1/16–inch sand skin layer was not used, since the PCA report did not list any force-movement data on the test that resulted in that figure. Instead, an estimate of 17.3 psi was found from extrapolating the data obtained from the unsuccessful push-off test on a cement-stabilized subbase with a test slab measuring 4 feet long, 2 feet wide, and 3–1/2 inches thick, also conducted for the first project report (Ref 6). The maximum force achieved by the equipment was 15.4 psi; however, a second-order polynomial curve fits the frictional restraint-movement data rather well, as shown in Fig 5.1. From this curve, a theoretical maximum value of 17.3 psi at 0.0018 inch was found and used as data input. This value, however, is still quite conservative. The data points used after the 17.3 psi maximum value were extrapolated from the data generated on push-off testing of the 3/4–inch asphalt-stabilized subbase bond breaker conducted by Wesevich et al. It was thought that the resulting sliding plane between the

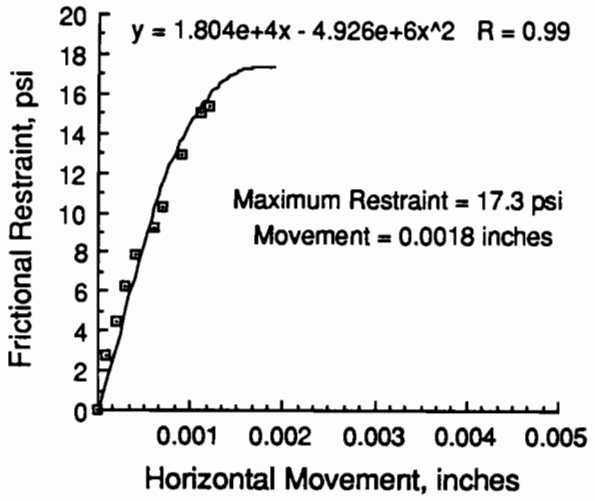

Fig 5.1. ***Second order polynomial curve fit.***

bond breaker and the cement-stabilized subbase from this successful push-off test would reflect the sliding plane of the cement-stabilized subbase if Wesevich et al had been able to achieve such a condition.

COLLECTION OF ACTUAL CRACK SPACING DATA

Data on observed crack spacings of sections of CRCP highways from Texas SDHPT Districts 1, 3, 4, 10, 13, 17, 19, 20, and 24 were used to obtain mean and mode crack spacing values for each measured section (Ref 15). These values for each section were then organized into tables according to the concrete pavement coarse aggregate and subbase combination, i.e., limestone aggregate concrete over cement-stabilized subbase, silicious river gravel concrete over lime-treated clay, and other combinations (Appendix D contains these tables). Finally, average mean and average mode crack spacing values were obtained for each combination, and these values were compared directly with the predicted values from the CRCP program. Only 8–inch–thick concrete pavements were considered, and overlaid pavements were not used in the correlation. No information was available on pavements overlying untreated clay and unbound shell material.

RESULTS OF THE CORRELATION BETWEEN ACTUAL AND PREDICTED CRACK SPACING

The predicted values from the CRCP program and the actual average mean and mode crack spacings are shown in Table 5.1 and organized by pavement-subbase combinations. One fact evident in the results is that the concrete's coefficient of thermal expansion and tensile strength affects the crack spacing values the most. However, the subbase friction data also significantly affect the results, with more than a one–foot difference in average crack spacings between limestone aggregate concrete pavements on lime-treated clay and cement-stabilized subbase.

TABLE 5.1. RESULTS OF THE CRACK SPACING CORRELATION USING TEXAS SDHPT MEASUREMENTS FROM DISTRICTS 1, 3, 4, 10, 13, 17, 19, 20, AND 24

Subbase Type	Coarse Aggregate Type	Predicted Crack Spacing (ft)	Actual Avg. Mean Crack Spacing (ft)	Actual Avg. Mode Crack Spacing (ft)	Number of Measurements
Lime Treated Clay	Limestone	7.4	6.10	5.83	15
	Siliceous River Gravel	3.7	3.72	2.75	14
Asphalt Stabilized	Limestone	7.4	7.31	7.00	16
	Siliceous River Gravel	3.7	3.56	2.65	20
Flexible	Limestone	7.0	7.79	8.00	3
	Siliceous River Gravel	3.5	3.39	2.00	2
Cement Treated	Limestone	6.3	6.52	5.66	31
	Siliceous River Gravel	3.1	3.93	2.71	58

Note: For limestone concrete, f'_t 443.27 psi at 28 days, thermalcoefficient = 4.0×10^{-6}
For siliceous river gravel, f'_t 312 psi at 28 days, thermalcoefficient = 6.00×10^{-6}

Also, the program predicts the actual CRCP crack spacing values very well. Figure 5.2 shows the comparison between the predicted and the actual average crack spacing values, with the diagonal line denoting a one–to–one correlation. The resulting data points come very close to such a perfect correlation. This means that the CRCP computer program, given the proper data, can be valuable in design of such a pavement type.

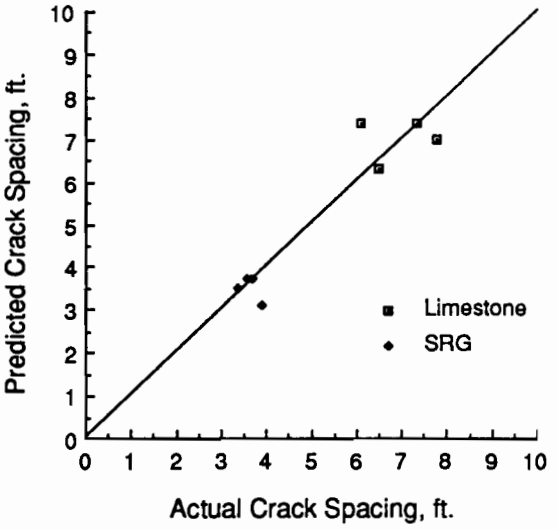

Fig 5.2. ***Predicted versus actual crack spacing.***

CHAPTER 6. A PROPOSED PROCEDURE FOR ESTIMATING SUBBASE FRICTION

This chapter discusses the feasibility of the indirect tensile testing of cores of several subbases to estimate the frictional resistances of the subbases. The reasons for such a procedure and the method used to find the indirect tensile strengths of two subbases tested in this project are discussed. The results of the correlation between frictional resistance and the indirect tensile strength are also presented.

REASONS FOR AN ALTERNATE PROCEDURE

As stated in this report, the push-off test procedure was used to find the maximum frictional restraint of several subbases. However, the time and expense involved in setting up and conducting the testing may make it unlikely to be conducted in the field at actual construction sites. Finding a suitable subbase area to test, constructing slabs, obtaining measurement equipment, and conducting the test all take time and money that may not be available. Therefore, this proposed procedure, which involves correlating the peak frictional resistance of the subbase with the indirect tensile strength of cores taken from the subbase, could be a less time consuming and less costly method.

In this study it was found, from the push-off tests conducted on stabilized subbases and on flexible and shell subbases, that the failure planes were within the subbase layer. This means that, in these cases, the material strength of the subbase governs. Since the indirect tensile test is a measure of material strength, it may be used as a way of estimating the frictional resistances of several subbases.

EXPERIMENTATION

Five cores of the cement-stabilized subbase used for the experimentation discussed in Research Report 459-1 at the Beltway 8 construction project in Houston and two cores of the 5-inch-thick asphalt concrete pavement used for the push-off tests at the Balcones Research Center in Austin are reported herein. The cement-stabilized subbase cores ranged from approximately 3-3/4 inches to 4 inches in diameter. The asphalt concrete cores were all 3-3/4 inches in diameter.

The five cement-stabilized subbase cores, which had lost almost all water content after they were cored and transported back to Austin, were remoisturized by soaking them in a container of water. The cores were taken from the tank and weighed approximately every week until their weight stabilized, meaning that they had reached moisture equilibrium conditions. They were then cut to approximately 2-inch thicknesses and their final dimensions were measured and recorded (one core provided two test specimens). Since the cylindrical surfaces of the cores were rather rough, and since the indirect tensile test apparatus needed a smooth specimen contact area, the cut cores were placed in circular molds containing plaster of paris. The cores and the plaster of paris caps on the cores are shown in Fig 6.1. They were then tested with the equipment shown in Fig 6.2, with the load applied at the plaster of paris surfaces.

The two asphalt pavement cores on the 5–inch–deep asphalt pavement were taken from the field in wet condition, placed in plastic bags, and tested one week after they were obtained. No remoisturization or preparation was necessary for these cores. The cores were cut into two test specimens each, their dimensions were recorded, and then they were tested at room temperature, approximately 77 degrees (although it would have been desirable to test these cores at the temperature during the push-off tests, which was between 109 and 115 degrees; the cores would have probably decompacted at that temperature).

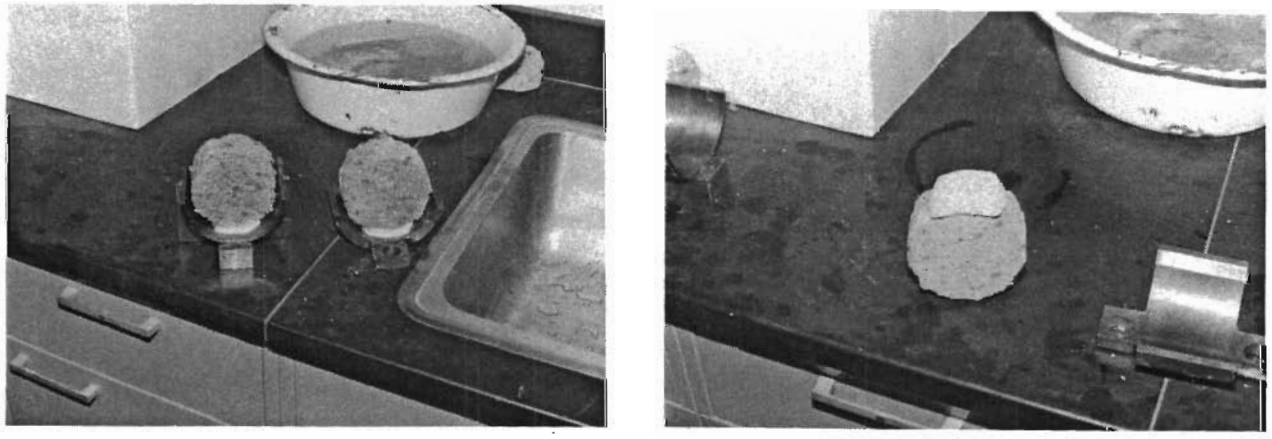

Fig 6.1. ***Cores being prepared for testing.***

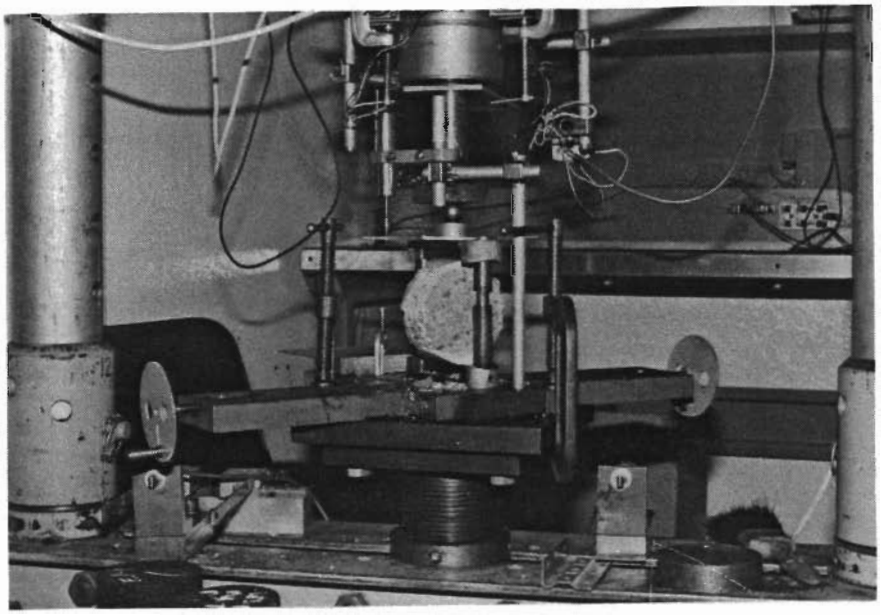

Fig 6.2. ***Indirect tensile test apparatus.***

The indirect tensile strengths of the asphalt pavement cores and the cement-stabilized subbase cores were obtained by the equation

$$S_t = C * P_{max} / t$$

where

S_t = indirect tensile strength of the specimen, psi;

P_{max} = load applied to the specimen by the test apparatus, lb;

t = specimen thickness, inches; and

C = indirect tensile strength correlation coefficient (0.1641 for 3–3/4 inch–diameter specimens, 0.1562 for 4–inch–diameter specimens) (Ref 14).

Cores could not be obtained from the lime-treated clay that Wesevich *et al* tested in Houston; the cores decompacted after they were removed from the subbase. The results in Research Report 98-4 (Ref 9) for tests of lime-treated clay specimens were used in lieu of values that could not be obtained from the field.

RESULTS

Results of the testing are shown in Tables 6.1 and 6.2. Specimens that came from the same core are noted by the letters "A" or "B" beside the specimen number.

The average indirect tensile strengths of the cement-stabilized subbase specimens and the asphalt concrete specimens, as shown in the tables, did not differ significantly - 89.8 psi for the asphalt concrete and 90.3 psi for the cement-stabilized subbase. However, the maximum values from the test series were very different - 155 psi and 97.4 psi for the cement-stabilized subbase and the asphalt concrete, respectively. These maximum values correlate rather closely to the average values for specimens reported on in Research Reports 98-2 (Ref 7) and 98-3 (Ref 8) on asphalt-stabilized and cement-stabilized materials, respectively - 138.2 psi for

TABLE 6.1. CEMENT-STABILIZED SUBBASE SPECIMEN RESULTS

Specimen Number	Indirect Tensile Strength (psi)
1	155.0
2	103.0
3	68.8
4	57.5
5A	81.0
5B	76.2

Average Indirect Tensile Strength = 90.3 psi
Standard Deviation = 35.1 psi

TABLE 6.2. ASPHALT CONCRETE PAVEMENT SPECIMEN RESULTS

Specimen Number	Indirect Tensile Strength (psi)
1A	97.4
1B	90.2
2A	91.3
2B	80.4

Average Indirect Tensile Strength = 89.8 psi
Standard Deviation = 7.0 psi

cement-stabilized, and 94.8 psi for asphalt-stabilized. The average value for lime-treated clay obtained from Research Report 98-4, then, could theoretically be used as the maximum value that might have been obtained from the field if cores could have been extracted.

The three graphs shown in Figs 6.3 through 6.5 compare the indirect tensile strength values to the maximum frictional resistances of asphalt-stabilized, cement-stabilized, and lime-stabilized clay subbases. The maximum frictional resistance values were obtained from the 7–inch test slab on the rough-textured 5–inch-thick asphalt concrete layer from this study (3.2 psi) ; the slab on the bituminous-coated cement-stabilized subbase with 1/16–inch sand skin layer from the PCA report (28 psi); and the 7–inch test slab on the lime-treated clay from Jim Wesevich's experiment (1.7 psi). All three graphs use the average tensile strength value obtained from CTR Research Report 98-4 for lime-stabilized clay (77 psi). Figure 6.3 is a correlation using the average values obtained from CTR Research Reports 98-2 (Ref 7), 98-3 (Ref 8), and 98-4 (Ref 9) on cement-stabilized materials, asphalt-stabilized materials, and lime-stabilized clay. Figure 6.4 uses the average values from the testing in this study on cement-stabilized subbase cores and asphalt concrete cores. Figure 6.5 uses the maximum values of the cement-stabilized and asphalt-stabilized cores.

The most accurate correlation is obtained from Fig 6.3, which shows that an estimation may be obtained by testing a very large number of cores for a subbase and computing the average. However, Fig 6.5 shows that it could be possible to correlate frictional resistance to the maximum indirect tensile strength value found from a small number of cores on each subbase. The main problem in this correlation procedure is the wide variation of values, as shown in the standard deviations. Obviously, more research needs to be conducted in this area. This test could not be used when subbase cores cannot be obtained, but the procedure could be useful in estimating the frictional resistances of subbases.

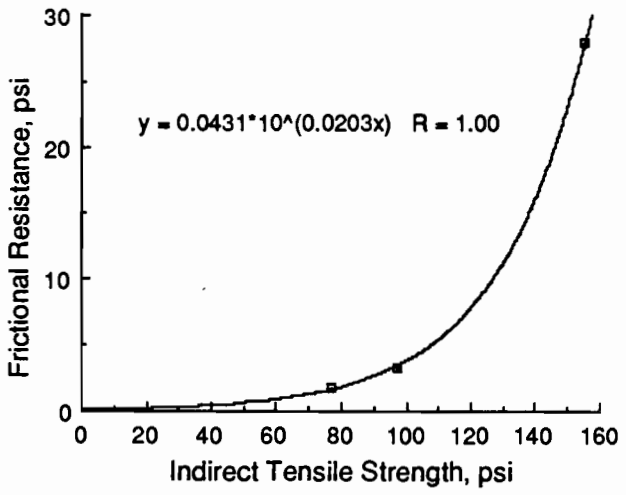

Fig 6.3. ***Frictional resistance vs. CTR Project 98 average values.***

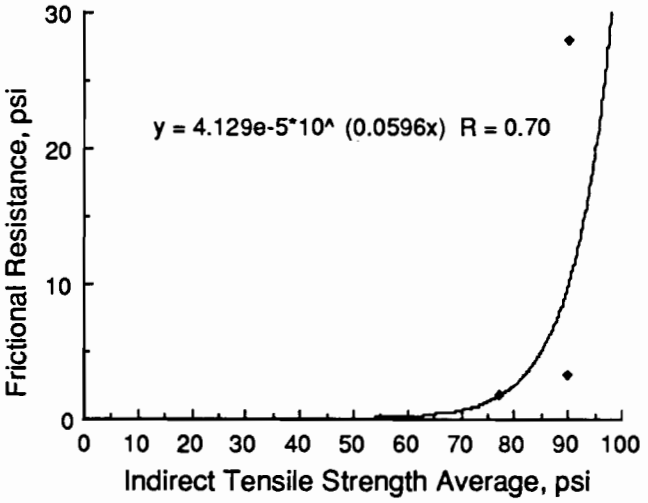

Fig 6.4. ***Frictional resistance vs. experimental average values.***

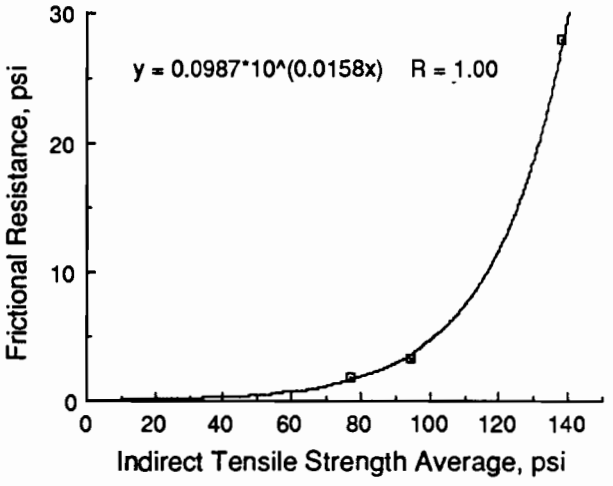

Fig 6.5. ***Frictional resistance vs. experimental maximum values.***

CHAPTER 7. DISCUSSION OF RESULTS

This chapter discusses the results of the push–off tests conducted for this report, the correlation between the indirect split tensile strengths of subbases and their frictional resistances, and the correlation between actual and predicted crack spacings on CRCP highways in Texas.

UNBOUND SHELL SUBBASE TESTS AT THE HOUSTON TEST SITE

The subbase under the pavement at IH-45 in Houston had the second lowest frictional restraint of any subbase tested in this project, exceeding only the values for untreated clay (0.6 psi for a 3–1/2–inch slab, 1.1 psi for a 7–inch slab). The low friction properties of this material are one major reason why this pavement stayed in such good condition for forty years. In addition, overburden pressure did not seem to have an effect on the frictional resistance, as shown by the results in Table 3.1.

Though this subbase is not currently used, it is an ideal material. From field observations, it seems that the material has good compactive properties - a pick, rather than a shovel, had to be used to excavate a hole for the anchor used in the push-off tests, since the material had compacted so well.

The tests were not conducted with the 0.3–gallon per square yard OA-175 base preservative, used to protect the subbase from construction operations, overlying the subbase material. This may have affected the friction between the JRCP slabs and the subbase. However, since the failure plane seemed to be within the subbase itself, it is likely that a surface coating would not affect the final outcome significantly.

ASPHALT CONCRETE PAVEMENT TESTS AT THE CTR TEST SITE

From the results shown in Table 4.1, the 1.65 psi maximum frictional restraint value for the 3–1/2–inch–thick test slab on the 2–inch-deep pavement subbase layer with the smooth texture seems to be too low, since the other values obtained from the three 7–inch–thick slabs on the same layer and the 3–1/2–inch–thick slabs on the 5–inch–deep layer all seem consistent with each other. The push–off test results for this slab, then, were not considered for the conclusions listed in this section.

Effect of Texture on Frictional Resistance

The texture did not make a significant difference in the maximum frictional resistance of the individual subbase layers. No difference between 3–1/2–inch slabs on the medium and rough textured 2–inch–thick subbase layer occurred, and an 0.8 percent difference between 7–inch–thick slabs on the smooth and medium textures of the same layer resulted. As for the 5–inch–thick subbase layer, the difference was 1.3 percent for the 3–1/2–inch–thick slabs on the medium and rough textures, and 12.8 percent for the same thickness slabs on the smooth and medium textures. It would seem likely, then, that, if values could have been obtained for the two simulated 7–inch–thick slabs on the layer for smooth and medium textures, no significant differences would have been found, either.

Effect of Subbase Depth on Frictional Resistance

The depth of the pavement subbase did make a difference in the frictional properties. The differences between 3–1/2–inch slabs on the 2–inch–thick and 5–inch–thick subbase layers were 20.3 percent for medium textures and 19.3 percent for rough textures; for the 7–inch slabs on rough surface textures, the difference was 25.1 percent. This variation in frictional properties was mainly due to the resulting failure planes. For the slabs on the 5–inch–thick asphalt pavement layer, the failure plane was within the pavement itself. However, for the slabs on the 2–inch–thick layer, the failure plane seemed to be at the interface between the asphalt pavement subbase layer and the flexible subbase layer. This is shown in Figs 7.1 through 7.3. For the 5–inch layer, the failure plane could be seen at the pavement edge, and no splitting of the layer occurred; the layer stayed intact. For the 2–inch layer, the layer split all around each test slab, with tears extending several inches away from each slab. The layer also buckled in several places during the testing. Some of the tears were so large that the underlying flexible subbase material could be seen. Thus, the maximum frictional restraint for the 5–inch subbase layer was due to the material properties of the subbase. The maximum frictional restraint for the 2–inch subbase layer, on the other hand, was dependent on the adhesive, bearing, and shear properties and the material characteristics of the asphalt pavement subbase and the flexible subbase at the interface between the two materials.

Effect of Overburden Pressure on Frictional Resistance

Overburden pressure (i.e., test slab thickness) was not a significant factor for this subbase, again assuming the 1.65 psi value obtained from the experiment is too low and thus not valid. This was the same as the result achieved in the previous tests on the stabilized subbases, the flexible subbase, and the unbound shell subbase. The difference between frictional restraints for 3–1/2–inch–thick slabs and simulated 7–inch–thick slabs on the 2–inch deep subbase layer was 9.8 percent for the medium texture and 5.0 percent for the rough texture; the difference was also 11.8 percent for the slabs on the rough-textured 5–inch–thick subbase layer.

Other Considerations

Temperature also affected the frictional characteristics of this subbase, as shown by the inability in this study to conduct push-off tests in the morning hours. Lower temperatures could increase the measured frictional restraint 1 to 2 psi, maybe even greater. More research should be done in this area over a range of temperatures for asphalt–stabilized materials.

The point at which the maximum frictional restraint occurred for the test slabs, also shown in Table 4.1, seems to be random. No correlation can be drawn from the data, based on texture, subbase depth, or test slab thickness. The only hypothesis that can be made is that the randomness of this data is most likely due to the variability of the asphalt pavement's material strength, compaction, and thickness under each slab. If no material variability was present, the same movement at sliding should be found for every test slab.

It is highly recommended that much deeper anchors, extending significantly into the material underlying the subbase, be used if future push–off tests are conducted on thick asphalt–stabilized subbase layers such as this one.

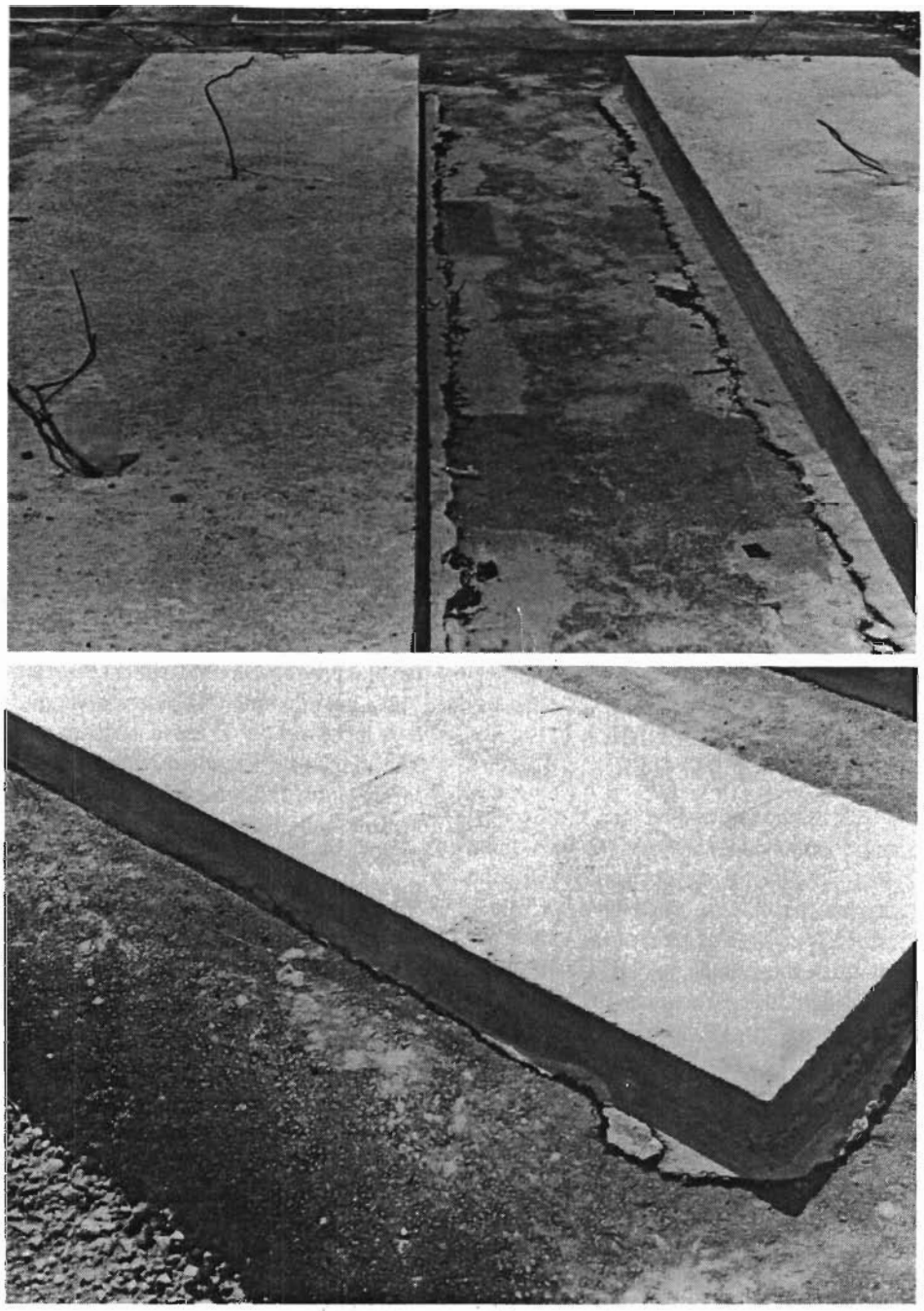

Fig 7.1. ***Failure planes for 5-inch-thick layer.***

The failure of an anchor in this study prevented push-off tests on one slab, and the inability of the anchors to resist loads effectively almost resulted in the failure to gather conclusive frictional information on the 5–inch–thick pavement layer.

INDIRECT TENSILE TEST CORRELATION RESULTS

The results of this testing are not conclusive. As stated in Chapter 6, a good correlation between maximum frictional restraint values can be achieved if a large number of subbase cores are tested. However, the maximum frictional restraint for untreated cement–stabilized subbases has not been found, which leads to some uncertainty in this particular correlation.

Another problem in this correlation is the wide variation of indirect tensile strengths observed between cores of the same subbase. The indirect tensile test, of course, does not accurately reflect failure conditions in the field, since small test samples are involved. However, the material properties of a subbase are usually not as consistent as the overlying concrete pavement, since the production

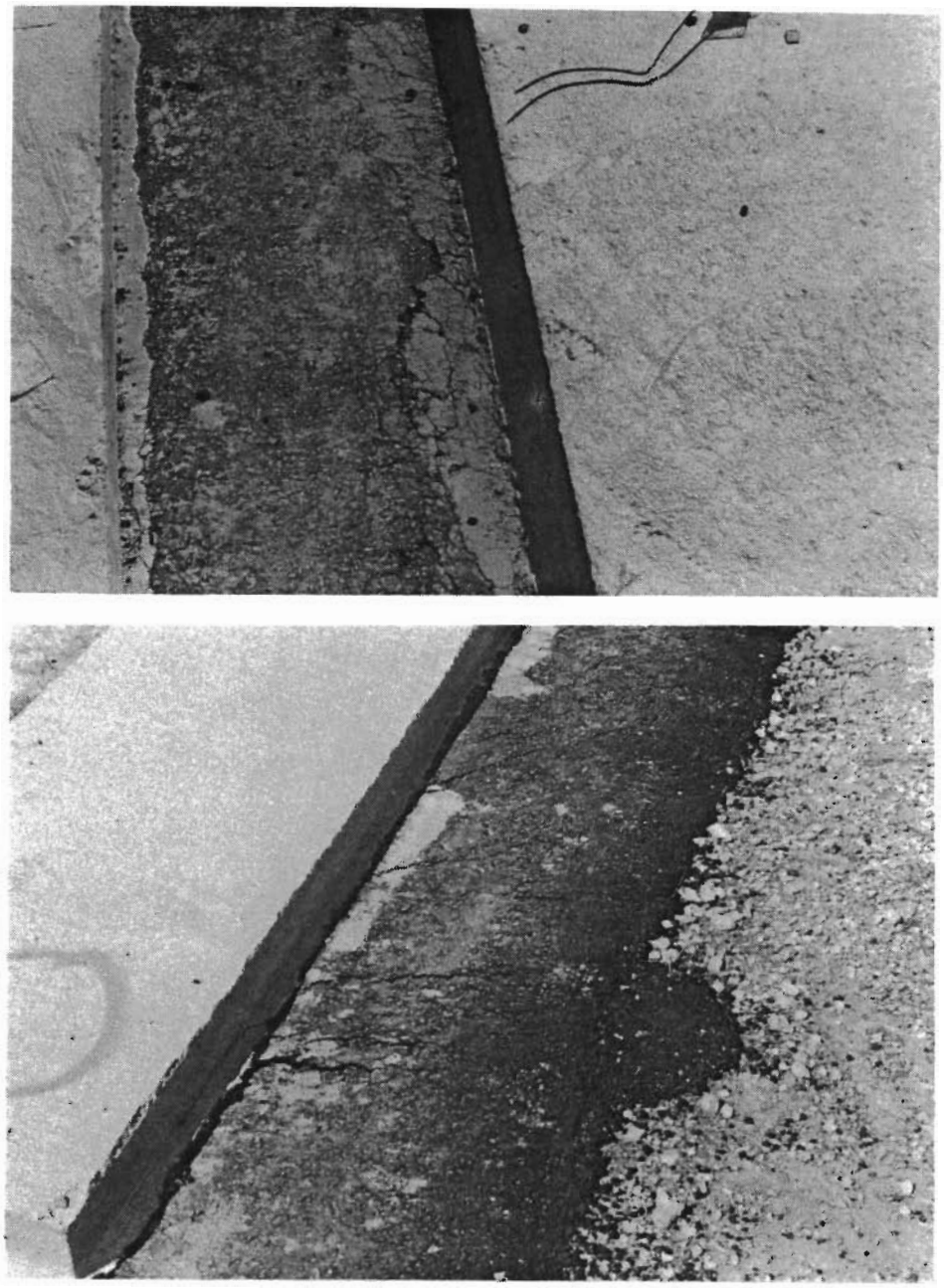

Fig 7.2. ***Failure in 2-inch-thick layer.***

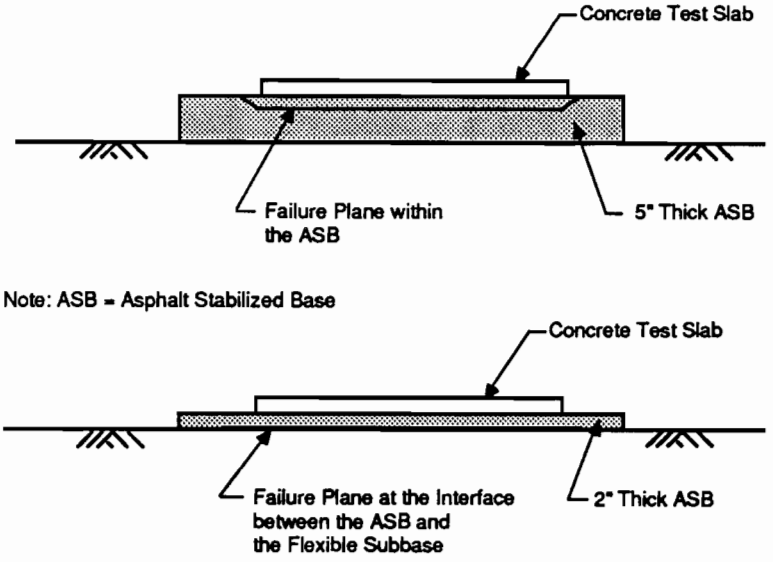

Fig 7.3. ***Resulting failure planes within the layers.***

and placement of a stabilized subbase is not as rigidly controlled as that of the concrete. In addition, certain subbases may be produced, for example, by using different aggregate types or aggregate gradations and varying contents of cement or lime.

A factor to consider in further testing, especially for asphalt–stabilized materials, is the temperature at which the cores are tested. As in the push-off tests for asphalt–stabilized subbases, a range of temperatures should be used in testing, or, when push-off tests are correlated with the indirect tensile test, both experiments should be conducted at the same temperature, preferably at a temperature at which the cores would not decompact.

Nevertheless, the results, though preliminary, are somewhat promising. More research should definitely be pursued in this area.

CRCP COMPUTER MODEL CORRELATION RESULTS

From the results of this correlation, the CRCP computer model does predict actual crack spacing very well. The differences between actual and predicted crack spacings can probably be negated by more accurate input data. For example, the soil support factor was kept constant at 640 pcf. However, lime-treated clay may not offer as much support as an asphalt–stabilized subbase or a cement–stabilized subbase. In addition, the flexible subbases used under certain CRCP highways may not consist of the same limestone aggregate that Wesevich et al tested in the first phase of the study. More accurate tensile strength curves for concrete should be used. The thermal coefficient for coarse aggregate types also varies, and it is possible that not all of the pavements had 0.6 percent steel with a steel thermal coefficient of 6.5×10^{-6}. Finally, a more accurate frictional restraint-movement curve for cement–stabilized subbases would have been more desirable.

CHAPTER 8. IMPLICATIONS OF THE FINDINGS FROM THIS STUDY

This chapter discusses the implications of the subbase frictional information from this project by using conceptual results from the PCP1 computer program developed by the Center for Transportation Research on a plain jointed concrete pavement containing limestone aggregate.

BACKGROUND

As shown in Chapter 5, the subbase frictional effect was a somewhat significant factor in the crack spacing of CRCP pavements in Texas, though not as important as the coarse aggregate types and tensile strengths of the pavements. However, jointed pavements and prestressed pavements are much more susceptible to the effects of subbase friction.

Using the frictional data generated from this study, the PCP1 program developed for prestressed pavement design produced tensile stress data for plain concrete slabs containing limestone aggregate. The output from this program is not intended to mirror what actually occurs in the field; it is, rather, used for comparative purposes to show the effect of frictional resistance on concrete pavement tensile stresses.

The purpose of the output from the PCP1 program is to show when the maximum tensile strength of the concrete is reached due to the frictional effect of the subbase. Therefore, slab lengths of 75 feet to 1000 feet were used so that the program could generate data for comparison.

PCP1 PROGRAM INPUT

The program generated results for five subbases - cement–stabilized subbase, lime–treated clay subbase, flexible subbase, asphalt–stabilized subbase, and unbound shell subbase. The properties were kept constant for the soil support and the concrete pavement, including 8–inch–thick pavements, 4.00 x 10^{-6} thermal coefficients, a 640 pci support value, and 9000 psi compressive strengths at 28 days. This design did not use any steel, and, as a result, the pavement was not prestressed.

The frictional restraint-movement data generated from this project's push-off testing was used as data input for all five subbases, up to their maximum frictional restraints. However, the maximum restraints were used for pavement movements exceeding the movements at the maximum frictional restraints. The shape of the resulting frictional restraint-movement curves is conceptually shown in Fig 8.1. Though this is not what actually occurred in the push–off tests, this was done for consistency, since the program could generate only reasonable values for the cement–stabilized subbase input in this format. The output, then, most likely overestimates the tensile stresses for this pavement design.

A 250–foot slab length was used for the asphalt–stabilized and flexible subbases. A 500–foot length had to be used for lime–treated clay, since the 400 psi tensile strength value was not reached for a slab length of 250 feet. The same problem was encountered for 250–foot and 500–foot slab lengths on the unbound shell subbase, and, to achieve tensile stress values above 400 psi, the length on that subbase was extended to 1000 feet. However, a 75–foot slab length had to be used for the cement–stabilized subbase, because the program could not handle any longer lengths since this subbase's frictional effect was so large.

This output results from an inputted 40-degree drop in slab temperature, from 90 degrees (the concrete curing temperature) to 50 degrees. There was a zero temperature differential between the top and bottom surfaces of the slabs.

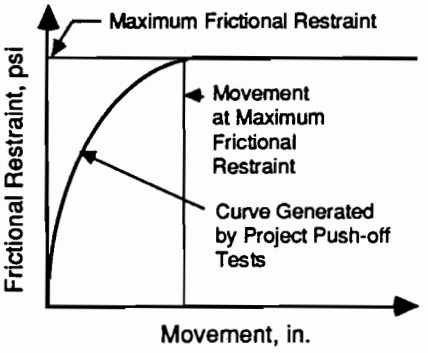

Fig 8.1. ***Conceptual frictional restraint movement curve for the subbases entered into the PCP1 program.***

RESULTS

The results of the program output are graphically shown in Fig 8.2, which shows that the 400 psi maximum tensile stress value was reached at 15 feet for the cement–stabilized subbase, around 79 feet for the flexible subbase, about 85 feet for the asphalt–stabilized subbase, approximately 154 feet for the lime–treated clay, and 380 feet for the unbound shell subbase. This means that the cement–stabilized subbase can cause approximately a twenty-five-fold increase in

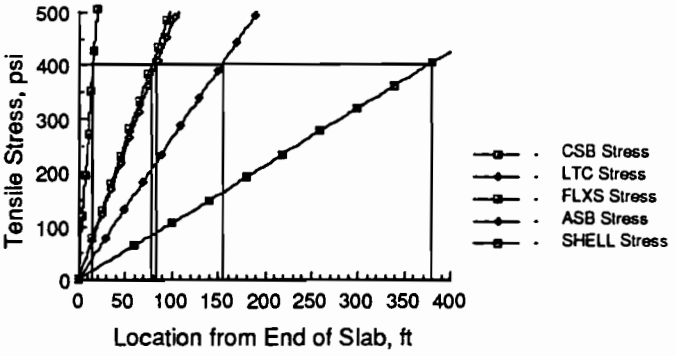

Fig 8.2. ***Tensile stress versus slab location.***

tensile stresses over the stresses caused by the unbound shell subbase, a tenfold increase over the lime–treated clay, and around a fivefold increase over the asphalt and lime–stabilized subbases at the same slab location for this pavement design.

Possible joint spacings can also be derived from this graph by multiplying the above values by a factor of two. This, in essence, is putting two ends of a long slab together to make a smaller slab with a maximum tensile stress of approximately 400 psi at the center. So, theoretically, joint spacings of 30, 160, 170, 300, and 760 feet can be achieved on cement–stabilized, flexible, asphalt–stabilized, lime–treated clay, and unbound shell subbases, respectively, using this design. However, ratios of the spacings can be helpful to find comparative joint spacings for conditions other than those input into the PCP1 program. For example, say that joint spacings of 30 feet have been found to be desirable for jointed pavements overlying asphalt–stabilized subbases. Using the joint spacings from the computer data, the resulting ratios are 1 to 0.19 for asphalt–stabilized subbase to cement–stabilized subbase; 1 to 0.94 for asphalt–stabilized subbase to flexible subbase; 1 to 1.8 for asphalt–stabilized subbase to lime–treated clay subbase; and 1 to 4.5 for asphalt–stabilized subbase to unbound shell subbase. Multiplying these resulting values by 30 feet generates the joint spacings shown in Fig 8.3. It is surprising that the cement–stabilized subbase causes such a relatively small joint spacing.

From the graph, it seems imperative that some sort of effective friction reducer be used between jointed and prestressed pavements and cement–stabilized subbases, as is the current practice. It would also explain why several concrete pavements overlying untreated cement–stabilized subbases have excessive amounts of cracks and punchouts. The results also show the very significant effect that frictional resistance, along with traffic loads, can have on pavement tensile stresses.

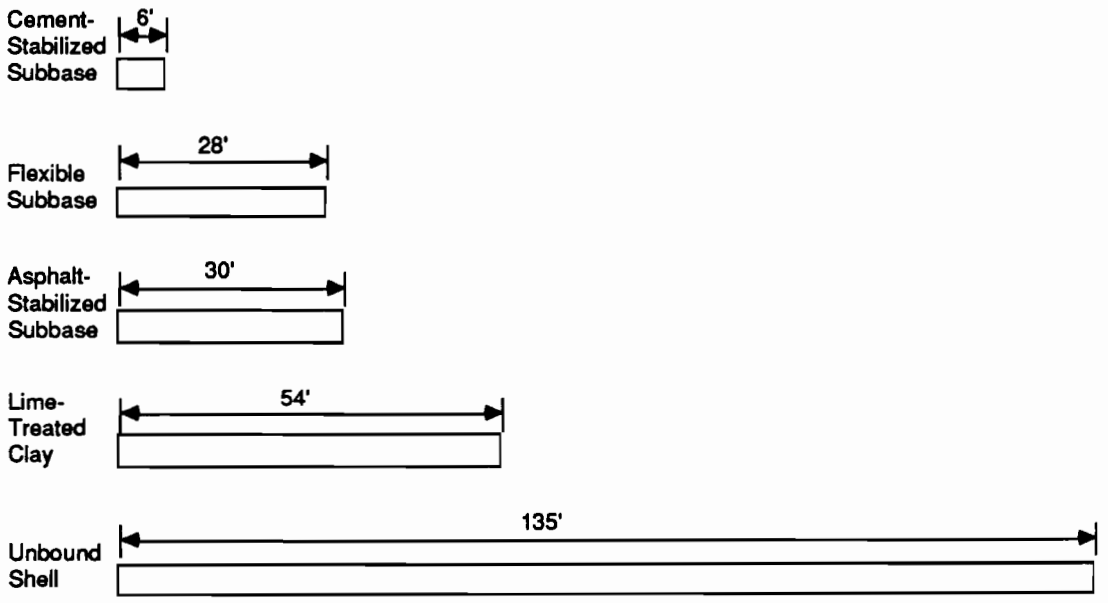

Fig 8.3. ***Comparative joint spacings from the computed results.***

CHAPTER 9. CONCLUSIONS AND RECOMMENDATIONS

CONCLUSIONS FROM THIS REPORT

1. For the Texas Specification Type "D" Asphalt Pavement subbase used in this report:
   (a) Texture was not significant in the frictional restraint.
   (b) Depth of the subbase layer can affect frictional restraint.
   (c) Higher temperatures decreased the frictional resistance; lower temperatures increased the resistance.
   (d) Overburden pressure, i.e., slab thickness, did not significantly affect frictional resistance.
   (e) For a subbase layer of 2 inches, the failure plane was at the interface between the subbase and the underlying material.
   (f) For a subbase layer of 5 inches, the failure plane was within the subbase.
2. The CRCP computer program, given proper concrete pavement and subbase data input, can predict actual crack spacing in the concrete pavement.
3. The indirect tensile test can be viable in estimating frictional resistance if a large number of cores are tested for each subbase that is considered for frictional properties. An example equation is presented in Fig 6.3.
4. According to the PCA Study for the FHWA, texture on a bituminous–coated cement–stabilized subbase material with a poor friction reducer, such as a 1/16–inch sand skin, can affect frictional resistance. However, when an effective friction reducer is used, such as polyethylene, texture is not a factor.
5. Subbase friction does have an effect on the performance of continuously reinforced concrete pavements, but such pavements are more sensitive to concrete coarse aggregate type and tensile strength.
6. For jointed concrete pavements, a cement–stabilized subbase can cause almost a twenty–five-fold increase in tensile stresses over the stresses caused by an unbound shell subbase, a tenfold increase over the lime-treated clay, and around a fivefold increase over the asphalt and lime–stabilized subbases at the same slab location.

RECOMMENDATIONS

1. For future push–off tests, shorter slabs should be used, such as the 4-foot by 4-foot by 6–inch slabs used in the PCA report for the FHWA discussed in this report.
2. If push–off testing is conducted on thick layers of asphalt–stabilized subbases, it is likely that the subbase cannot take any bearing pressure. If anchors are used for loading the slabs, the holes excavated for the anchors should significantly extend into the material under the subbase.
3. More testing needs to be done on asphalt–stabilized subbases for a range of temperature values, since the temperature of the subbase affects its material properties and, thus, its frictional resistance.
4. More research should be done in the indirect tensile test correlation to frictional resistance. It is also recommended for this test that asphalt–stabilized subbase cores be tested under a range of temperatures.
5. If texture on stabilized subbase materials is to be considered in the future, another method of texturing should be considered, since the wedge-hammer method used in this report was time consuming and cumbersome. Rotomilling and varying the aggregate gradation of the subbase are suggested methods for asphalt–stabilized and cement–stabilized subbases.
6. If more research is to be done in correlating actual crack spacing to predicted crack spacing using the CRCP computer model, more accurate data concerning the concrete pavement and reinforcing steel properties should be used.

MAJOR CONCLUSIONS FROM CENTER FOR TRANSPORTATION RESEARCH REPORT 459-1 (REF 6)

1. The magnitude of frictional resistance and the point at which sliding occurs vary from subbase to subbase.
2. The addition of stabilizing agents to a subbase will offer higher frictional resistance and the point at which sliding occurs will be a smaller movement as compared to that for an unbound subbase.
3. The magnitude of subbase friction is dependent on three components, namely bearing, shear, and adhesion at the slab-subbase interface.
4. If the adhesion component is high enough, the failure plane at sliding will not be at the slab-subbase interface but within the subbase. This holds true for all stabilized subbases tested in this project.
5. The failure plane at sliding will be at the slab-subbase interface for loose unbound subbases.
6. If failure occurs within the subbase as it does for stabilized subbases, frictional information can be looked at as a two-dimensional stress analysis, where the shearing is only slightly influenced by the overburden pressure supplied by slab weight.
7. If failure occurs at the slab-subbase interface, then the magnitude of frictional resistance is directly dependent on slab weight.

8. A coefficient of friction can be used in design of concrete pavements for determining frictional resistances for loose unbound subbases but not for stabilized subbases.
9. Subbase friction for stabilized subbases must be determined by a friction-movement profile obtained through a push-off test.
10. Push-off tests should be repeated over time because it is known that the initial test will yield higher frictional resistances than will result under steady-state conditions.

REFERENCES

1. Goldbeck, A. T., "Friction Tests of Concrete on Various Subbases," *Public Roads*, United States Department of Agriculture, July 1924.
2. Timms, A. G., "Evaluating Subbase Friction Reducing Mediums for Rigid Pavements," *Highway Research Record 60*, Highway Research Board, Washington, D. C., 1963.
3. McCullough, B. Frank, and Alberto Mendoza, "Report on a Mechanistic Analysis of the PCC Aprons at King Fahd International Airport, Kingdom of Saudi Arabia," Austin Research Engineers, October 1985.
4. "Methods For Reducing Friction Between Concrete Slabs and Cement-Treated Subbases," an unpublished report by the Cement and Concrete Research Institute (a division of the Portland Cement Association) for the Federal Highway Administration, September 1971.
5. Stott, J. P., "Tests on Materials for Use as Sliding Layers Under Concrete Road Slabs," Road Research Laboratory, DSIR, 1961.
6. Wesevich, J. W., B. F. McCullough, and N. H. Burns, "Stabilized Subbase Friction Study for Concrete Pavements," Research Report 459-1, Center for Transportation Research, The University of Texas at Austin, November 1987.
7. Hadley, W. O., T. W. Kennedy, and W. R. Hudson, "An Evaluation of Factors Affecting the Tensile Properties of Asphalt-Treated Materials," Research Report 98-2, Center for Highway Research, The University of Texas at Austin, March 1969.
8. Pendola, H. J., T. W. Kennedy, and W. R. Hudson, "Evaluation of Factors Affecting the Tensile Properties of Cement-Treated Materials," Research Report 98-3, Center for Highway Research, The University of Texas at Austin, September 1969.
9. Miller, S. P., T. W. Kennedy, and W. R. Hudson, "An Evaluation of Factors Affecting the Tensile Properties of Lime-Treated Materials," Research Report 98-4, Center for Highway Research, The University of Texas at Austin, March 1970.
10. Bertrand, Carl, "CTR Project 422 and 472 Notes," Center for Transportation Research, The University of Texas at Austin, February 1987.
11. Information was obtained from a conversation with Mr. W. V. Ward (Former District Engineer for Texas State Department of Highways and Public Transportation District 12, and an inspector at the facility when it was constructed), Center for Transportation Research, The University of Texas at Austin, October 1987.
12. *Plans for Houston Urban Expressways: Interurban Expressway From 700 West of Scott Street to St. Bernard Street, U.S. Highway No. 75, Harris County*, State of Texas State Highway Department and Mitchell & Hunt Consulting Engineers, August 1946.
13. *Highway Design Division Operations and Procedures Manual, Appendix A*, Texas State Department of Highways and Public Transportation, June 1986 revision.
14. Correlation values were obtained from Mr. J. N. Anagnos, Research Associate, Center for Transportation Research, The University of Texas at Austin, June 1987. The equation and the indirect tensile test are discussed in Anagnos, J. N., and T. W. Kennedy, "Practical Method of Conducting the Indirect Tensile Test," Research Report 98-10, Center for Highway Research, The University of Texas at Austin, August, 1972.
15. Machado, J. P., B. F. McCullough, and H. J. Williamson, "Continuously Reinforced Concrete Pavement: Prediction of Distress Quantities," Research Report 177-8, Center for Highway Research, The University of Texas at Austin, March 1977 (unpublished).

APPENDIX A. INDIRECT TENSILE STRENGTH RESULTS FROM CENTER FOR HIGHWAY RESEARCH PROJECT 98

TABLE A.1. INDIRECT TENSILE STRENGTH DATA FOR ASPHALT TREATED SPECIMENS (REF 7)

Specimen Number	Indirect Tensile Strength (psi)	Horizontal Failure Deformation	Specimen Number	Indirect Tensile Strength (psi)	Horizontal Failure Deformation
20	74.5	0.0100	55	23.9	0.0076
21	108.4	0.0064	56	13.5	0.0154
22	105.1	0.0056	57	30.9	0.0098
23	65.5	0.0074	58	41.5	0.0102
24	60.7	0.0098	59	82.8	0.0064
25	62.9	0.0136	60	65.6	0.0078
26	80.5	0.0072	61	54.6	0.0136
27	35.9	0.0080	62	50.8	0.0078
28	29.8	0.0144	63	25.5	0.0034
29	37.0	0.0052	64	83.0	0.0062
30	15.6	0.0073	90	30.2	0.0070
31	14.3	0.0088	66	29.2	0.0068
32	95.7	0.0112	67	53.5	0.0102
89	111.3	0.0164	68	43.6	0.0064
34	148.5	0.0040	69	43.2	0.0064
35	82.9	0.0068	70	120.4	0.0068
36 *	91.5	0.0184	88	191.3	0.0056
37 *	82.3	0.0218	72	169.4	0.0068
38	127.8	0.0176	73	117.1	0.0126
39	156.3	0.0114	74	82.8	0.0190
40	133.5	0.0178	75 *	124.2	0.0132
41	69.4	0.0210	76 *	126.7	0.0140
42	137.7	0.0093	77	73.4	0.0262
43	134.3	0.0106	78	55.5	0.0228
44	120.1	0.0077	79	149.0	0.0176
45	131.2	0.0122	80	231.3	0.0090
46	185.0	0.0051	81	179.8	0.0170
47	158.7	0.0044	82	78.8	0.0282
48	166.5	0.0068	83	129.2	0.0128
49	85.8	0.0254	84 *	195.1	0.0052
50	122.5	0.0190	85 *	204.9	0.0065
51	148.1	0.0124	86	116.7	0.0180
52	125.0	0.0180	87	107.2	0.0072
53 *	7.6	0.0090			
54 *	12.8	0.0092			

*Duplicate specimens.

TABLE A.2. INDIRECT TENSILE STRENGTH DATA FOR CEMENT TREATED SPECIMENS (REF 8)

Specimen Number	Indirect Tensile Strength (psi)	Specimen Number	Indirect Tensile Strength (psi)
1	34.7	46	74.3
2	126.4	47	113.7
3	20.3	48	39.4
4	174.6	49	72.2
5	14.3	50	225.4
6	248.9	51	272.5
7	123.3	52	243.3
8	140.5	53	25.3
9	212.0	54	238.0
10	257.2	55	91.6
11	174.6	56	242.6
12	90.5	57	103.1
13 *	139.0	58	111.3
14	39.3	59	187.7
15	54.1	60	101.9
16	50.0	61	84.9
17	268.9	62 *	206.5
18 *	252.0	63	105.7
19	57.8	64	183.5
20	66.6	65	40.4
21	103.8	66 *	190.5
22	237.9	67	137.6
23	290.7	68	60.4
24	197.5	69	99.6
25	366.5	70	32.3
26	260.2	71 *	202.6
27	157.5	72	134.0
28	115.6	73	283.2
29	431.8	74	70.9
30 *	129.3	75 *	127.7
31	118.0	76	114.8
32	80.8	77	70.5
33	89.8	78	212.9
34	44.0	79	37.0
35	169.6	80 *	145.4
36	74.2	81	102.1
37	41.6	82	139.8
38	68.0	83	221.7
39	364.1	84	57.0
40	57.7	85	162.4
41	86.4	86	131.1
42	27.0	87	45.2
43	316.0	88	169.4
44	41.1	89	251.8
45	53.7	90	100.1
91	375.2	136	102.8
92	196.8	137	122.6
93	117.1	138	113.4
94	47.1	139	106.9
95	41.4	140	147.2
96	44.8	141	48.0
97	175.8	142	77.0
98	96.0	143	132.9
99	385.3	144	159.1
100	63.7	145 *	82.3
101	26.0	146	147.5
102	497.1	147	55.0
103	54.3	148	207.4
104 *	70.9	149	113.9
105	259.2	150 *	74.5
106	71.8	151	122.0
107	41.1	152	170.3
108	374.3	153	128.2
109	254.1	154	365.1
110	106.3	155 *	93.5
111	245.6	156	197.8
112	54.7	157	104.5
113 *	105.6	158	26.4
114	63.8	159	59.5
115 *	98.1	160	74.7
116	108.5	161	192.3
117	98.0	162	37.0
118	283.3	163	123.0
119	62.0	164	13.1
120	40.6	165	303.8
121	93.1	166	247.5
122 *	136.8	167	291.2
123	115.5	168	108.3
124	63.7	169	73.1
125	30.9	170	40.4
126	127.1	171	42.0
127	227.6	172	146.4
128	142.4	173	233.5
129	157.8	174	43.6
130	495.5	175	162.9
131	39.6	176 *	92.4
132	88.0	177	280.2
133	50.3	178	252.8
134	125.9	179	68.0
135	180.3	180	22.4

*Duplicate specimen.

(continued)

*Duplicate specimen.

TABLE A.3. INDIRECT TENSILE STRENGTH DATA FOR LIME TREATED CLAY SPECIMENS (REF 9)

Specimen Number*	Indirect Tensile Strength (psi)	Specimen Number*	Indirect Tensile Strength (psi)	Specimen Number*	Indirect Tensile Strength (psi)
1 ***	318	21	73	40 **	66
2 **	115	22	259	41 ***	150
3 **	75	23	120	42	124
4	160	24	45	43	64
6 ***	68	25	68	44	56
7	36	26	83	45	32
9	36	28	46	46	25
10	73	29	50	47	33
11	59	30	42	49	65
12	63	31	74	50	98
13	58	32	56	51	97
14 ***	92	33	178	52	75
15	29	35 **	70	53	89
17	101	36 **	43	54	24
18	43	37	92	55	33
19	28	38	109	56	50
20 **	26	39	19	57	46

* Treatment combinations for each specimen given in Ref 9.

** Duplicate specimens.

*** These values are from replacement specimens (Ref 9).

APPENDIX B. RESULTS OF THE PUSH-OFF TESTS ON ASPHALT CONCRETE PAVEMENT AT THE BALCONES RESEARCH CENTER

TABLE B.1. PUSH-OFF TEST, 7 IN. SIMULATED SLAB ON 5 IN. ASPHALT PAVEMENT WITH ROUGH TEXTURE

Push-off Test No.: 1 BRC
Date: 8-11-1987
Subbase: 5" Asphalt
Slab Area: 4032 in.^{2}
Slab Thickness: 7" Simulated
Texture: Rough

Time (Hr:Min)	Load (klps)	Ram Pressure (ksi)	Horizontal Movement (in.)	Vertical Movement (in.)	Slab Temp. (°F)	Frictional Resistance (psi)	μ
16:33	0.850	0.100	0.0000	0.0000	115.124	0.211	0.361
16:34	1.583	0.300	0.0002	0.0001	114.980	0.393	0.673
16:34	2.924	0.600	0.0011	0.0000	114.998	0.725	1.243
16:35	4.259	0.850	0.0030	0.0008	114.998	1.056	1.811
16:35	6.023	1.200	0.0053	0.0021	115.052	1.494	2.561
16:35	7.896	1.550	0.0080	0.0038	115.070	1.958	3.357
16:35	8.782	1.850	0.0132	0.0069	115.214	2.178	3.734
16:36	10.777	2.100	0.0183	0.0106	115.250	2.673	4.582
16:36	11.583	2.350	0.0283	0.0176	115.232	2.873	4.925
16:36	13.009	2.500	0.0355	0.0252	115.268	3.226	5.531
16:36	12.536	2.500	0.0474	0.0363	115.286	3.109	5.330
16:37	12.399	2.550	0.0563	0.0470	115.340	3.075	5.272
16:37	12.315	2.500	0.0651	0.0587	115.304	3.054	5.236
16:37	12.005	2.500	0.0756	0.0723	115.286	2.977	5.104
16:38	12.078	2.500	0.0920	0.0918	115.160	2.996	5.135
16:38	11.143	2.300	0.1165	0.1223	115.070	2.764	4.738
16:38	10.242	2.050	0.1447	0.1743	115.088	2.540	4.355
16:39	8.279	1.600	0.2060	0.2858	115.016	2.053	3.520
16:39	6.635	1.300	0.2840	0.3663	114.908	1.646	2.821
16:39	5.624	1.100	0.3812	0.1721	114.872	1.395	2.391
16:40	4.642	0.900	0.4877	0.1963	114.854	1.151	1.974
16:40	3.976	0.800	0.5818	0.2053	114.854	0.986	1.690

TABLE B.2. PUSH-OFF TEST, 3-1/2-IN. SLAB ON 5-IN. ASPHALT PAVEMENT WITH ROUGH TEXTURE

Push-off Test No.: 4 BRC
Date: 8-11-1987
Subbase: 5" Asphalt
Slab Area: 4032 in.^{2}
Slab Thickness: 3 1/2"
Texture: Rough

Time (Hr:Min)	Load (kips)	Ram Pressure (ksi)	Horizontal Movement (in.)	Vertical Movement (in.)	Slab Temp. (°F)	Frictional Resistance (psi)	μ
16:09	0.817	0.000	0.0000	0.0000	114.944	0.203	0.695
16:09	1.462	0.250	0.0000	0.0001	114.962	0.363	1.243
16:10	2.789	0.500	0.0000	0.0002	115.016	0.692	2.372
16:10	4.116	0.800	0.0015	0.0007	115.070	1.021	3.500
16:10	5.271	1.100	0.0057	0.0022	115.052	1.307	4.482
16:10	7.341	1.500	0.0115	0.0060	115.088	1.821	6.242
16:11	9.413	1.900	0.0199	0.0119	115.052	2.335	8.004
16:11	10.901	2.200	0.0322	0.0202	115.034	2.704	9.270
16:11	11.477	2.300	0.0488	0.0310	115.106	2.846	9.759
16:12	11.506	2.300	0.0620	0.0428	115.124	2.854	9.784
16:12	10.964	2.200	0.0729	0.0506	115.232	2.719	9.323
16:12	10.768	2.100	0.0824	0.0580	115.304	2.671	9.156
16:13	10.225	2.000	0.0933	0.0656	115.286	2.536	8.695
16:13	10.082	1.900	0.1058	0.0742	115.304	2.500	8.573
16:13	9.748	1.800	0.1166	0.0823	115.196	2.418	8.289
16:13	9.305	1.700	0.1280	0.0925	115.214	2.308	7.912
16:14	8.829	1.600	0.1438	0.1042	115.232	2.190	7.508
16:14	8.058	1.500	0.1574	0.1179	115.142	1.999	6.852
16:14	7.491	1.400	0.1804	0.1351	115.160	1.858	6.370
16:14	6.649	1.300	0.2083	0.1619	115.008	1.649	5.654
16:15	5.527	1.100	0.2583	0.2117	114.872	1.371	4.700
16:15	4.160	0.950	0.3298	0.2477	114.728	1.032	3.537
16:15	2.719	0.900	0.4329	0.2715	114.872	0.674	2.312
16:16	1.846	2.000	0.4521	0.2482	114.944	0.458	1.570

TABLE B.3. PUSH-OFF TEST, 3-1/2-IN. SLAB ON 5-IN. ASPHALT PAVEMENT WITH SMOOTH TEXTURE

Push-off Test No.: 5 BRC
Date: 8-11-1987
Subbase: 5" Asphalt
Slab Area: 4032 in.^{2}
Slab Thickness: 3 1/2"
Texture: Smooth

Time (Hr:Min)	Load (kips)	Ram Pressure (ksi)	Horizontal Movement (in.)	Vertical Movement (in.)	Slab Temp. (°F)	Frictional Resistance (psi)	μ
15:05	0.188	0.000	0.0000	0.0000	115.034	0.047	0.160
15:07	0.985	0.120	0.0000	0.0000	115.052	0.244	0.838
15:07	1.485	0.250	0.0001	-0.0001	115.070	0.368	1.263
15:07	2.111	0.400	0.0001	0.0000	115.034	0.524	1.795
15:08	3.000	0.600	0.0001	0.0002	115.016	0.744	2.551
15:08	3.594	0.750	0.0004	0.0008	114.908	0.891	3.056
15:08	4.544	1.000	0.0016	0.0015	114.908	1.127	3.864
15:09	5.400	1.100	0.0036	0.0024	114.890	1.339	4.592
15:09	6.304	1.300	0.0060	0.0034	114.908	1.563	5.361
15:09	7.783	1.600	0.0095	0.0053	114.890	1.930	6.618
15:10	8.576	1.800	0.0150	0.0085	114.908	2.127	7.293
15:10	9.293	1.900	0.2060	0.0128	114.890	2.305	7.902
15:10	9.986	2.000	0.0266	0.0184	114.818	2.477	8.491
15:11	9.854	2.100	0.0365	0.0251	114.890	2.444	8.379
15:11	9.890	2.100	0.0494	0.0335	114.908	2.453	8.410
15:12	10.212	2.100	0.0663	0.0396	114.980	2.533	8.684
15:12	9.102	2.000	0.0777	0.0498	114.998	2.257	7.740
15:12	9.296	2.000	0.0866	0.0576	114.998	2.306	7.905
15:13	8.966	1.900	0.0951	0.0655	115.052	2.224	7.624
15:13	8.461	1.700	0.1028	0.0738	115.034	2.098	7.195
15:14	8.144	1.500	0.1099	0.0833	115.070	2.020	6.925
15:15	7.367	1.400	0.1282	0.1073	115.214	1.827	6.264
15:15	7.568	1.400	0.1401	0.1228	115.268	1.877	6.435

TABLE B.4. PUSH-OFF TEST, 3-1/2-IN. SLAB ON 5-IN. ASPHALT PAVEMENT WITH MEDIUM TEXTURE

Push-off Test No.: 6 BRC
Date: 8-11-1987
Subbase: 5" Asphalt
Slab Area: 4032 in.^{2}
Slab Thickness: 3 1/2"
Texture: Medium

Time (Hr:Min)	Load (kips)	Ram Pressure (ksi)	Horizontal Movement (in.)	Vertical Movement (in.)	Slab Temp. (°F)	Frictional Resistance (psi)	μ
17:29	0.596	0.060	0.0000	0.0000	113.882	0.148	0.507
17:30	1.107	0.200	0.0003	0.0000	113.738	0.275	0.941
17:31	1.782	0.350	0.0010	0.0001	113.630	0.442	1.515
17:31	3.450	0.750	0.0024	0.0006	113.594	0.856	2.934
17:31	5.479	1.400	0.0047	0.0036	113.648	1.359	4.659
17:31	7.268	1.600	0.0064	0.0065	113.684	1.803	6.180
17:32	8.753	2.000	0.0088	0.0101	113.738	2.171	7.443
17:32	10.117	2.300	0.0122	0.0143	113.756	2.509	8.603
17:32	11.468	2.700	0.0161	0.0193	113.594	2.844	9.752
17:32	11.715	2.800	0.0215	0.0272	113.486	2.906	9.962
17:33	11.464	2.500	0.0264	0.0367	113.522	2.843	9.748
17:33	11.308	2.700	0.0323	0.0484	113.540	2.805	9.616
17:33	11.640	2.800	0.0404	0.0625	113.594	2.887	9.898
17:34	11.318	2.500	0.0484	0.0739	113.558	2.807	9.624
17:34	10.201	2.500	0.0611	0.0992	113.486	2.530	8.674
17:35	9.716	2.200	0.0683	0.1117	113.540	2.410	8.262
17:35	10.267	2.400	0.1056	0.1517	113.504	2.546	8.730
17:36	9.638	2.100	0.1484	0.2047	113.180	2.390	8.196
17:36	9.129	1.900	0.2006	0.2658	113.072	2.264	7.763
17:36	7.360	1.500	0.2502	0.3683	113.126	1.825	6.259
17:37	4.900	1.500	0.3184	0.4430	113.180	1.215	4.167
17:37	2.842	3.000	0.3578	0.4433	113.306	0.705	2.417

TABLE B.5. PUSH-OFF TEST, 7-IN. SIMULATED SLAB ON 2-IN. ASPHALT PAVEMENT WITH ROUGH TEXTURE

Push-off Test No.: 7 BRC
Date: 8-12-1987
Subbase: 2" Asphalt
Slab Area: 4032 in. ^{2}
Slab Thickness: 7" Simulated
Texture: Rough

Time (Hr:Min)	Load (kips)	Ram Pressure (ksi)	Horizontal Movement (in.)	Vertical Movement (in.)	Slab Temp. (°F)	Frictional Resistance (psi)	μ
17:43	0.453	0.14	0.0000	0.0000	110.174	0.112	0.193
17:43	0.991	0.28	0.0000	0.0000	110.318	0.246	0.421
17:44	1.951	0.48	0.0000	0.0000	110.336	0.484	0.830
17:44	2.971	0.68	0.0004	0.0002	110.336	0.737	1.263
17:44	4.019	0.90	0.0012	0.0005	110.390	0.997	1.709
17:44	5.221	1.12	0.0025	0.0012	110.336	1.295	2.220
17:45	6.090	1.28	0.0040	0.0021	110.300	1.510	2.589
17:45	7.207	1.50	0.0063	0.0036	110.264	1.787	3.064
17:45	8.302	1.68	0.0103	0.0068	110.318	2.059	3.530
17:45	8.932	1.80	0.0162	0.0116	110.390	2.215	3.798
17:46	9.561	1.90	0.0229	0.0176	110.300	2.371	4.065
17:46	9.757	1.90	0.0337	0.0273	110.246	2.420	4.148
17:46	9.277	1.88	0.0535	0.0414	110.102	2.301	3.944
17:47	9.040	1.75	0.0739	0.0498	110.192	2.242	3.844
17:47	8.719	1.62	0.0959	0.0644	110.174	2.162	3.707
17:47	7.372	1.50	0.1270	0.0824	110.264	1.828	3.134
17:47	7.231	1.40	0.1537	0.0950	110.372	1.793	3.074
17:48	6.866	1.28	0.1957	0.1100	110.372	1.703	2.919
17:48	6.083	1.16	0.2420	0.1215	110.390	1.509	2.586
17:48	5.596	1.06	0.2897	0.1319	110.408	1.388	2.379
17:48	5.281	1.00	0.3294	0.1372	110.300	1.310	2.245
17:49	5.150	0.98	0.3840	0.1459	110.264	1.277	2.190
17:49	7.481	0.90	0.4348	0.1551	110.228	1.855	3.181
17:49	4.366	0.78	0.5998	0.1347	110.210	1.083	1.856
17:50	3.98	0.70	0.6888	-0.0699	110.228	0.987	1.692

TABLE B.6. PUSH-OFF TEST, 7-IN. SIMULATED SLAB ON 2-IN. ASPHALT PAVEMENT WITH SMOOTH TEXTURE

Push-off Test No.: 8 BRC
Date: 8-12-1987
Subbase: 2" Asphalt
Slab Area: 4032 in.^{2}
Slab Thickness: 7" Simulated
Texture: Smooth

Time (Hr:Min)	Load (kips)	Ram Pressure (ksi)	Horizontal Movement (in.)	Vertical Movement (in.)	Slab Temp. (°F)	Frictional Resistance (psi)	μ
16:48	0.723	0.06	0.0000	0.0000	112.550	0.179	0.307
16:48	2.308	0.40	0.0003	0.0002	112.568	0.572	0.981
16:48	4.069	0.80	0.0013	0.0008	112.550	1.009	1.730
16:49	6.614	1.28	0.0066	0.0042	112.586	1.640	2.812
16:49	8.194	1.60	0.0148	0.0098	112.748	2.007	3.441
16:49	9.692	1.90	0.0251	0.0205	112.694	2.404	4.121
16:49	10.251	1.90	0.0390	0.0359	112.766	2.542	4.358
16:50	9.882	1.80	0.0698	0.0556	112.802	2.451	4.202
16:50	8.115	1.50	0.1242	0.0949	112.874	2.013	3.450
16:50	6.782	1.20	1.1998	0.1196	112.892	1.682	2.884
16:51	5.777	1.10	0.2629	0.1363	112.928	1.433	2.456
16:51	5.253	0.90	0.3195	0.1472	113.054	1.303	2.233
16:51	4.767	0.90	0.3917	-0.0777	113.036	1.182	2.027
16:51	4.309	0.80	0.4500	-0.0713	113.144	1.069	1.832

TABLE B.7. PUSH-OFF TEST, 7-IN. SIMULATED SLAB ON 2-IN. ASPHALT PAVEMENT WITH MEDIUM TEXTURE

Push-off Test No.: 9 BRC
Date: 8-12-1987
Subbase: 2" Asphalt
Slab Area: 4032 in.^{2}
Slab Thickness: 7" Simulated
Texture: Medium

Time (Hr:Min)	Load (kips)	Ram Pressure (ksi)	Horizontal Movement (in.)	Vertical Movement (in.)	Slab Temp. (°F)	Frictional Resistance (psi)	μ
15:40	1.099	0.180	0.0000	0.0000	113.504	0.273	0.467
15:42	2.130	0.480	0.0001	-0.0001	113.486	0.528	0.906
15:43	3.324	0.740	0.0004	-0.0001	113.522	0.824	1.413
15:43	4.878	1.100	0.0013	0.0000	113.612	0.210	2.074
15:43	6.684	1.500	0.0027	0.0006	113.792	1.658	2.842
15:44	7.370	1.700	0.0043	0.0016	113.810	1.828	3.134
15:44	8.217	1.900	0.0058	0.0026	113.810	2.038	3.494
15:45	8.907	2.000	0.0084	0.0046	113.774	2.209	3.787
15:45	9.814	2.200	0.0139	0.0097	113.828	2.434	4.173
15:45	10.336	2.300	0.0258	0.0206	113.828	2.563	4.395
15:45	9.960	2.200	0.0428	0.0325	113.756	2.470	4.235
15:46	9.887	2.100	0.0636	0.0427	113.450	2.452	4.204
15:46	9.905	2.000	0.0930	0.0527	113.432	2.457	4.211
15:47	9.305	1.750	0.1279	0.0604	113.486	2.308	3.956
15:47	8.421	1.600	0.1682	0.0635	113.504	2.089	3.580
15:47	7.365	1.500	0.1999	0.0605	113.396	1.827	3.131
15:48	6.380	1.400	0.2315	0.0579	113.360	1.582	2.713
15:48	5.344	1.100	0.2988	-0.0087	113.360	1.325	2.272
15:48	4.180	0.700	0.3764	-0.0408	113.270	1.037	1.777

TABLE B.8. PUSH-OFF TEST, 3-1/2-IN. SLAB ON 2-IN. ASPHALT PAVEMENT WITH ROUGH TEXTURE

Push-off Test No.: 10 BRC
Date: 8-12-1987
Subbase: 2" Asphalt
Slab Area: 4032 in.^{2}
Slab Thickness: 3 1/2" Simulated
Texture: Rough

Time (Hr:Min)	Load (kips)	Ram Pressure (ksi)	Horizontal Movement (in.)	Vertical Movement (in.)	Slab Temp. (°F)	Frictional Resistance (psi)	μ
18:03	0.415	0.180	0.0000	0.0000	109.796	0.103	0.353
18:04	1.093	0.340	0.0000	0.0000	109.688	0.271	0.929
18:04	2.191	0.540	0.0002	0.0002	109.706	0.543	1.863
18:04	2.878	0.720	0.0010	0.0004	106.616	0.714	2.447
18:05	3.614	0.880	0.0021	0.0007	109.634	0.896	3.073
18:05	4.375	1.020	0.0040	0.0013	109.598	1.085	3.720
18:05	5.973	1.380	0.0088	0.0035	109.598	1.481	5.079
18:05	6.703	1.520	0.0133	0.0062	109.562	1.662	5.700
18:06	7.218	1.620	0.0187	0.0032	109.526	1.790	6.138
18:06	7.728	1.740	0.0247	0.0094	109.490	1.917	6.571
18:06	8.045	1.800	0.0319	0.0182	109.418	1.995	6.841
18:06	8.240	1.820	0.0402	0.0298	109.418	2.044	7.007
18:07	9.263	1.920	0.0501	0.0461	109.472	2.297	7.877
18:07	7.616	1.700	0.0660	0.0759	109.490	1.889	6.476
18:07	6.919	1.600	0.0813	0.0901	109.400	1.716	5.884
18:07	5.994	1.500	0.0969	0.1169	109.454	1.487	5.097
18:08	5.239	1.400	0.1127	0.1372	109.364	1.299	4.455
18:08	5.573	1.300	0.1242	0.1511	109.544	1.382	4.739
18:08	5.180	1.200	0.1407	0.1652	109.508	1.285	4.405
18:09	4.918	1.160	0.1562	0.1715	109.508	1.220	4.182
18:09	4.595	1.060	0.1720	0.1830	109.472	1.140	3.907
18:09	4.419	0.980	0.1866	0.1951	109.490	1.096	3.758
18:10	4.336	0.940	0.2043	0.2073	109.490	1.075	3.687
18:11	4.159	0.820	0.2578	0.2337	109.508	1.007	3.452
18:11	3.869	0.800	0.2973	0.2519	109.562	0.960	3.290

TABLE B.9. PUSH-OFF TEST, 3-1/2" SLAB ON 2" ASPHALT PAVEMENT WITH SMOOTH TEXTURE

Push-off Test No.: 11 BRC
Date: 8-12-1987
Subbase: 2" Asphalt
Slab Area: 4032 in.^{2}
Slab Thickness: 3 1/2"
Texture: Smooth

Time (Hr:Min)	Load (kips)	Ram Pressure (ksi)	Horizontal Movement (in.)	Vertical Movement (in.)	Slab Temp. (°F)	Frictional Resistance (psi)	μ
17:18	0.474	0.060	0.0000	0.0000	111.092	0.118	0.403
17:18	0.865	0.120	0.0000	0.0000	110.948	0.215	0.736
17:18	1.560	0.280	0.0002	0.0000	110.840	0.387	1.327
17:19	2.623	0.500	0.0006	0.0002	110.768	0.651	2.230
17:19	3.652	0.720	0.0032	0.0016	110.912	0.906	3.105
17:19	4.270	0.850	0.0088	0.0043	110.894	1.059	3.631
17:19	5.065	1.000	0.0156	0.0070	110.912	1.256	4.307
17:20	5.715	1.100	0.0200	0.0093	111.020	1.417	4.860
17:20	6.210	1.220	0.0240	0.0111	111.074	1.540	5.281
17:20	6.525	1.400	0.0286	0.0146	111.056	1.618	5.548
17:20	6.668	1.300	0.0352	0.0191	111.020	1.654	5.670
17:21	6.479	1.200	0.0424	0.0232	111.092	1.607	5.509
17:21	6.266	1.220	0.0506	0.0267	111.110	1.554	5.328
17:21	6.020	1.200	0.0575	0.0314	111.200	1.493	5.119
17:21	5.732	1.000	0.0644	0.0343	111.128	1.422	4.874
17:22	5.470	1.000	0.0756	0.0388	111.056	1.357	4.651
17:22	5.765	0.900	0.0863	0.0423	111.002	1.430	4.902
17:23	5.574	0.900	0.1037	0.0466	110.768	1.380	4.740
17:23	5.246	0.800	0.1159	0.0493	110.558	1.301	4.461

TABLE B.10. PUSH-OFF TEST, 3-1/2-IN. SLAB ON 2-IN. ASPHALT PAVEMENT WITH MEDIUM TEXTURE

Push-off Test No.: 12 BRC
Date: 8-12-1987
Subbase: 2" Asphalt
Slab Area: 4032 in.^{2}
Slab Thickness: 3 1/2"
Texture: Medium

Time (Hr:Min)	Load (kips)	Ram Pressure (ksi)	Horizontal Movement (in.)	Vertical Movement (in.)	Slab Temp. (°F)	Frictional Resistance (psi)	μ
16:17	0.530	0.060	0.0000	0.0000	112.946	0.131	0.451
16:19	1.623	0.320	0.0011	-0.0002	113.036	0.403	1.380
16:19	2.589	0.560	0.0016	-0.0002	113.000	0.642	2.202
16:20	3.044	0.640	0.0020	-0.0002	113.000	0.755	2.588
16:20	4.013	0.820	0.0031	0.0000	113.036	0.995	3.412
16:20	4.581	1.000	0.0051	0.0007	113.036	1.136	3.895
16:21	5.979	1.300	0.0075	0.0017	113.180	1.483	5.084
16:21	6.777	1.460	0.0145	0.0064	113.180	1.681	5.763
16:21	6.974	1.600	0.0262	0.0142	113.216	1.730	5.930
16:21	8.061	1.700	0.0341	0.0208	113.126	1.999	6.855
16:22	9.310	1.900	0.0472	0.0351	113.198	2.309	7.917
16:22	9.318	1.800	0.0643	0.0529	113.216	2.311	7.923
16:22	8.925	1.820	0.0781	0.0664	113.270	2.214	7.589
16:23	8.853	1.800	0.0981	0.0877	113.288	2.196	7.528
16:23	8.303	1.800	0.1231	0.1086	113.306	2.059	7.060
16:23	8.838	1.700	0.1495	0.1288	113.018	2.192	7.515
16:23	8.308	1.600	0.1761	0.1472	112.856	2.061	7.065
16:24	7.048	1.400	0.2282	0.1634	112.766	1.748	5.993
16:24	6.448	1.300	0.2715	0.1657	112.892	1.599	5.483
16:25	5.162	1.000	0.3423	-0.0972	112.820	1.280	4.389
16:25	3.989	0.700	0.4274	-0.1274	112.874	0.989	3.392
16:26	3.435	1.400	0.4675	-0.1362	112.982	0.852	2.921

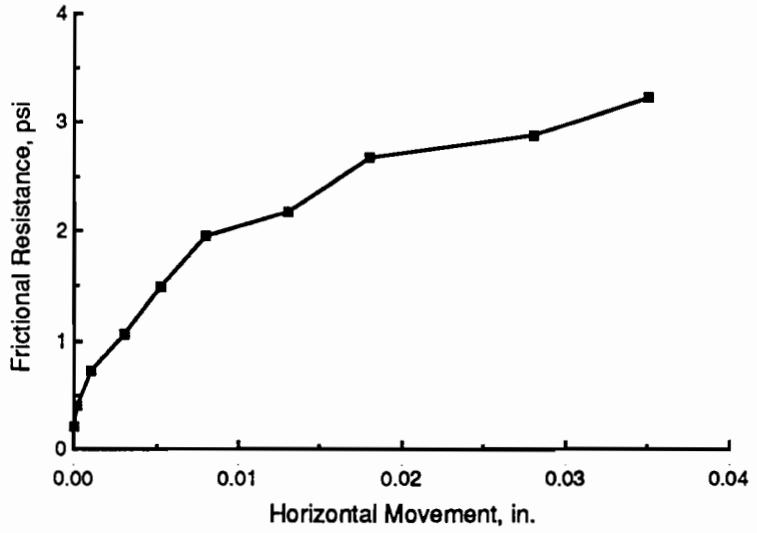

Fig B.1. *Horizontal movement to peak frictional resistance for push-off tests on simulated 7-inch slab over a 5-inch-thick asphalt pavement with a rough texture.*

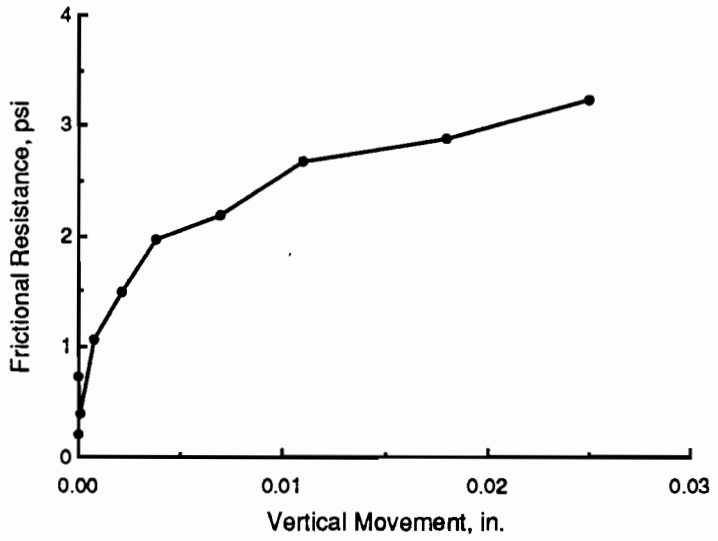

Fig B.2. *Vertical movement to peak frictional resistance for push-off test on 7-inch slab over a 5-inch-thick asphalt pavement with a rough texture.*

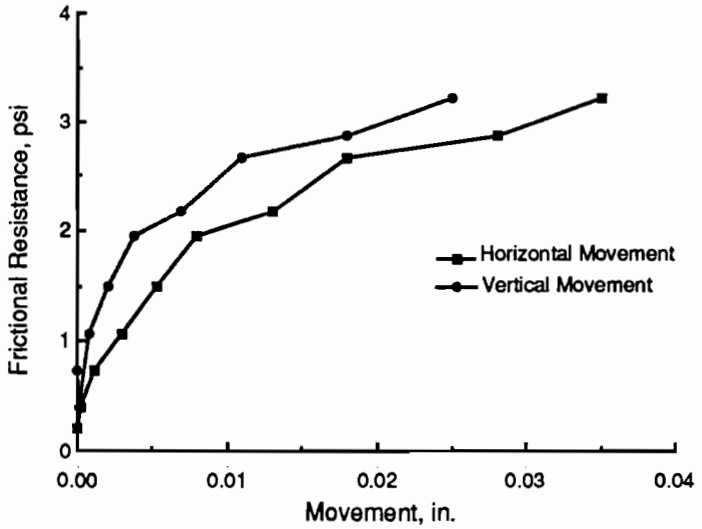

Fig B.3. *Horizontal and vertical movements to peak frictional resistance for push-off test on simulated 7-inch slab over a 5-inch-thick asphalt pavement with a rough texture.*

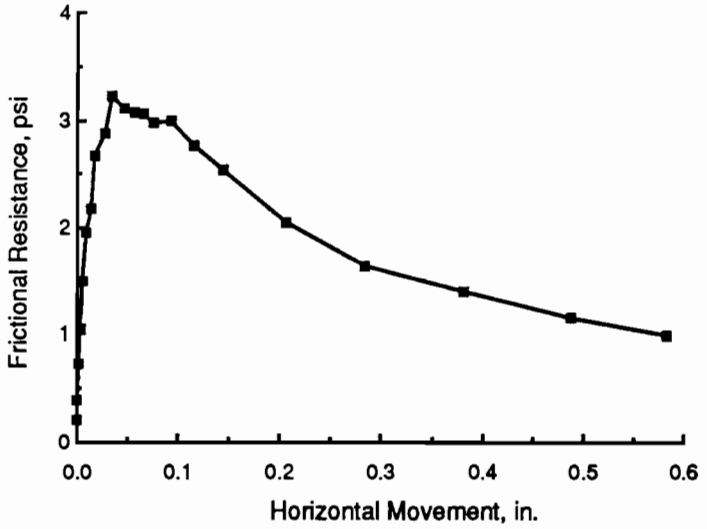

Fig B.4. ***Horizontal movement for push-off test on simulated 7-inch slab over a 5-inch-thick asphalt pavement with a rough texture.***

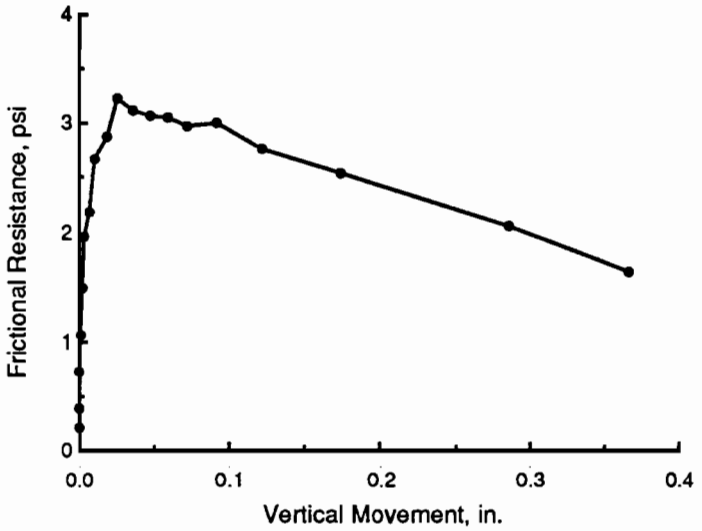

Fig B.5. ***Vertical movement for push-off test on simulated 7-inch slab over a 5-inch-thick asphalt pavement with a rough texture.***

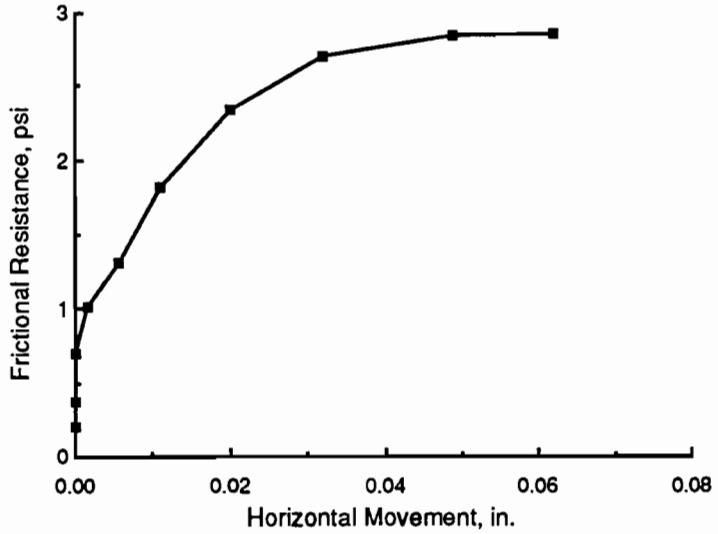

Fig B.6. ***Horizontal movement to peak frictional resistance for push-off tests on 3-1/2-inch slab over a 5-inch-thick asphalt pavement with a rough texture.***

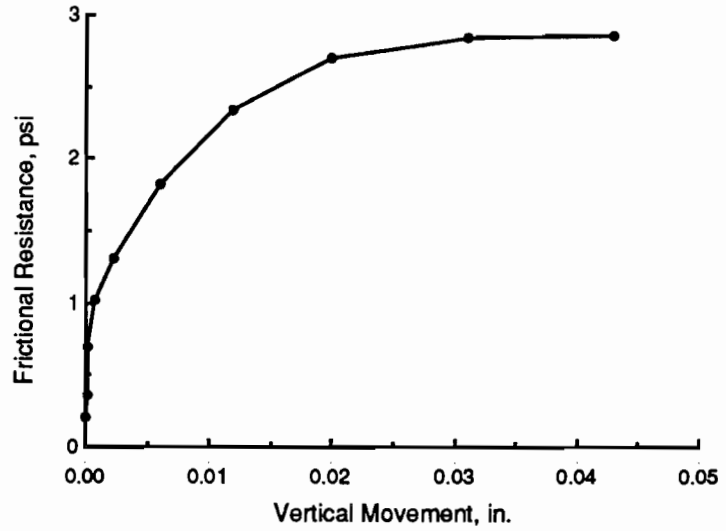

Fig B.7. ***Vertical movement to peak frictional resistance for push-off test on 3-1/2-inch slab over a 5-inch-thick asphalt pavement with a rough texture.***

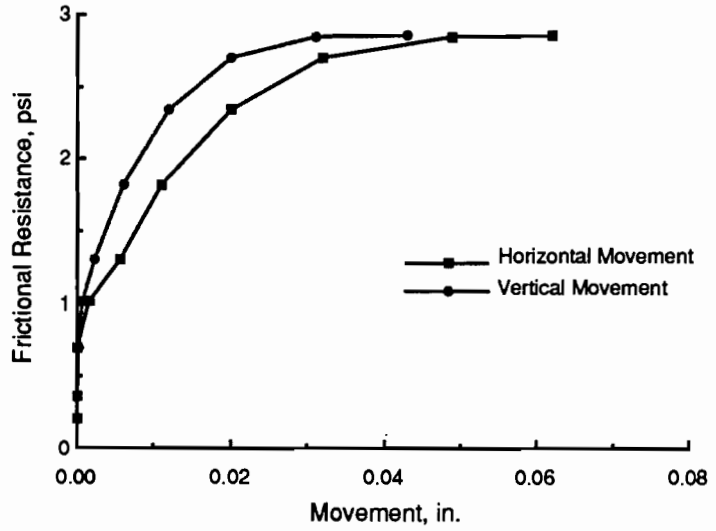

Fig B.8. ***Horizontal and vertical movements to peak frictional resistance for push-off test on 3-1/2-inch slab over a 5-inch-thick asphalt pavement with a rough texture.***

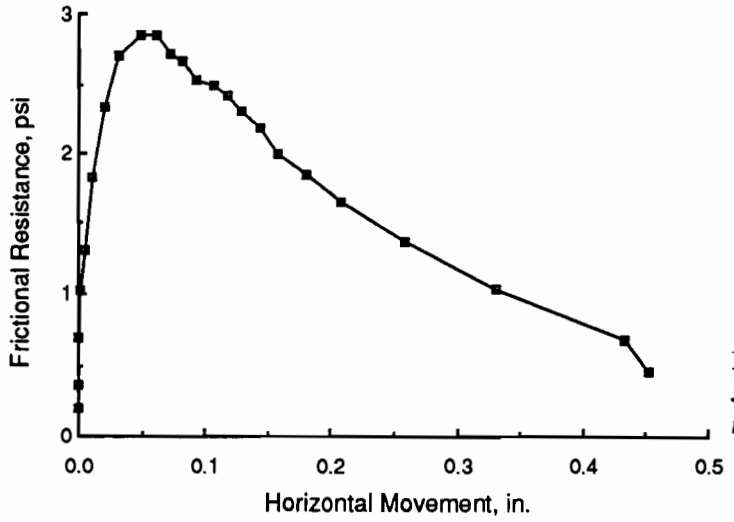

Fig B.9. ***Horizontal movement for push-off test on 3-1/2-inch slab over a 5-inch-thick asphalt pavement with a rough texture.***

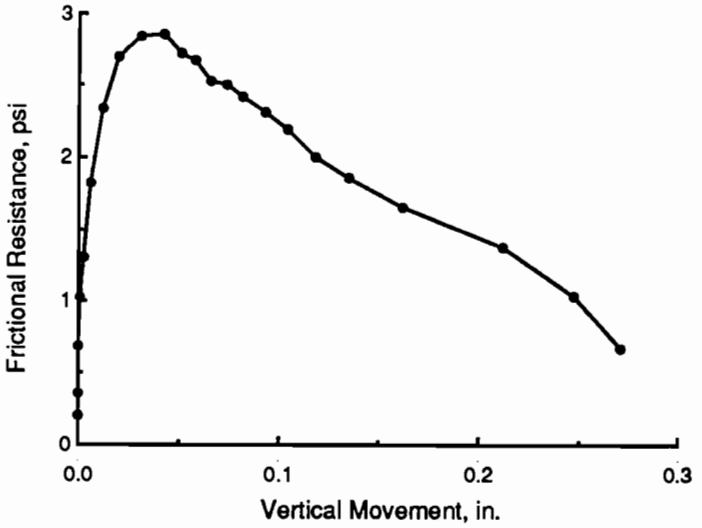

Fig B.10. *Vertical movement for push-off test on 3-1/2-inch slab over a 5-inch-thick asphalt pavement with a rough texture.*

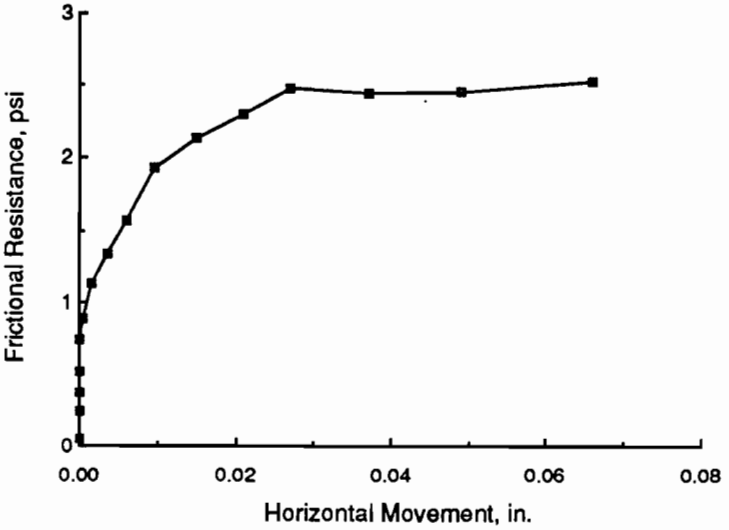

Fig B.11. *Horizontal movement to peak frictional resistance for push-off tests on 3-1/2-inch slab over a 5-inch-thick asphalt pavement with a smooth texture.*

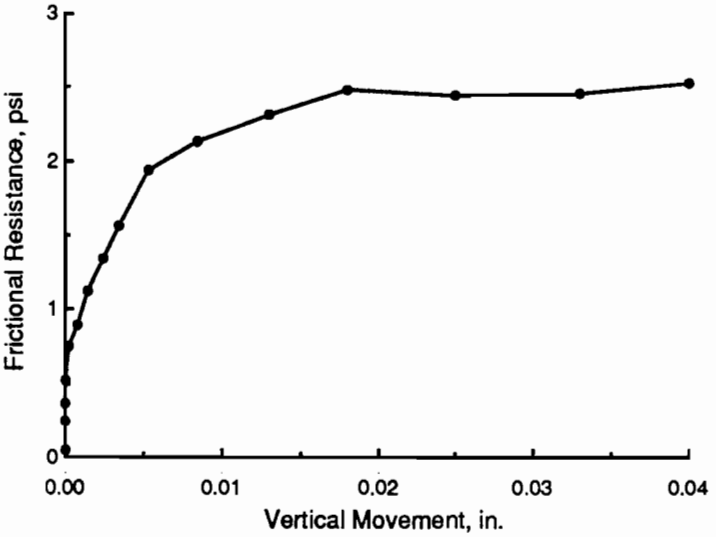

Fig B.12. *Vertical movement to peak frictional resistance for push-off test on 3-1/2-inch slab over a 5-inch-thick asphalt pavement with a smooth texture.*

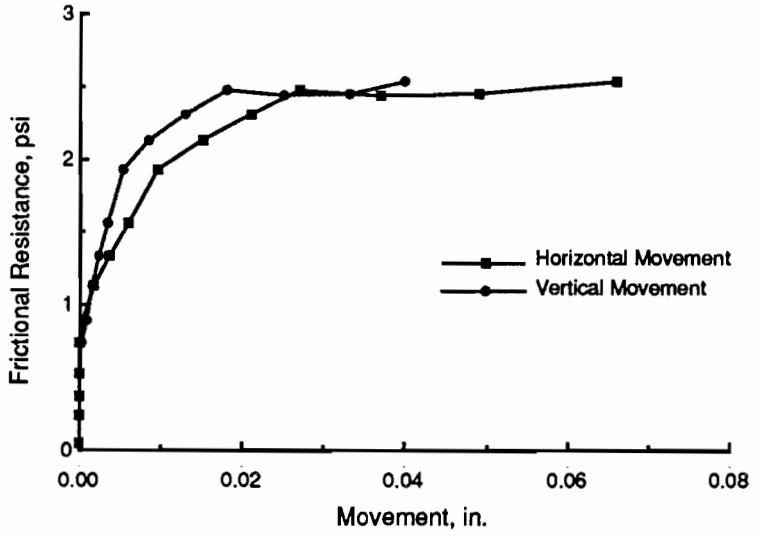

Fig B.13. *Horizontal and vertical movements to peak frictional resistance for push-off test on 3-1/2-inch slab over a 5-inch-thick asphalt pavement with a smooth texture.*

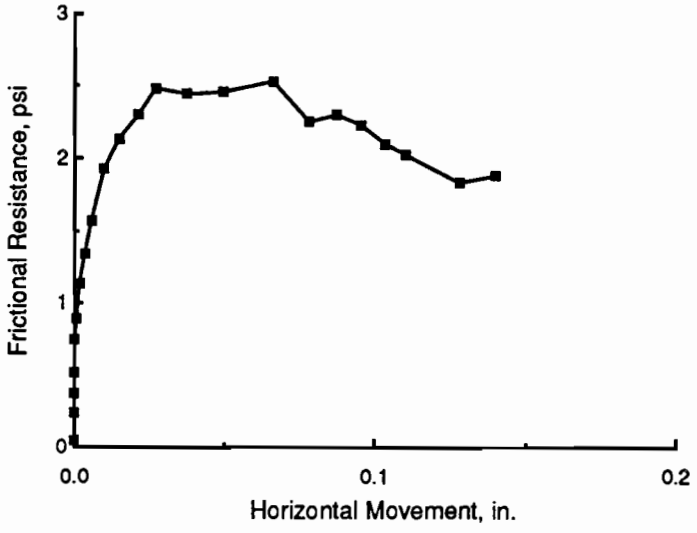

Fig B.14. *Horizontal movement for push-off test on 3-1/2-inch slab over a 5-inch-thick asphalt pavement with a smooth texture.*

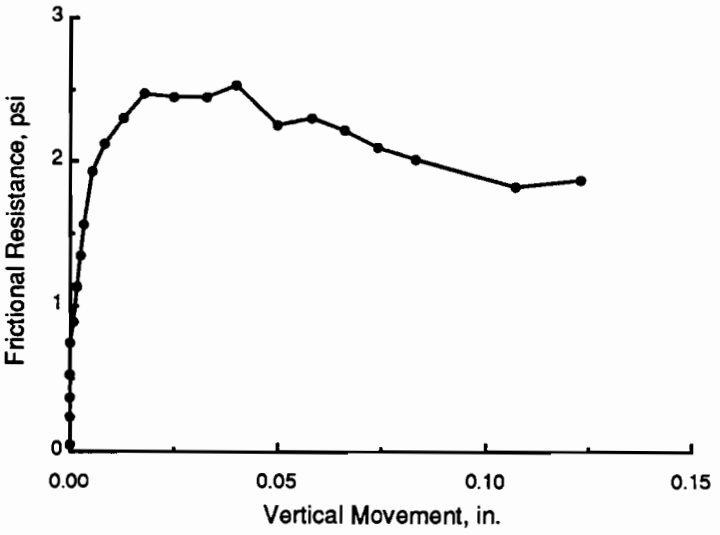

Fig B.15. *Vertical movement for push-off test on 3-1/2-inch slab over a 5-inch-thick asphalt pavement with a smooth texture.*

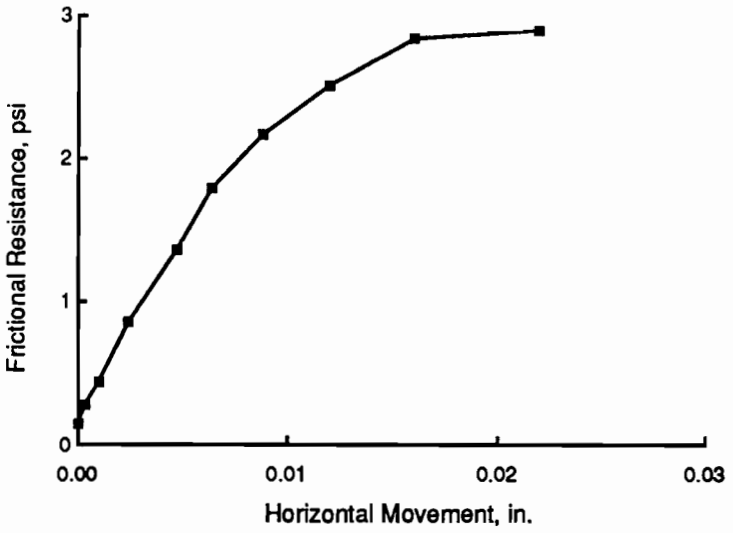

Fig B.16. *Horizontal movement to peak frictional resistance for push-off tests on 3-1/2-inch slab over a 5-inch-thick asphalt pavement with a medium texture.*

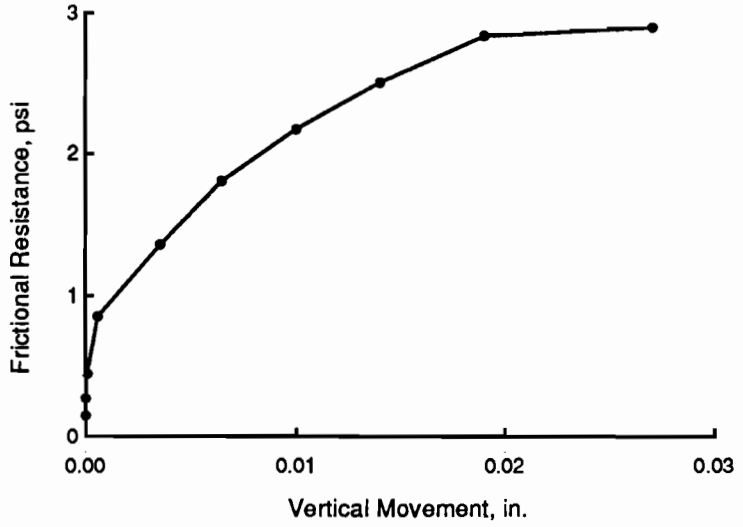

Fig B.17. *Vertical movement to peak frictional resistance for push-off test on 3-1/2-inch slab over a 5-inch-thick asphalt pavement with a medium texture.*

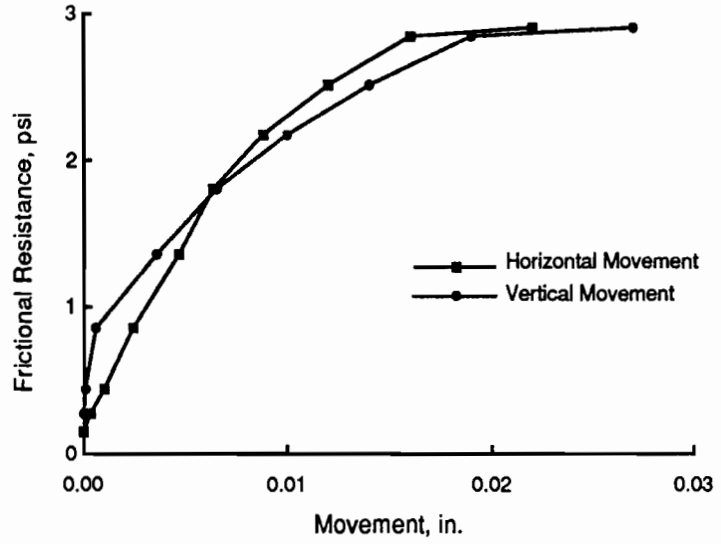

Fig B.18. *Horizontal and vertical movements to peak frictional resistance for push-off test on 3-1/2-inch slab over a 5-inch-thick asphalt pavement with a medium texture.*

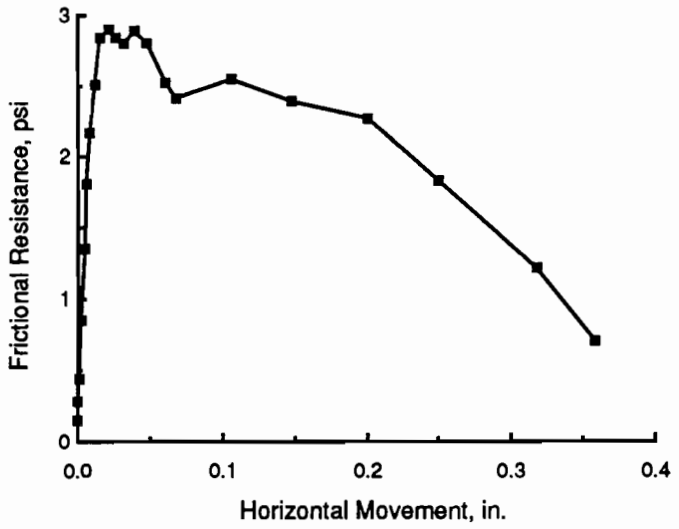

Fig B.19. ***Horizontal movement for push-off test on 3-1/2-inch slab over a 5-inch-thick asphalt pavement with a medium texture.***

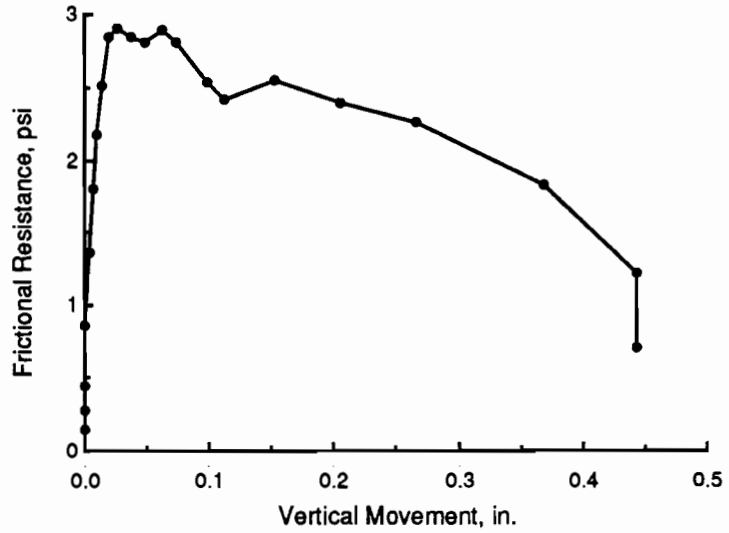

Fig B.20. ***Vertical movement for push-off test on 3-1/2-inch slab over a 5-inch-thick asphalt pavement with a medium texture.***

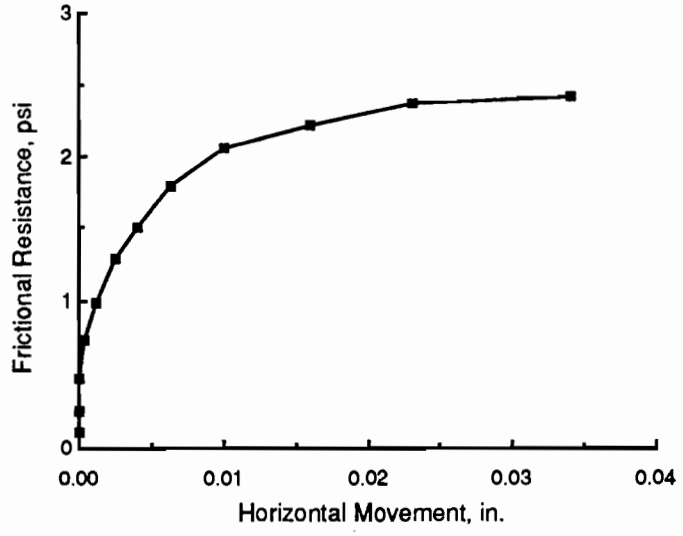

Fig B.21. ***Horizontal movement to peak frictional resistance for push-off tests on simulated 7-inch slab over a 2-inch-thick asphalt pavement with a rough texture.***

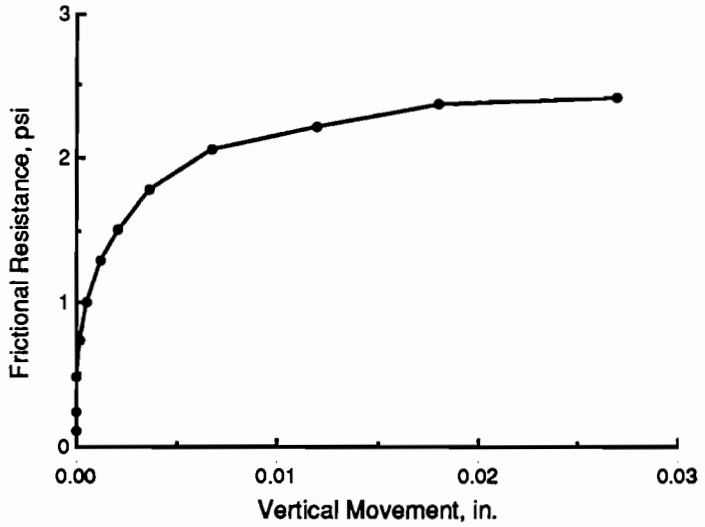

Fig B.22. *Vertical movement to peak frictional resistance for push-off test on simulated 7-inch slab over a 2-inch-thick asphalt pavement with a rough texture.*

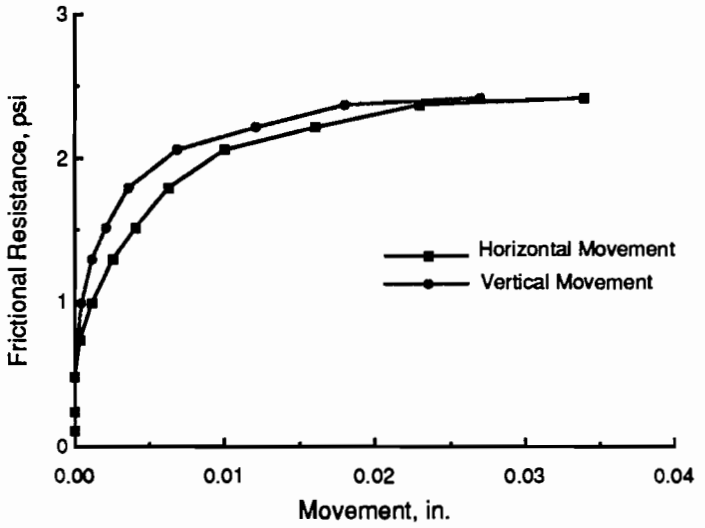

Fig B.23. *Horizontal and vertical movements to peak frictional resistance for push-off test on simulated 7-inch slab over a 2-inch-thick asphalt pavement with a rough texture.*

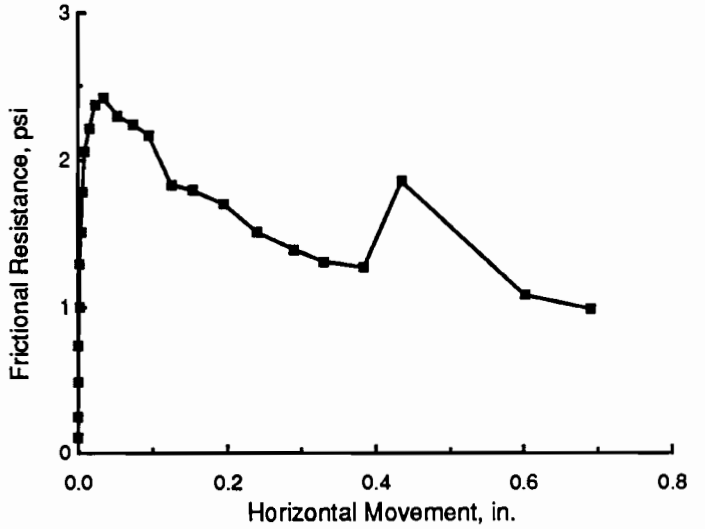

Fig B.24. *Horizontal movement for push-off test on simulated 7-inch slab over a 2-inch-thick asphalt pavement with a rough texture.*

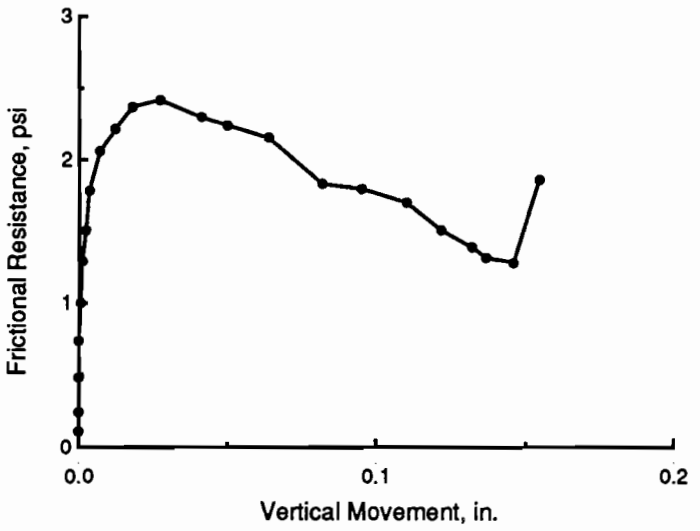

Fig B.25. ***Vertical movement for push-off test on simulated 7-inch slab over a 2-inch-thick asphalt pavement with a rough texture.***

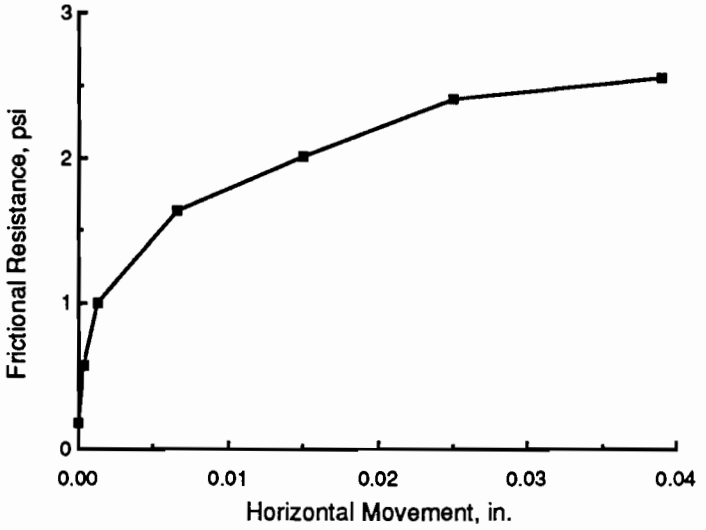

Fig B.26. ***Horizontal movement to peak frictional resistance for push-off tests on simulated 7-inch slab over a 2-inch-thick asphalt pavement with a smooth texture.***

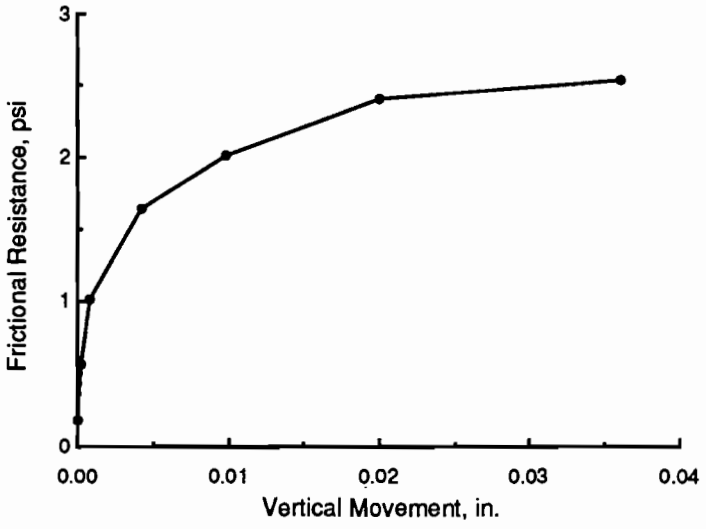

Fig B.27. ***Vertical movement to peak frictional resistance for push-off test on simulated 7-inch slab over a 2-inch-thick asphalt pavement with a smooth texture.***

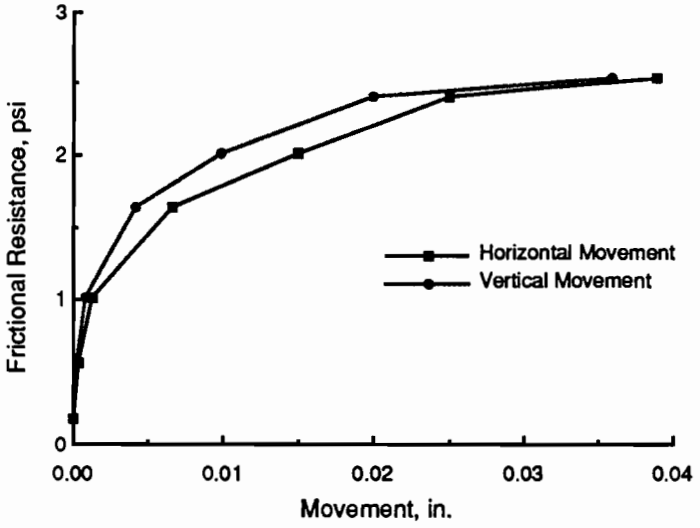

Fig B.28. *Horizontal and vertical movements to peak frictional resistance for push-off test on simulated 7-inch slab over a 2-inch-thick asphalt pavement with a smooth texture.*

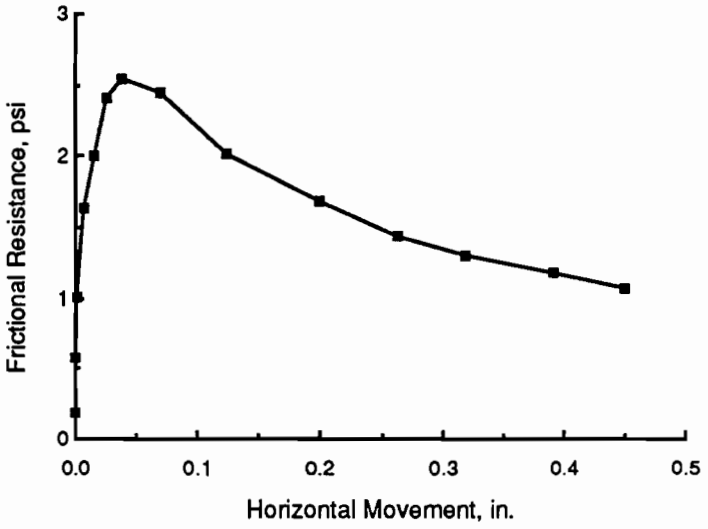

Fig B.29. *Horizontal movement for push-off test on simulated 7-inch slab over a 2-inch-thick asphalt pavement with a smooth texture.*

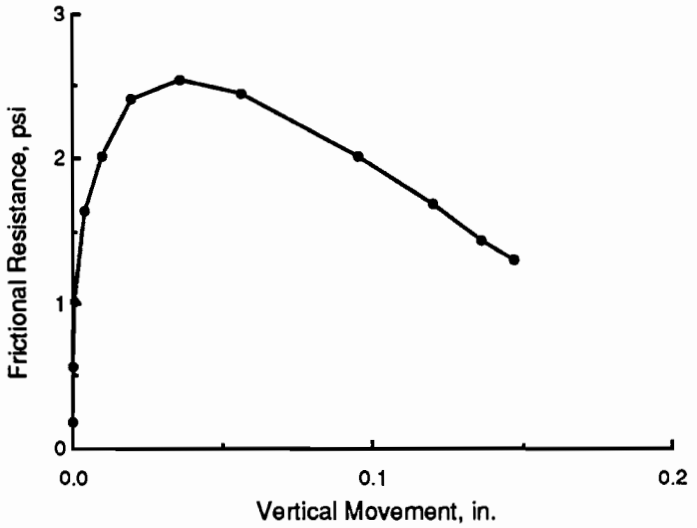

Fig B.30. *Vertical movement for push-off test on simulated 7-inch slab over a 2-inch-thick asphalt pavement with a smooth texture.*

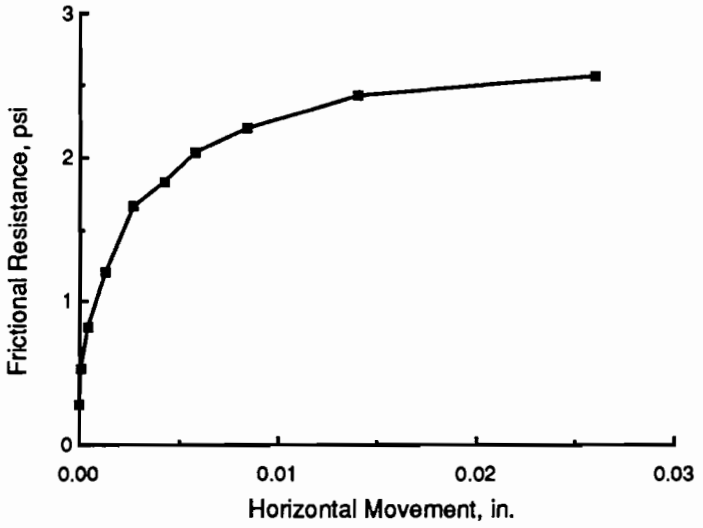

Fig B.31. *Horizontal movement to peak frictional resistance for push-off tests on simulated 7-inch slab over a 2-inch-thick asphalt pavement with a medium texture.*

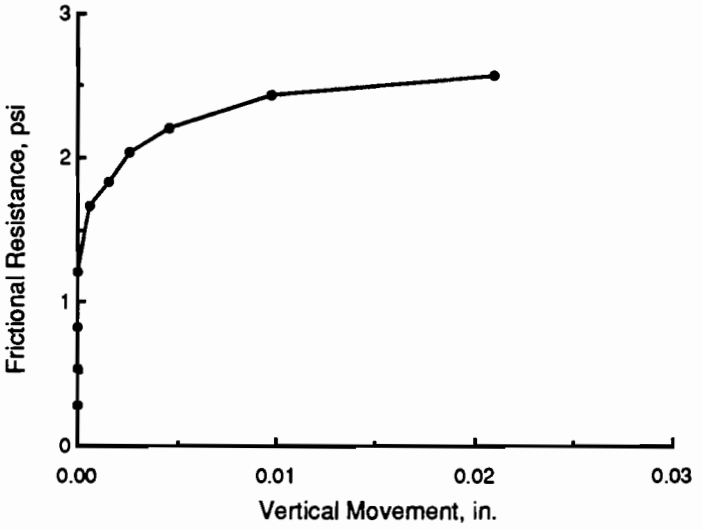

Fig B.32. *Vertical movement to peak frictional resistance for push-off test on simulated 7-inch slab over a 2-inch-thick asphalt pavement with a medium texture.*

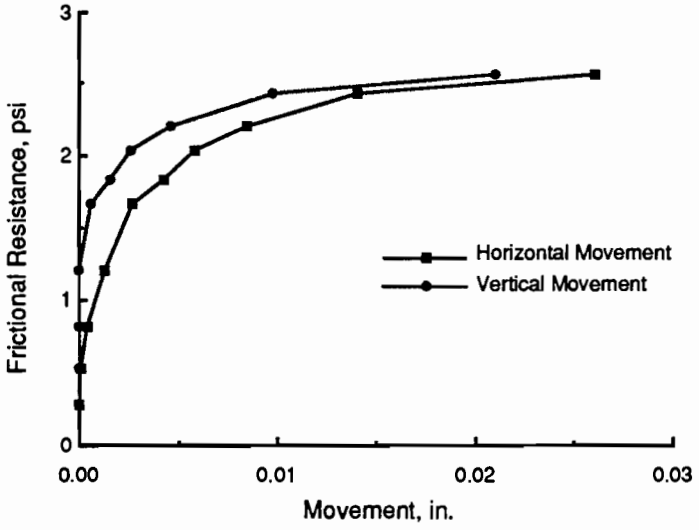

Fig B.33. *Horizontal and vertical movements to peak frictional resistance for push-off test on simulated 7-inch slab over a 2-inch-thick asphalt pavement with a medium texture.*

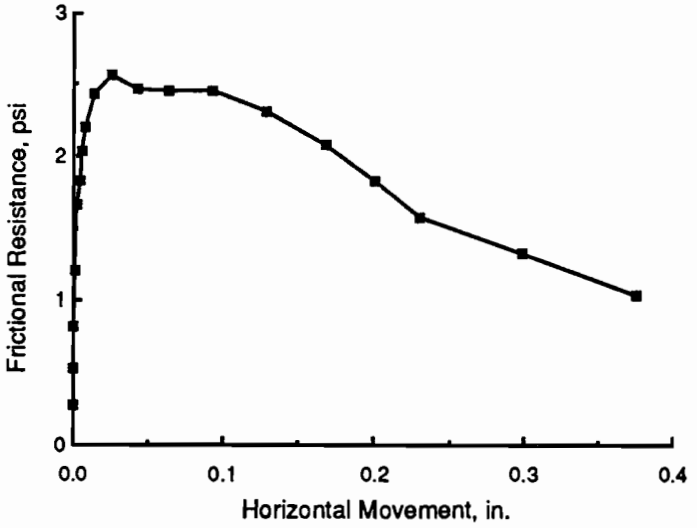

Fig B.34. *Horizontal movement for push-off test on simulated 7-inch slab over a 2-inch-thick asphalt pavement with a medium texture.*

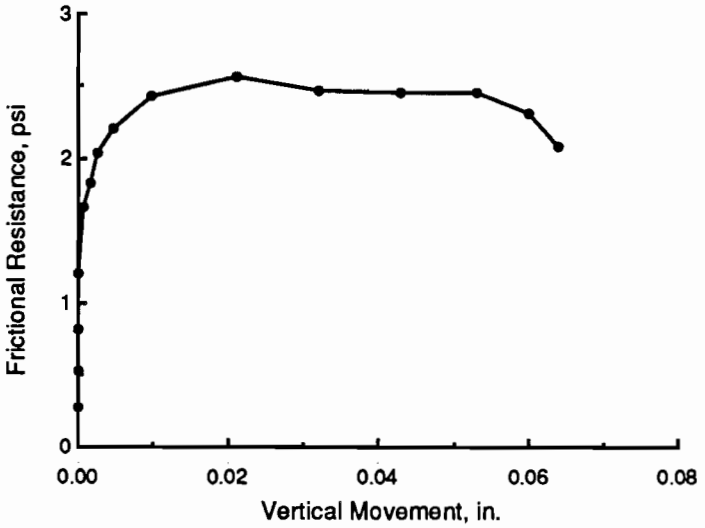

Fig B.35. *Vertical movement for push-off test on simulated 7-inch slab over a 2-inch-thick asphalt pavement with a medium texture.*

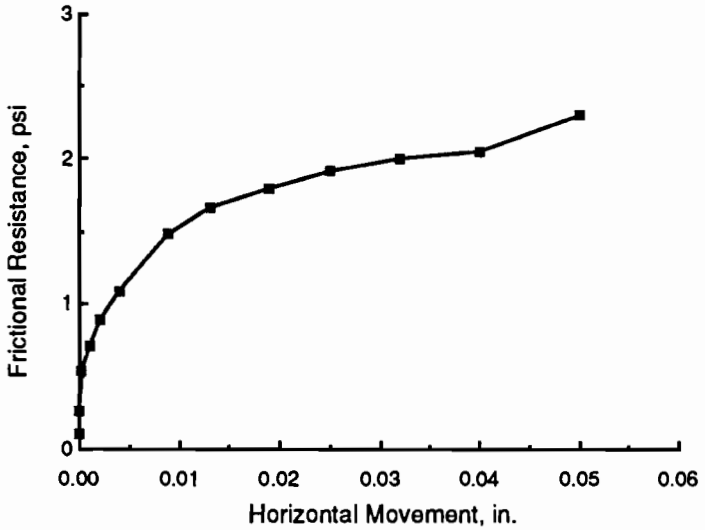

Fig B.36. *Horizontal movement to peak frictional resistance for push-off tests on 3-1/2-inch slab over a 2-inch-thick asphalt pavement with a rough texture.*

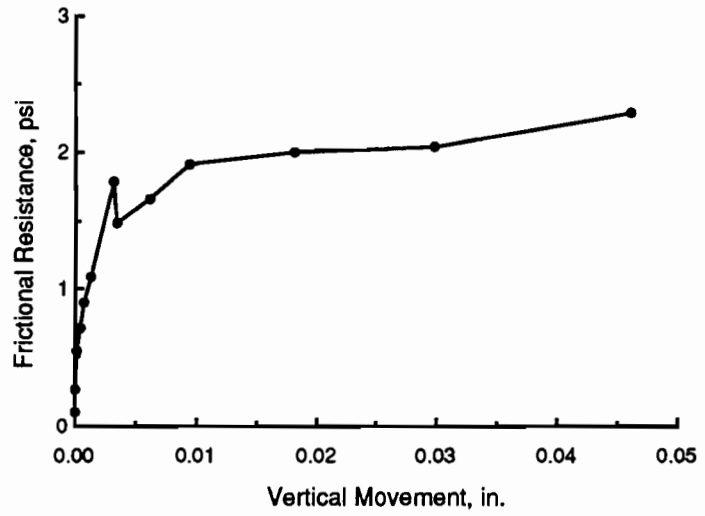

Fig B.37. *Vertical movement to peak frictional resistance for push-off test on 3-1/2-inch slab over a 2-inch-thick asphalt pavement with a rough texture.*

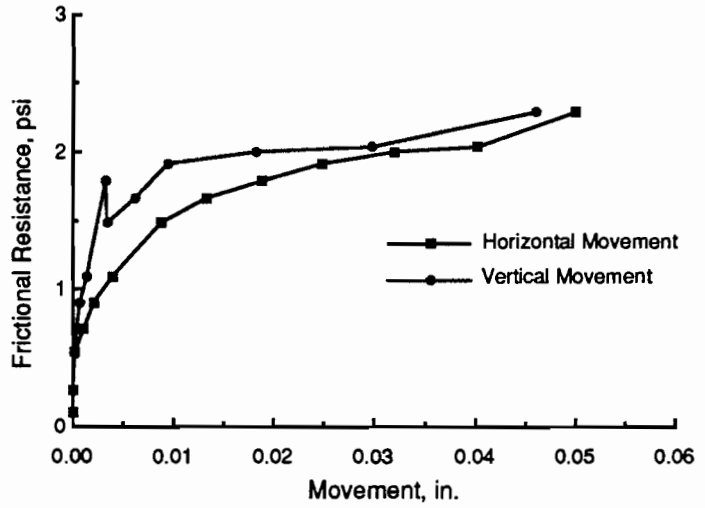

Fig B.38. *Horizontal and vertical movements to peak frictional resistance for push-off test on 3-1/2-inch slab over a 2-inch-thick asphalt pavement with a rough texture.*

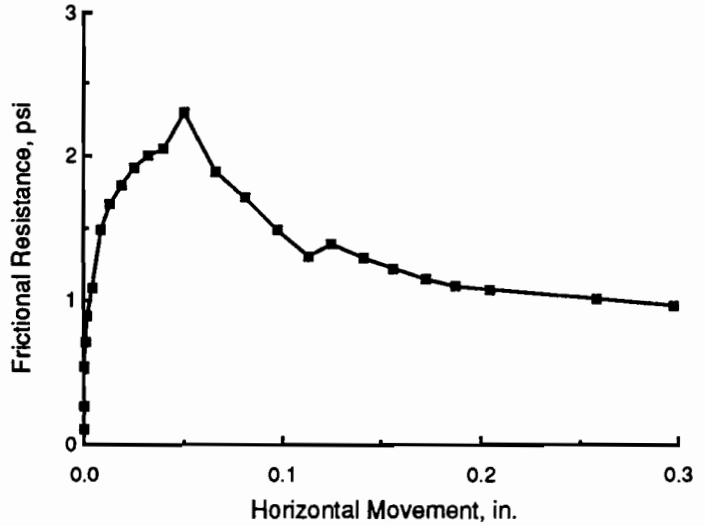

Fig B.39. *Horizontal movement for push-off test on 3-1/2-inch slab over a 2-inch-thick asphalt pavement with a rough texture.*

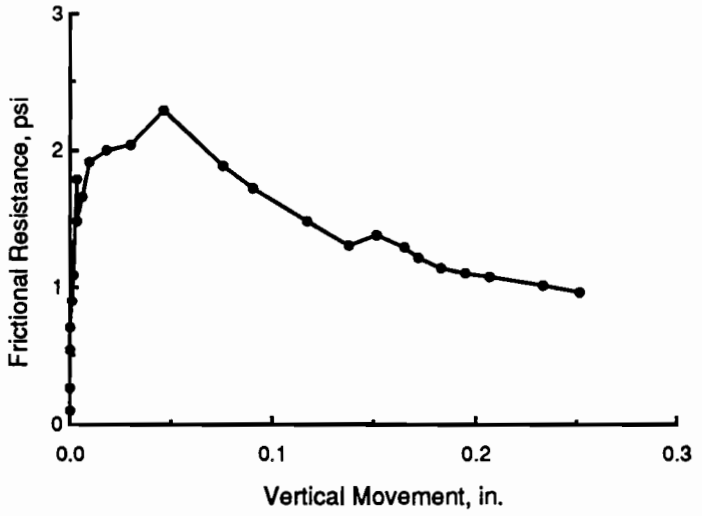

Fig B.40. *Vertical movement for push-off test on 3-1/2-inch slab over a 2-inch-thick asphalt pavement with a rough texture.*

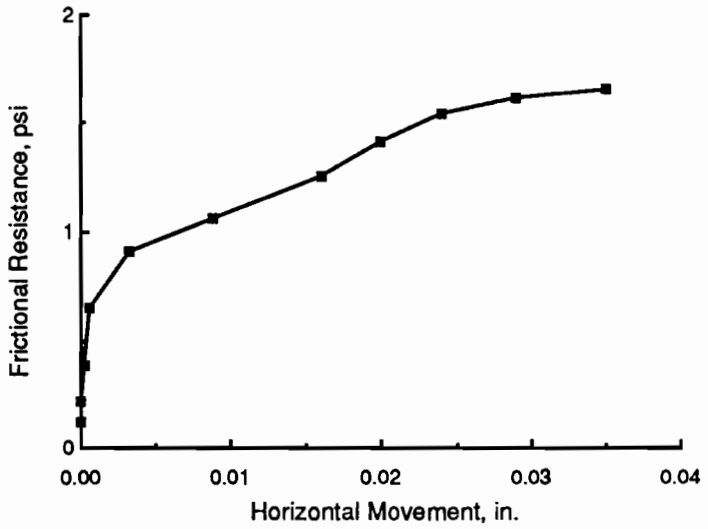

Fig B.41. *Horizontal movement to peak frictional resistance for push-off tests on 3-1/2-inch slab over a 2-inch-thick asphalt pavement with a smooth texture.*

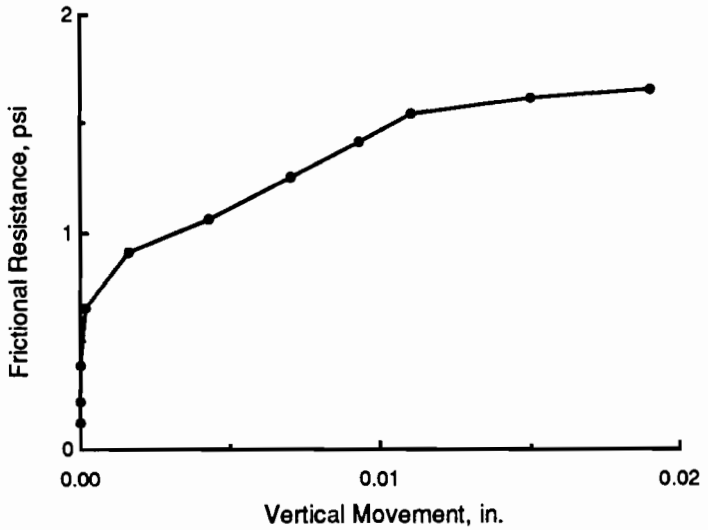

Fig B.42. *Vertical movement to peak frictional resistance for push-off test on 3-1/2-inch slab over a 2-inch-thick asphalt pavement with a smooth texture.*

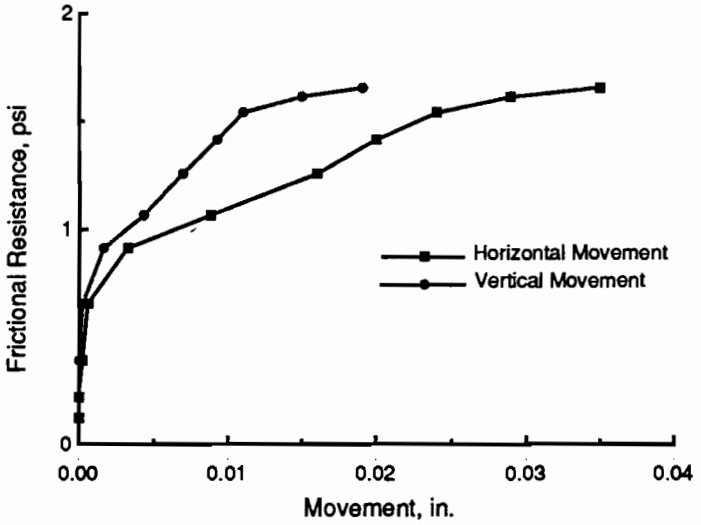

Fig B.43. Horizontal and vertical movements to peak frictional resistance for push-off test on 3-1/2-inch slab over a 2-inch-thick asphalt pavement with a smooth texture.

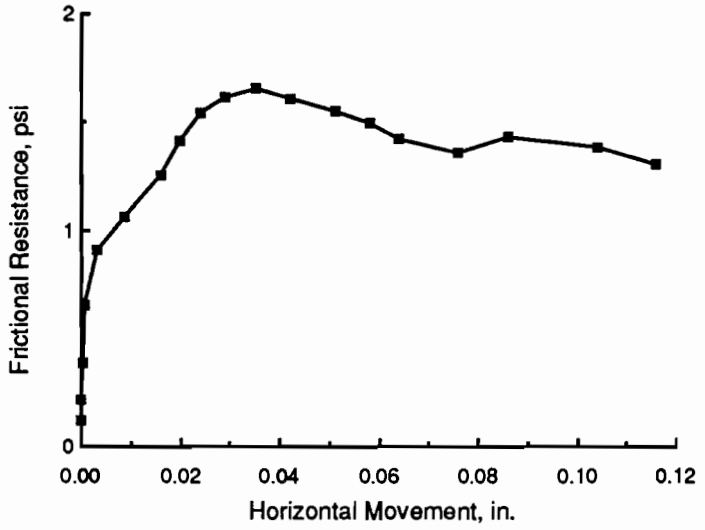

Fig B.44. *Horizontal movement for push-off test on 3-1/2-inch slab over a 2-inch-thick asphalt pavement with a smooth texture.*

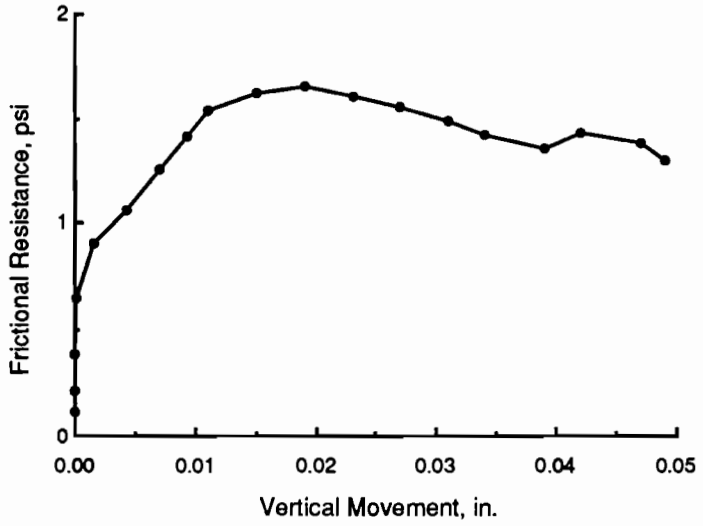

Fig B.45. *Vertical movement for push-off test on 3-1/2-inch slab over a 2-inch-thick asphalt pavement with a smooth texture.*

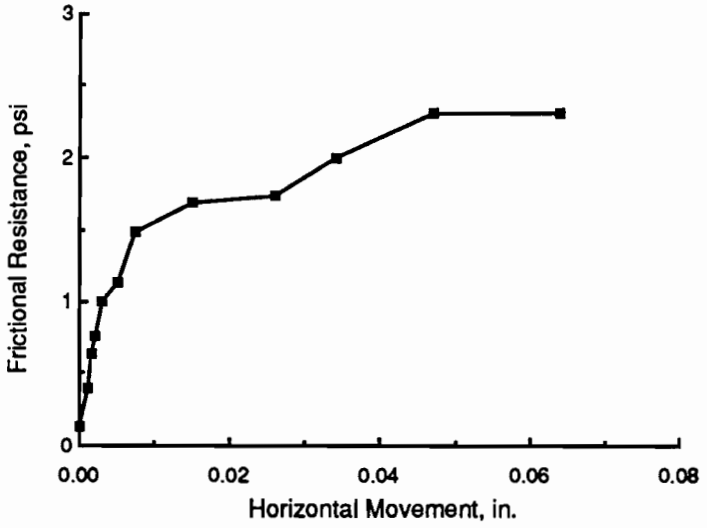

Fig B.46. *Horizontal movement to peak frictional resistance for push-off tests on 3-1/2-inch slab over a 2-inch-thick asphalt pavement with a medium texture.*

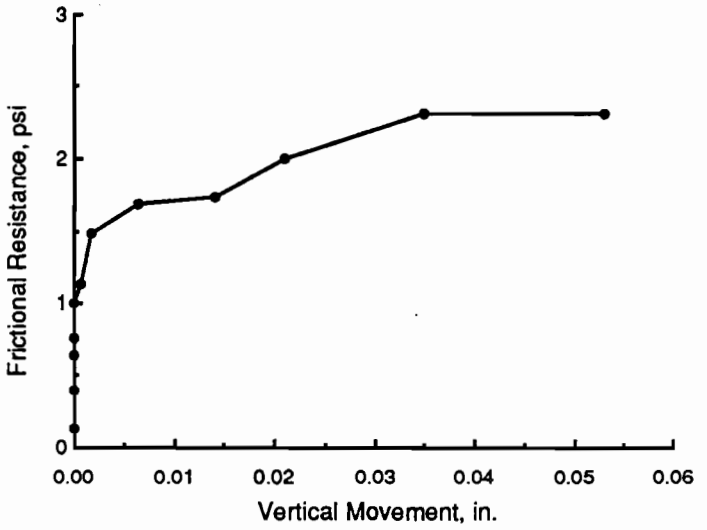

Fig B.47. *Vertical movement to peak frictional resistance for push-off test on 3-1/2-inch slab over a 2-inch-thick asphalt pavement with a medium texture.*

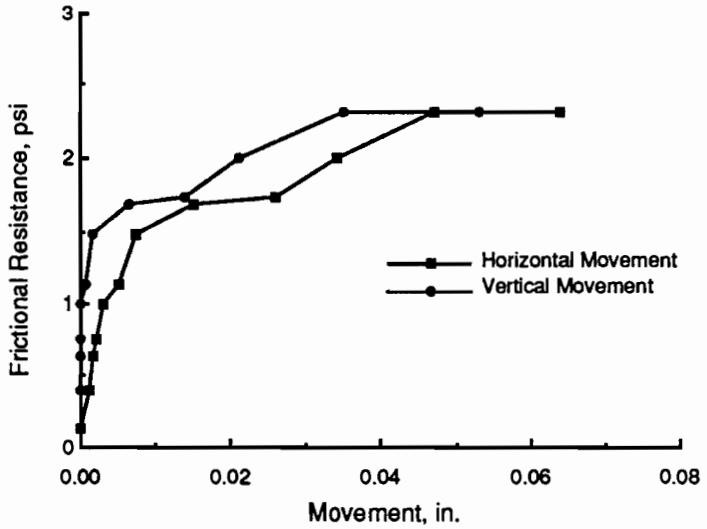

Fig B.48. *Horizontal and vertical movements to peak frictional resistance for push-off test on 3-1/2-inch slab over a 2-inch-thick asphalt pavement with a medium texture.*

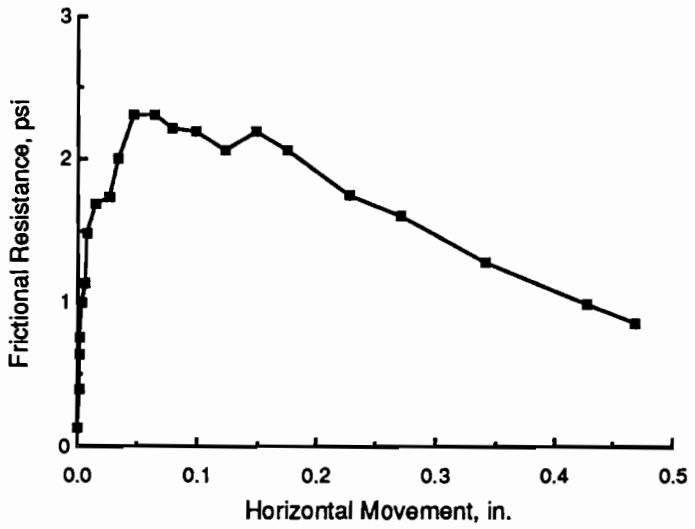

Fig B.49. ***Horizontal movement for push-off test on 3-1/2-inch slab over a 2-inch-thick asphalt pavement with a medium texture.***

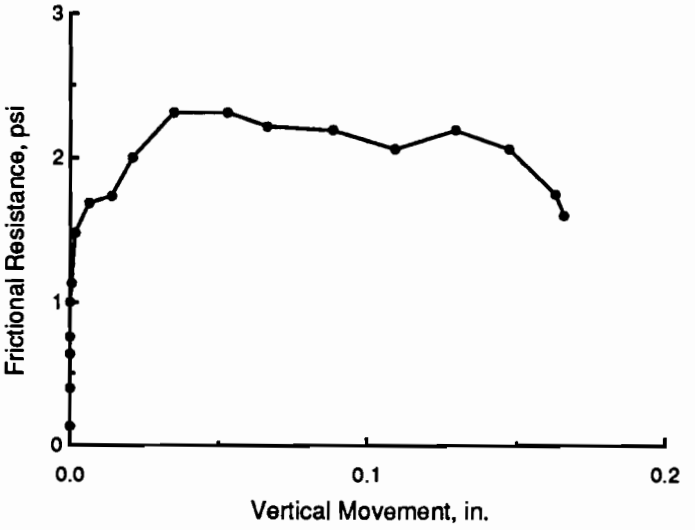

Fig B.50. ***Vertical movement for push-off test on 3-1/2-inch slab over a 2-inch-thick asphalt pavement with a medium texture.***

APPPENDIX C. DATA INPUT FOR THE CRCP PROGRAM TO PREDICT CRACK SPACING

TABLE C.1. PROPERTIES OF CONCRETE PAVEMENT WITH SILICEOUS RIVER GRAVEL

```
**************************************************
*                                                *
*                STEEL PROPERTIES                *
*                                                *
**************************************************

      TYPE OF LONGITUDINAL REINFORCEMENT IS
                  DEFORMED BARS

      PERCENT REINFORCEMENT = 6.000E-01
      BAR DIAMETER          = 7.500E-01
      YIELD STRESS          = 6.000E+04
      ELASTIC MODULUS       = 3.020E+07
      THERMAL COEFFICIENT   = 6.500E-06

**************************************************
*                                                *
*              CONCRETE PROPERTIES               *
*                                                *
**************************************************

      SLAB THICKNESS       = 8.000E+00
      THERMAL COEFFICIENT = 6.000E-06
      TOTAL SHRINKAGE      = 2.525E-04
      UNIT WEIGHT CONCRETE= 1.440E+02
      COMPRESSIVE STRENGTH= 3.500E+03

      TENSILE STRENGTH DATA AS INPUT BY USER

     AGE,    TENSILE
    (DAYS)  STRENGTH
       -0      -0
      1.0    165.0
      3.0    223.0
      5.0    248.0
      7.0    266.0
     14.0    302.0
     21.0    310.0
     28.0    312.0
```

TABLE C.2. PROPERTIES OF CONCRETE PAVEMENT WITH LIMESTONE AGGREGATE

```
**************************************************
*                                                *
*              STEEL PROPERTIES                  *
*                                                *
**************************************************

     TYPE OF LONGITUDINAL REINFORCEMENT IS
               DEFORMED BARS


     PERCENT REINFORCEMENT = 6.000E-01
     BAR DIAMETER          = 7.500E-01
     YIELD STRESS          = 6.000E+04
     ELASTIC MODULUS       = 3.020E+07
     THERMAL COEFFICIENT   = 6.500E-06



**************************************************
*                                                *
*            CONCRETE PROPERTIES                 *
*                                                *
**************************************************

     SLAB THICKNESS       = 8.000E+00
     THERMAL COEFFICIENT = 4.000E-06
     TOTAL SHRINKAGE      = 2.525E-04
     UNIT WEIGHT CONCRETE= 1.440E+02
     COMPRESSIVE STRENGTH= 3.500E+03
     STRENGTH MULTIPLIER = 1.0


    TENSILE STRENGTH DATA
    *********************

     NO TENSILE STRENGTH DATA IS INPUT BY USER
     THE FOLLOWING AGE-TENSILE STRENGTH RELATIONSHIP
     IS USED WHICH IS BASED ON THE RECOMMENDATION
     GIVEN BY U.S. BUREAU OF RECLAMATION

     AGE,  TENSILE
    (DAYS) STRENGTH

        0       0
      1.0   171.8
      3.0   273.5
      5.0   323.0
      7.0   352.2
     14.0   401.8
     21.0   430.2
     28.0   443.7
```

TABLE C.3. TEMPERATURE AND STRENGTH DATA

```
**********************************
*                                *
*       TEMPERATURE DATA         *
*                                *
**********************************

     CURING TEMPERATURE= 80.0

          MINIMUM       DROP IN
DAY     TEMPERATURE   TEMPERATURE

  1         69.0          11.0
  2         70.0          10.0
  3         72.0           8.0
  4         73.0           7.0
  5         74.0           6.0
  6         76.0           4.0
  7         73.0           7.0
  8         74.0           6.0
  9         74.0           6.0
 10         75.0           5.0
 11         75.0           5.0
 12         68.0          12.0
 13         66.0          14.0
 14         59.0          21.0
 15         59.0          21.0
 16         59.0          21.0
 17         64.0          16.0
 18         62.0          18.0
 19         67.0          13.0
 20         70.0          10.0
 21         71.0           9.0
 22         78.0           2.0
 23         76.0           4.0
 24         74.0           6.0
 25         72.0           8.0
 26         72.0           8.0
 27         74.0           6.0
 28         70.0          10.0

  DAYS BEFORE CONCRETE GAINS
  FULL STRENGTH                        =   28 DAYS
  MINIMUM TEMPERATURE EXPECTED AFTER
  CONCRETE GAINS FULL STRENGTH         = 24.0 DEGREES FAHRENHEIT
  DAYS BEFORE REACHING MIN. TEMP.      = 28.0 DAYS
```

TABLE C.4. EXTERNAL LOAD AND PROGRAM CONTROLS

```
**************************************************
*                                                *
*                 EXTERNAL LOAD                  *
*                                                *
**************************************************

      WHEEL LOAD (LBS)        = 9.000E+03
      WHEEL BASE RADIUS (IN) = 1.800E+01
      SUBGRADE MODULUS (PCI) = 6.400E+02
      CONCRETE MODULUS (PSI) = 3.374E+06
      LOAD APPLIED AT         =  14. TH DAY
      CALC.LOAD STRESS (PSI) = 6.265E+01




**************************************************
*                                                *
*       ITERATION AND TOLERANCE CONTROL          *
*                                                *
**************************************************


 MAXIMUM ALLOWABLE NUMBER OF ITERATIONS=   60

 RELATIVE CLOSURE TOLERANCE=  1.0 PERCENT
```

TABLE C.5. FRICTION-MOVEMENT DATA FOR LIME-TREATED CLAY

TYPE OF FRICTION CURVE IS A MULTILINEAR CURVE

F(I)	Y(I)
0	-0
.7800	-.0012
1.1900	-.0034
1.5200	-.0065
1.7200	-.0118
1.5400	-.0335
1.0100	-.1277
.7800	-.3994
.7200	-.6753
.6700	-.9725

TABLE C.6. FRICTION-MOVEMENT DATA FOR FLEXIBLE SUBBASE

TYPE OF FRICTION CURVE IS A MULTILINEAR CURVE

F(I)	Y(I)
0	0
1.7300	-.0009
2.0500	-.0017
2.6900	-.0028
3.0600	-.0070
3.3100	-.0149
3.3600	-.0362
3.0900	-.0697
2.0000	-.1527
1.0000	-.5938

TABLE C.7. FRICTION MOVEMENT DATA FOR ASPHALT-STABILIZED SUBBASE

TYPE OF FRICTION CURVE IS A MULTILINEAR CURVE

F(I)	Y(I)
0	-0
.3900	-.0002
1.4900	-.0053
2.1800	-.0132
2.6700	-.0183
2.8700	-.0287
3.2200	-.0355
3.1000	-.0474
2.7600	-.1165
1.3900	-.3812

TABLE C.8. FRICTION MOVEMENT DATA FOR CEMENT-TREATED SUBBASE

TYPE OF FRICTION CURVE IS A MULTILINEAR CURVE

F(I)	Y(I)
0	-0
2.8000	-.0001
7.8500	-.0004
10.2900	-.0007
12.8600	-.0009
15.3500	-.0012
17.2700	-.0018
2.0000	-.0100
1.7500	-.1008
1.2700	-.5000

APPENDIX D. CRCP CRACK SPACING DATA FOR SELECTED TEXAS HIGHWAYS IN DISTRICTS 1, 3, 4, 10, 13, 15, 17, 19, 20, AND 24

TABLE D.1. DATA FOR CRCP SECTIONS - LIMESTONE AGGREGATE CONCRETE OVER LIME-TREATED CLAY SUBBASE

Section ID No.	Mean Crack Spacing (ft)	Std. Dev. (ft)	Mode (ft)
1015E	7.38	4.45	6
1015W	7.25	3.43	8
10002E	9.09	4.09	8
10002W	7.27	4.06	6
17008N	3.10	1.58	1.5, 3
17008S	6.15	3.57	8
24010E	7.14	2.86	8, 10
24010W	7.31	3.58	8
24011E	5.60	2.96	5
24011W	4.62	1.49	4
24012E	4.07	1.77	5
24012W	5.64	2.17	7
24014E	6.64	2.07	6
24014W	5.65	2.34	5
24015W	4.60	2.55	2

Avg. Mean Crack Spacing = 6.10 ft
Avg. Mode Crack Spacing = 5.95 ft
(For sections containing two or more mode values, the values were averaged for that section, and that average was used as the section value in the calculation for the average mode for the whole table.)

TABLE D.2. DATA FOR CRCP SECTIONS - SILICIOUS RIVER GRAVEL AGGREGATE CONCRETE OVER LIME-TREATED CLAY SUBBASE

Section ID No.	Mean Crack Spacing (ft)	Std. Dev. (ft)	Mode (ft)
1012N	2.43	1.17	2
1013N	3.54	1.78	2
1013S	4.20	2.26	5
4005E	2.88	1.05	2.5
4005W	2.59	1.06	2.5
13029S	3.00	1.53	3
13030N	2.92	1.38	3
13030S	3.07	1.66	2.5
19006E	3.33	1.83	2
19006W	6.60	5.93	2
19008W	3.71	2.18	2
24020E	4.56	2.62	2, 6
24020W	4.23	2.47	5
24023E	4.98	2.71	3, 6

Avg. Mean Crack Spacing = 3.72
Avg. Mode Crack Spacing = 3.00
(For sections containing two or more mode values, the values were averaged for that section, and that average was used as the section value in the calculation for the average mode for the whole table.)

TABLE D.3. DATA FOR CRCP SECTIONS - LIMESTONE AGGREGATE CONCRETE OVER ASPHALT-STABILIZED SUBBASE

Section ID No.	Mean Crack Spacing (ft)	Std. Dev. (ft)	Mode (ft)
3004S	6.49	3.87	2, 8
3005S	6.01	3.33	2, 4, 8
3015W	7.19	4.80	4
3016N	4.85	2.68	3, 6
3018N	10.22	4.18	10, 12
3018S	6.79	3.28	8
13016E	5.72	2.03	6
13016W	5.51	2.13	6
13020E	9.12	4.33	14
13020W	10.86	5.82	12
13021E	10.74	3.87	12
13021W	12.29	4.26	16
17002N	4.40	2.54	2
17002S	4.07	2.17	2, 4
24009E	6.75	3.03	6
24009W	5.98	2.39	5

Avg. Mean Crack Spacing = 7.31 ft
Avg. Mode Crack Spacing = 6.70 ft
(For sections containing two or more mode values, the values were averaged for that section, and that average was used as the section value in the calculation for the average mode for the whole table.)

TABLE D.4. DATA FOR CRCP SECTIONS - SILICIOUS RIVER GRAVEL AGGREGATE CONCRETE OVER ASPHALT-STABILIZED SUBBASE

Section ID No.	Mean Crack Spacing (ft)	Std. Dev. (ft)	Mode (ft)
4006E	3.16	1.53	2.5
4006W	3.10	1.33	3
4010E	2.78	1.44	2, 3
4010W	3.10	1.44	3
13023N	4.85	3.11	2
13024S	5.32	3.06	7
17003N	2.86	1.27	2
17003S	3.46	1.49	2
17004N	2.95	1.29	2
17004S	3.03	1.33	2
17007N	3.02	1.48	2.5
17007S	2.89	1.21	2.5
17010N	4.64	1.72	4
17010S	5.00	1.84	5
17011N	5.00	3.49	2
17011S	4.97	4.06	1
19001E	2.23	1.08	1.5
19001W	1.86	1.02	1
19004E	3.20	1.67	3
19004W	3.82	1.98	3

Avg. Mean Crack Spacing = 3.56 ft
Avg. Mode Crack Spacing = 2.68 ft
(For sections containing two or more mode values, the values were averaged for that section, and that average was used as the section value in the calculation for the average mode for the whole table.)

TABLE D.5. DATA FOR CRCP SECTION - LIMESTONE AGGREGATE CONCRETE OVER FLEXIBLE SUBBASE

Section ID No.	Mean Crack Spacing (ft)	Std. Dev. (ft)	Mode (ft)
1008N	8.93	4.36	12
1008S	7.26	3.89	6
1011S	7.18	3.79	6, 6, 8

Avg. Mean Crack Spacing = 7.79 ft
Avg. Mode Crack Spacing = 8.22 ft
(For sections containing two or more mode values, the values were averaged for that section, and that average was used as the section value in the calculation for the average mode for the whole table.)

TABLE D.6. DATA FOR CRCP SECTIONS - SILICIOUS RIVER GRAVEL AGGREGATE CONCRETE OVER FLEXIBLE SUBBASE

Section ID No.	Mean Crack Spacing (ft)	Std. Dev. (ft)	Mode (ft)
4002E	3.42	2.23	2
4002W	3.37	2.19	2

Avg. Mean Crack Spacing = 3.39 ft
Avg. Mode Crack Spacing = 2.00 ft

TABLE D.7. DATA FOR CRCP SECTIONS - LIMESTONE AGGREGATE CONCRETE OVER CEMENT-STABILIZED SUBBASE

Section ID No.	Mean Crack Spacing (ft)	Std. Dev. (ft)	Mode (ft)
1001E	8.08	5.64	2
1001W	7.05	3.24	8
1002E	8.98	4.82	10
1002W	10.12	7.03	6, 8
1003E	6.24	3.22	6
1003W	6.22	3.26	6
1005E	5.56	2.99	6
1005W	6.64	3.32	6
3001S	5.14	2.72	5
3003S	5.98	3.05	4
3006E	4.43	2.13	5
3006W	5.54	2.76	4
3007E	5.13	2.31	5
3007W	5.51	2.45	3, 5
3008E	2.58	1.25	2.5
3008W	5.41	2.12	6
3010N	5.02	2.99	2
3010S	5.47	2.92	4
3011N	9.90	4.82	12, 14
3011S	8.51	3.39	6
3019S	7.07	2.08	7
3020N	8.21	4.39	8
3022N	7.04	4.05	10
13015E	6.54	3.27	6
13015W	6.13	2.44	6
13017E	7.65	2.99	6
13017W	8.58	3.80	8, 12
20009E	5.43	3.08	6
20009W	5.82	3.72	2
20011S	4.85	3.45	2
20019W	7.22	3.52	6

TABLE D.8. DATA FOR CRCP SECTIONS - SILICIOUS RIVER GRAVEL AGGREGATE CONCRETE OVER CEMENT-STABILIZED SUBBASE

Section ID No.	Mean Crack Spacing (ft)	Std. Dev. (ft)	Mode (ft)
4011E	5.38	2.67	6
4011W	3.46	1.58	3
13001E	3.36	1.88	2
13001W	3.51	2.37	1, 2
13002E	4.00	2.20	2, 4
13002W	4.11	2.69	2
13003E	4.62	2.78	4
13003W	4.80	2.58	2
13005N	3.22	1.66	2
13005S	2.83	1.49	1.5
13006E	2.27	1.03	1.5
13006W	3.43	1.55	2
13007E	2.83	1.47	2.5
13007W	2.49	1.23	2
13008N	8.27	3.43	8, 10
13008S	5.83	4.00	2
13009N	4.28	3.29	2
13009S	3.23	2.06	2
13010N	5.91	4.52	2
13010S	4.42	3.28	2
13011E	3.44	1.58	2.5
13011W	3.64	2.09	2
13012N	4.31	2.90	3
13012S	5.15	2.90	6
13013E	3.55	2.06	3
13013W	5.01	2.68	8
13018N	3.48	2.32	2
13018S	4.35	2.19	3
13019N	3.55	2.10	2
13019S	4.48	2.56	3
13022N	5.25	2.87	1, 5
13022S	5.16	3.23	3
13032N	5.27	2.82	2, 6
13032S	4.68	2.69	3
13033N	4.28	2.85	2

TABLE D.8. DATA FOR CRCP SECTIONS - SILICIOUS RIVER GRAVEL AGGREGATE CONCRETE OVER CEMENT-STABILIZED SUBBASE (cont.)

Section ID No.	Mean Crack Spacing (ft)	Std. Dev. (ft)	Mode (ft)
19003W	2.12	1.08	2
19011E	2.58	1.20	2.5
19011W	3.12	1.33	2.5
19014E	2.50	1.11	2
19014W	3.37	1.46	3
19019E	2.75	1.03	3.5
19019W	2.69	1.23	1.5
20003W	5.87	4.01	2
20014S	3.19	1.63	3
20015S	5.07	2.76	3
20016S	4.16	2.11	5
20017E	3.02	2.12	2
20018E	3.91	2.22	2
20021E	4.21	3.40	2
20022N	4.02	2.18	3
20022S	4.46	2.70	3
20023N	2.59	0.94	2.5
20023S	2.62	0.90	2.5
20026W	2.62	1.50	3

Avg. Mean Crack Spacing = 3.93 ft
Avg. Mode Crack Spacing = 2.84 ft
(For sections containing two or more mode values, the values were averaged for that section, and that average was used as the section value in the calculation for the average mode for the whole table.)